COUNTER TELESCOPE INVESTIGATIONS OF K MESON PHOTOPRODUCTION

and

PRODUCTION OF PION PAIRS BY 1 BEV PHOTONS

Thesis by

Marshall P. Ernstene

In Partial Fulfillment of the Requirements

For the Degree of

Doctor of Philosophy

California Institute of Technology

Pasadena, California

1959

ACKNOWLEDGMENTS

The earlier K meson experiments reported here were supervised by Dr. Alvin V. Tollestrup, whose guidance throughout the author's graduate career has been invaluable. Dr. Robert L. Walker supervised the later experiments and suggested the pion pair work; his constant encouragement is gratefully acknowledged.

Dr. Arthur B. Clegg and Dr. Ricardo Gomez provided considerable assistance in planning and running the experiments, and in interpreting the results. Much of the necessary equipment was constructed by Mr. Henry R. Myers, who also shared fully in the operation of the experiment. Mr. Myers, together with Mr. Earle B. Emery, constructed and maintained the pressure-fed hydrogen target used here. All members of the synchrotron staff, and in particular Dr. Matthew Sands, were responsible for valuable discussions of the results and calculations reported here. Mr. Larry Loucks, Mr. Alfred Neubieser, and the entire synchrotron crew provided continuing assistance.

The interest of Dr. Robert F. Bacher is appreciated. The partial financial support of the Atomic Energy Commission is gratefully acknowledged.

ABSTRACT

A number of counter telescope systems were set up to detect K mesons produced by the photon beam from the California Institute of Technology synchrotron. A common feature of these experiments was the presence of a very large background from other particles, which largely obscured the K mesons. Four methods for separating K's were investigated: observing their decay in a scintillator, and in a Cerenkov counter, detecting the decay products with separate counters, and counting protons from Λ particles produced in association with the K's. Tentative cross section values were obtained, but none of the methods was completely successful. However, the advanced telescope techniques developed here and the experimental arrangements are of interest for future work.

The photoproduction of pion pairs was studied by observing protons and charged pions produced simultaneously in a liquid hydrogen target. Protons of a given energy were counted in a five-counter range telescope; energetic pions were detected as they passed through a three-counter array. The reaction yield was measured as a function of peak photon energy, of pion angle, and especially of proton angle. Cross sections obtained by photon differences were compared to the predictions of certain phenomenological models, but statistical uncertainties in the experimental results prevent definite conclusions from being drawn. Further experiments are mentioned which might give more definite information about the mechanism of pion pair production.

Contents

COUNTER TELESCOPE INVESTIGATION OF K MESON PHOTOPRODUCTION

PRODUCTION OF PION PAIRS BY 1 BEV PHOTONS

COUNTER TELESCOPE INVESTIGATIONS OF K MESON PHOTOPRODUCTION

I. INTRODUCTION

The study of K mesons and hyperons has been a chief concern of high-energy physics since these "strange" particles were discovered. First seen in cosmic ray observations, many of their properties have been determined in experiments with large accelerators. Their plentiful production in pion-nucleon and nucleon-nucleon reactions is well known, but their production in photon-nucleon reactions had not been observed when the experiments reported here were begun. The cross section for K^+ photoproduction in liquid hydrogen has since been measured by Donoho and Walker (1, 2), who used a large magnetic spectrometer. Peterson, Roos, and Terman (3) have observed K^+ mesons from hydrogen in nuclear emulsion stacks. Silverman, Wilson, and Woodward (4, 5) at Cornell have used a magnetic spectrometer to study K photoproduction. More recently Brody, Walker, and Wetherell (6) have extended the methods of Donoho and Walker to other kinematic regions.

This thesis will describe attempts to measure K^+ photoproduction by means of scintillation counter telescopes. These attempts were started at the same time as the spectrometer experiments of Donoho and Walker, as soon as the California Institute of Technology synchrotron began operation above 1 Bev. A detailed comparison of telescope and spectrometer methods is given later. Here it will only

be mentioned that the K telescope offered a higher counting rate (because of larger solid angle), and particularly promised to be more suitable for measuring K's of low energy, most of which decayed before being counted in the large spectrometer. Furthermore, complementary measurements of reaction cross sections by both spectrometer and telescope had been found useful in the past, regardless of the special advantages of each method. Systematic experimental errors are clearly revealed by such measurements.

A common feature of K meson photoproduction experiments is the presence of a very large background from other particles. Considerably more elaborate experimental arrangements are required for clear identification of K's than are necessary to measure pions or protons. Examples of this complexity are found in the experiment of Donoho and Walker, who made a time of flight measurement within their spectrometer, and in the Cornell experiment where K decay particles were observed behind the spectrometer.

Four successive telescope arrangements for separating K's from pions and protons were tried in the course of the work discussed here. First, pulses from a counter in which K mesons stopped were photographed from a fast oscilloscope; delayed pulses from K decay were sought. Second, K mesons were stopped in a water Cerenkov counter, in which the mesons themselves could not give a signal but their decay particles could. Third, side counters were placed next to a stopping counter to look for decay particles. Finally, a second telescope was set up to look for protons from the Λ particles

produced in association with the K's.

The first of these experiments was perhaps the most successful, in that it alone gave a reliable figure for K meson yield and lifetime. However, it had a low counting rate and required tedious and subjective film analysis. The later experiments were attempts to avoid these drawbacks and at the same time to improve discrimination against other particles. These attempts, while not very successful, involved some interesting new experimental techniques. The advantages and drawbacks of each method will be fully described in the hope that the experience gained here will be of use in future research with scintillation and Cerenkov counter systems.

II. EXPERIMENTAL TECHNIQUES

A. Telescope Principles

Figure 1a shows a basic counter telescope. Particles of interest stop in counter 2 or absorber C, giving signals in counters 1 and 2 but none in 3. Counters 2 and 3 thus restrict the range to lie between R and R + ΔR. The curves of figure 1b show (in qualitative fashion) rate of energy loss in counter material versus residual range. Absorber B provides sufficient residual range so that energy loss in counter 1 distinguishes various types of particles. Counters such as 1 are commonly called dE/dx counters; 2 may be called the ΔR counter, and 3 the veto counter. In the example shown, the pulse from counter 1 is about twice as large for protons as for pions, corresponding to a residual range of 2 cm of copper. A pulse height spectrum for such a telescope with 0.8 cm of copper as ΔR is shown in figure 1c; proton and pion peaks are well resolved. Finally, absorber A adjusts the range R and so selects the energy of the particles being examined.

The rate at which a telescope counts particles is proportional to ΔR. For low yield experiments, such as those with K mesons, large ΔR is very desirable. As figure 2a shows, however, large ΔR causes pion and proton peaks to overlap. A method for increasing ΔR without sacrificing peak resolution was suggested by Dr. Gomez at this laboratory, and was used in much of the experimental work described here. The method consists of omitting absorber C and making counter 2 very thick--thick enough to provide the desired ΔR. The signal in this counter then increases with residual range as

Figures 1, 2, 3, 4,

Counter Telescope Principles

1a Basic telescope configuration.

1b Rate of energy loss versus residual range, showing pion and proton peaks.

1c Observed pion and proton peaks.

2a Overlap of peaks caused by excessive ΔR.

2b Signal in ΔR counter versus residual range.

2c Sum of dE/dx and ΔR signals, showing peaks.

3a Observed dE/dx spectrum with excessive ΔR.

3b Observed peaks from $dE/dx + \Delta R$ signal.

4 Distribution of energy losses in 1 gram/cm^2 of counter material.
ΔE is energy loss; ΔE_o is most probable loss.

5a Spectrum with excessive electron background.

5b Spectrum with electrons vetoed by Cerenkov counter; dashed line shows protons lost by scintillation in Cerenkov counter.

5c Spectrum with Cerenkov counter in coincidence; dashed line shows protons scintillating in Cerenkov counter.

a

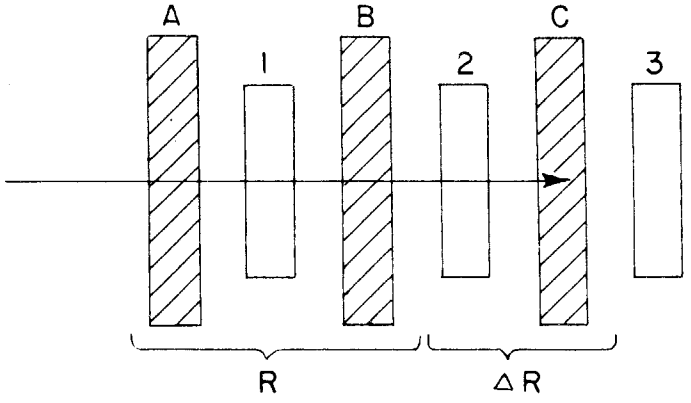
A
B
C
1
2
3
R
ΔR

b

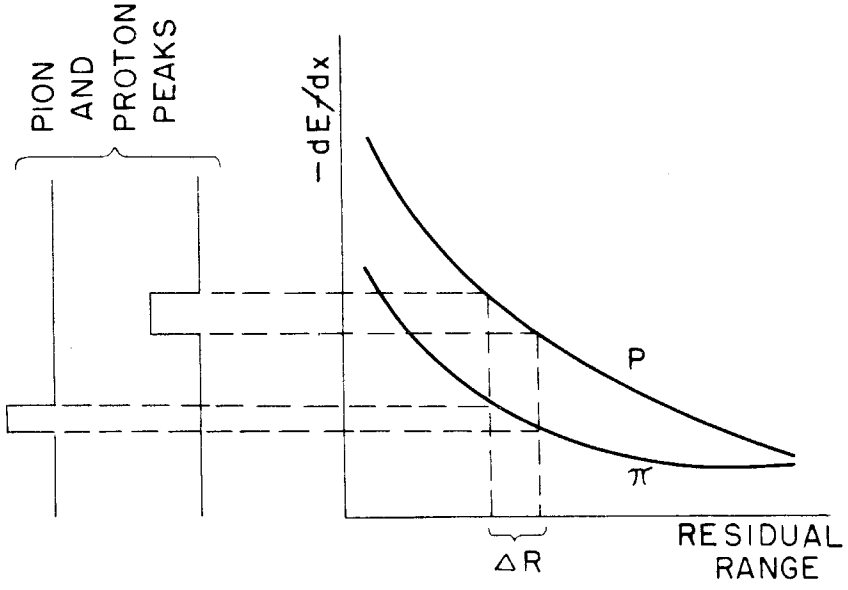
PION AND PROTON PEAKS
-dE/dx
P
π
ΔR
RESIDUAL RANGE

c

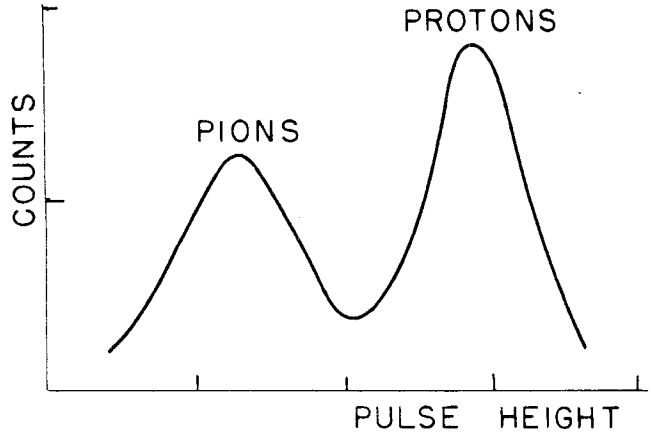
PROTONS
PIONS
COUNTS
PULSE HEIGHT

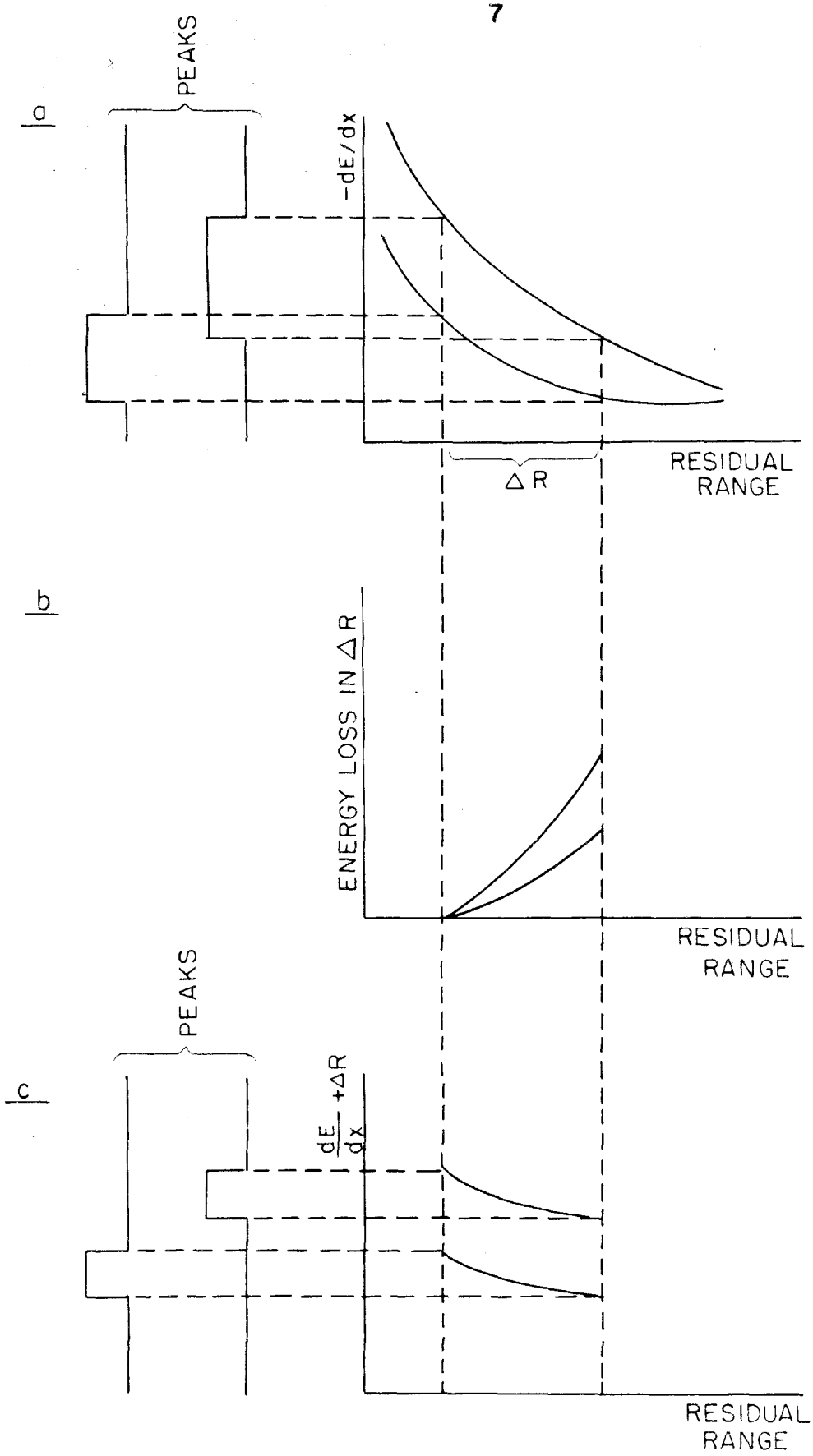
a
PEAKS
-dE/dx
ΔR
RESIDUAL RANGE
b
ENERGY LOSS IN ΔR
RESIDUAL RANGE
c
PEAKS
dE/dx +ΔR
RESIDUAL RANGE

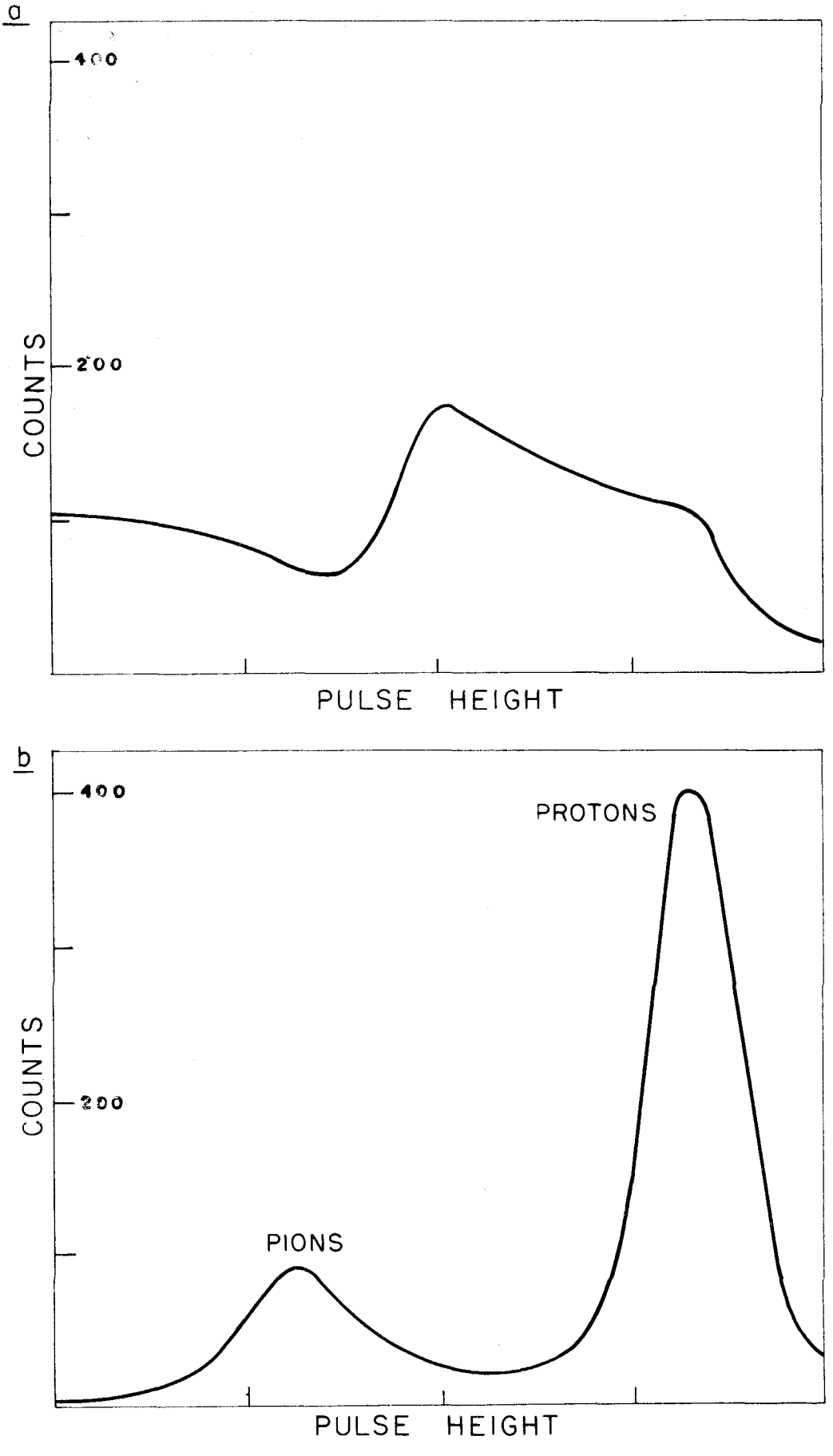
a
400
200
COUNTS
PULSE HEIGHT
b
400
200
COUNTS
PROTONS
PIONS
PULSE HEIGHT

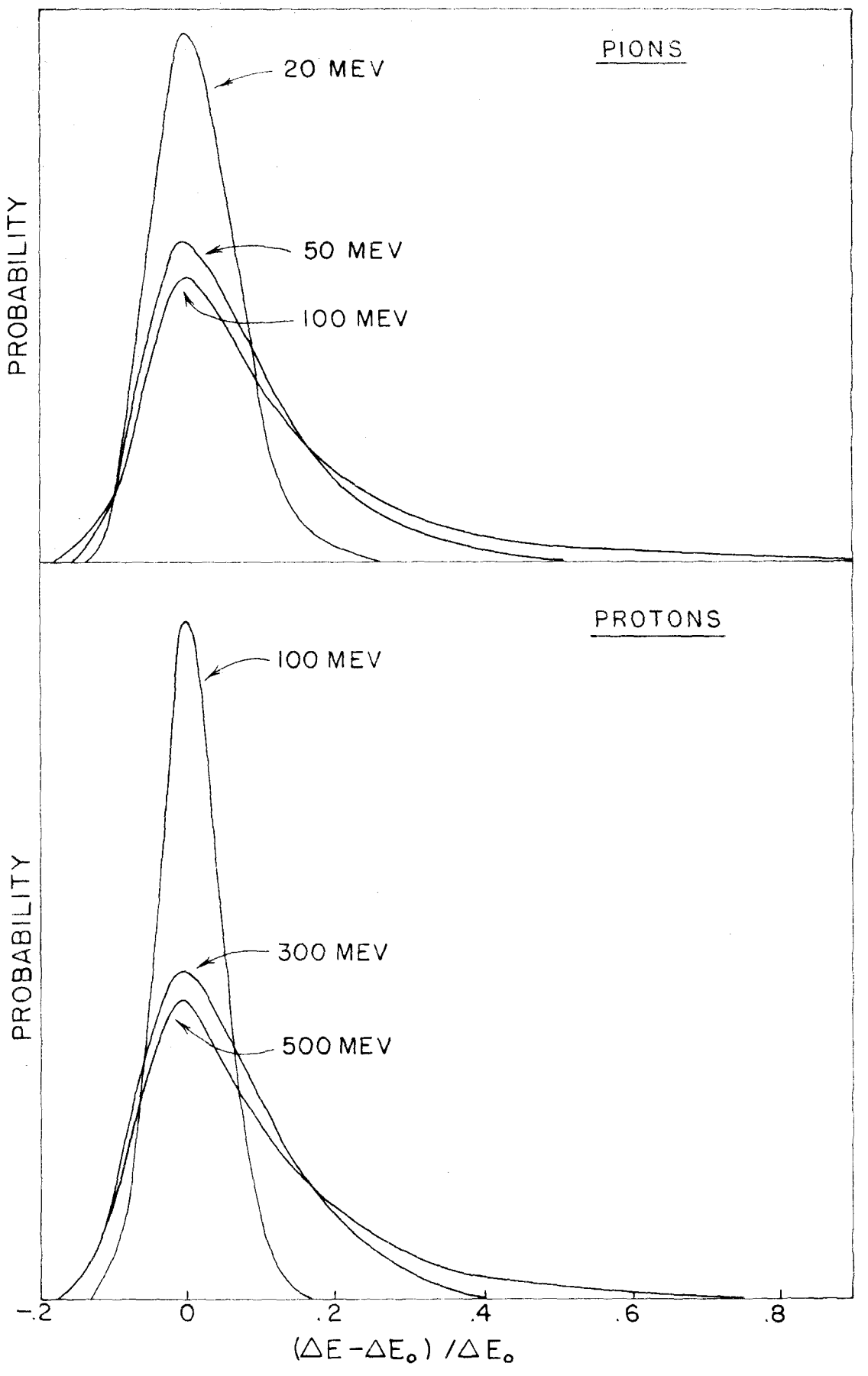
PIONS
20 MEV
50 MEV
100 MEV
PROBABILITY
PROTONS
100 MEV
300 MEV
500 MEV
PROBABILITY
-.2
0
.2
.4
.6
.8
(ΔE - ΔE₀) / ΔE₀

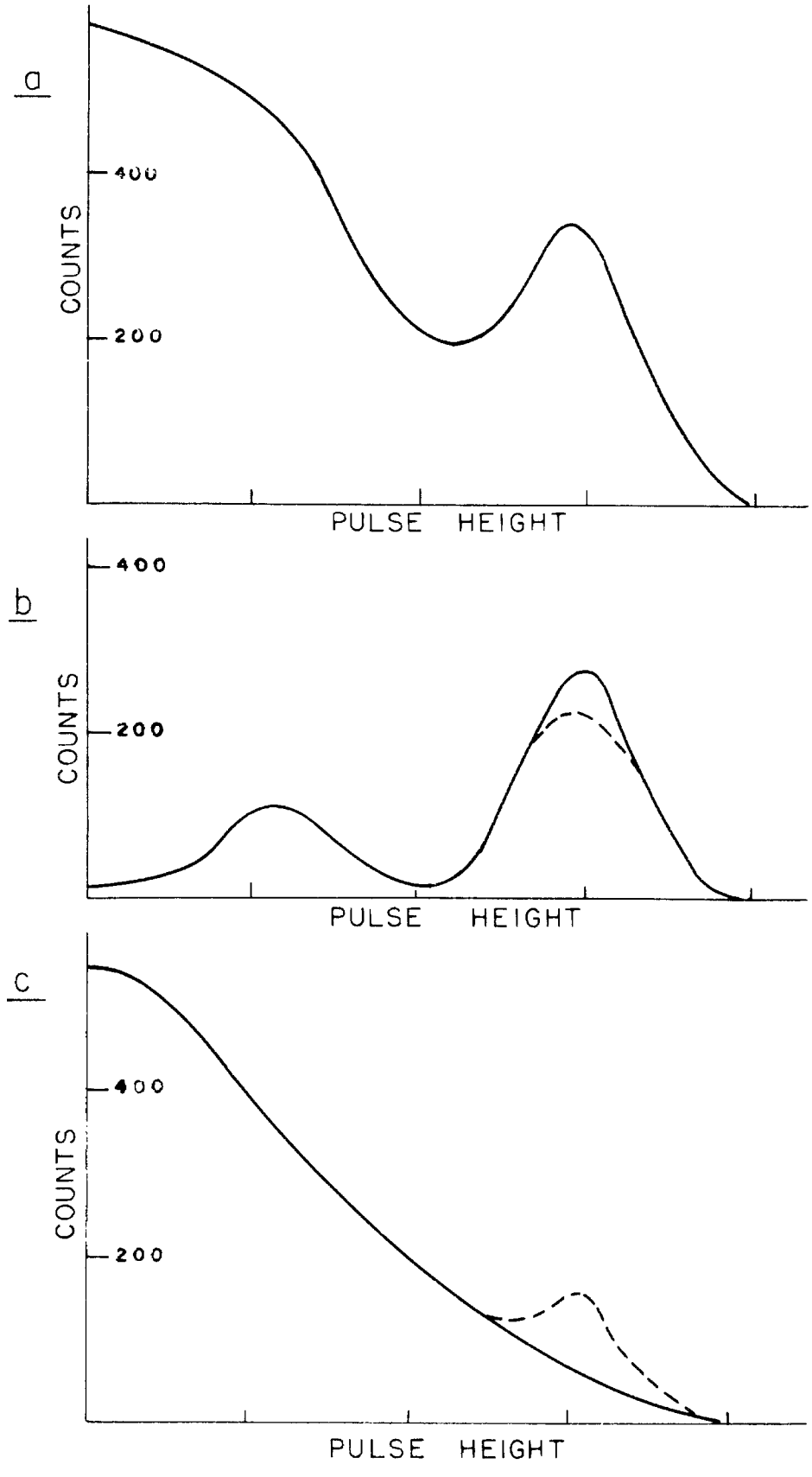
a
400
200
COUNTS
PULSE HEIGHT
b
400
200
COUNTS
PULSE HEIGHT
c
400
200
COUNTS
PULSE HEIGHT

indicated in figure 2b. By adding an appropriate amount of this signal to the dE/dx signal, the curves of figure 2c can be obtained. Pion and proton peaks are again clearly separated.

The product of the ΔR and dE/dx signals would give an even better separation of particles; this system of analysis has been described by several authors (7, 8). But electronic addition requires only a simple resistor network rather than a complex (and probably slow) multiplication circuit, and it gives results sufficiently good for these experiments. Figure 3a shows a dE/dx spectrum observed at 36° from a liquid hydrogen target, using a 2" thick ΔR counter and 0. 2 cm of copper residual range. 3b shows the spectrum with enough ΔR signal added to give good peaks. In practice, different amounts of signal are added until the setting which gives the narrowest peaks is found. This setting is slightly different for protons than for pions.

For an actual counter telescope, the width of pion and proton peaks is always greater than indicated by the size of ΔR. Imperfect resolution in a scintillation counter is caused by non-uniform light collection, and by the statistical nature of energy loss in the scintillator and of electron multiplication in the phototube. The statistics of energy loss as a particle traverses matter have been considered by Symon (9). His results, as reproduced by Rossi (10), show that the distribution of energy loss depends only on β (the particle velocity relative to that of light) for the energies of interest here. The curves of figure 4 give distributions for various particle energies in 1 gram/cm^2 of counter material. For higher energy

($\beta \approx 1$) the curves are all similar to the 100 Mev pion curve. The distribution width is roughly proportional to counter thickness, although the "tail" of the curve becomes less pronounced for thicker counters.

It is this "tail" of large energy loss for pions that is the most harmful aspect of these distributions. It smears the pion peak up into the protons, making particle separation quite difficult. To avoid this trouble, most counter telescopes contain more than one dE/dx counter. The chance that a pion will make an extra large pulse in two successive counters is quite small. Two counters are also advisable for avoiding spurious counts from nuclear interactions. In the telescope of figure 1a, for example, a pion or neutron can interact in absorber A to produce a secondary proton; if this passes through the telescope it may be counted as a proton. Thus there should be a front dE/dx counter preceded by as little absorber as possible.

The statistical nature of energy loss leads to a fluctuation of particle range, commonly called "straggling." Symon's results (10) show that straggling gives an uncertainty in $\Delta R/R$ of one to three percent, for the energies of interest here; this causes a percent or less variation in dE/dx, and hence is negligible compared to the distribution widths of figure 4.

Multiple scattering for a particle going through the telescope also gives a range variation. Numerical integration of the usual scattering formula (10) through a range R (in copper absorber, for example) shows that pions travel, on the average, about 1.025 R.

Fluctuations from scattering therefore cause dE/dx variations which again are small compared to the widths of figure 4.

A large background of electrons is present near any target in the synchrotron beam. Electromagnetic interactions in a telescope can largely obscure pion and proton counts, particularly at foreward angles. A typical spectrum with this background is shown in figure 5a. To eliminate electron counts, a Cerenkov counter is often included in the telescope. This vetoes any event with a fast electron passing through. Such a counter can eliminate enough electrons to give th spectrum of figure 5b. Care must be taken to avoid losing proton counts through scintillation in the Cerenkov counter. If a lucite counter is used the UVT variety scintillates much less than the UVA, but even in UVT 100 Mev protons give at least 1/10 as much signal as do fast electrons (11). If the counter gain is set too high some protons will be missed, as shown by the dashed curve in 5b. A sensitive test for this consists of putting the Cerenkov counter in coincidence with the rest of the telescope, giving the dE/dx spectrum of figure 5c. Scintillation in the counter then causes a small proton peak (dashed curve). The Cerenkov gain should be lowered until this peak just disappears.

The procedures for setting an elaborate counter system into operation are complicated, and they vary according to the particles to be detected, the specific counter arrangement, and the types of electronic analyzing equipment. Some fairly general methods for proton or pion telescopes will be given here; extra techniques for K detection will be discussed throughout this thesis.

Photomultiplier voltages can be set roughly by observing signals from cobalt 60 or (for Cerenkov counters) from fast cosmic ray particles. Signals from either source should typically be a few volts, according to the electronic circuits which use the signals. Next, pulses to the various coincidence and gate circuits must be timed, usually with the synchrotron beam and a target as a source of counts. Timing is done roughly by observing the signals on a fast oscilloscope, but for accurate timing it is necessary to measure coincidence rates as various delays are inserted in the signal lines. Note that photomultiplier timing depends on tube voltage, and will change slightly if the tube gain is changed.

Once the signals are properly timed, the dE/dx pulse spectrum can be examined. There is no infallible method for obtaining good peaks. In one system, the phototube and amplifier gains of the ΔR and veto counters (2 and 3, figure 1a) are simply set to give equal, large signals from cobalt 60. This insures that a particle will not have to penetrate either counter very far to count; since scintillators show saturation effects the necessary penetration distance may be hard to calculate, but if it is equal for the two counters then ΔR can be accurately found from the absorber and counter thicknesses. The dE/dx counters should then show peaks, and unwanted protons or pions can be biased out.

A more sophisticated system for setting gain and bias can be used if proton counts are desired. This consists of first placing the ΔR and veto counters in coincidence, and lowering the latter's gain

until only protons stopping near its back surface are counted. These protons have longer range than those observed in normal operation; if the ΔR counter gain and bias are set just to accept them, few normal protons will be lost and there will be good discrimination against pions and electrons. The gain of the veto counter must then be raised, and the counter must be placed in anticoincidence as usual. The dE/dx counters should now show a good proton peak, and pions can be further biased out here. If pions are rejected well by the dE/dx counters, the veto counter can have a low gain and not be required to count pions at all. This reduces the telescope dead time, which is often controlled by the recovery time of the veto circuits.

With different gains in the ΔR and veto counters, one might question whether the range interval ΔR in which particles must stop is still given accurately by the thickness of absorber C and the ΔR counter. This interval can be measured by plotting the counting rate versus absorber C as the latter is varied, adjusting absorber B to keep the total range constant. Extrapolating the counting rate to zero shows the amount which must be added to C to give ΔR.

When recognizable pion and proton peaks are obtained, several harmful effects should be checked. Saturation of dE/dx counters or of their amplifiers may cause the peak separation to be less than expected. Insufficient magnetic shielding around phototubes will cause the peaks to drift, especially when the fields of nearby magnetic spectrometers are changed. If the radiation shielding around the telescope or near the target is inadequate or is improperly adjusted,

there will be background counts which will broaden the peaks and impair telescope resolution. The elimination of these effects is tedious, but it is a necessary requirement for successful telescope operation.

B. Counting Rate for Telescope

Consider the photons striking a small element of target dx dy dz, with the z-coordinate along the photon beam. The synchrotron beam contains N(k) dk photons per Bip (for Beam integrator pulse) with energy between k and k + dk. N(k) is given by $Q\,B(k)/k$, where B(k) respresents the deviation from a 1/k bremsstrahlung distribution and Q is the total energy per Bip divided by E_o, the upper limit of photon energy.

The beam is generally monitored by a thick-walled ion chamber of a type developed at Cornell. Q per Bip for this chamber can be obtained from the work of Gomez (12). These values must be corrected for the effects of temperature and pressure in the laboratory. B(k) has been measured by Donoho, Emery, and Walker (13) with a pair spectrometer. They tentatively find a thin-target bremsstrahlung spectrum, with $B(k) \approx 1.35 \left(1 - \frac{k}{E_o} + \frac{3k^2}{4E_o^2}\right)$ for $k < \frac{2}{3} E_o$, and $B(k) \approx 0.9$ for $\frac{2}{3} E_o < k < E_o$.

N(k) dk n(x, y) dx dy photons strike the target element, n(x, y) being the spatial density of the beam at the target. If there are N_t target nucleons per unit volume, the element contains N_t dz nucleons per unit area. Then the counting rate for particles emerging at the angle θ' (in the center of mass system, hereafter abbreviated cm) is

$$dC = N_T\, dz\ \sigma'\, d\Omega'\ N(k)\, dk\ \ \eta(x,y)\, dx\, dy$$

where $d\Omega'$ is the cm solid angle within which particles are counted, and σ' is the cm differential cross section for the production of the particles.

A counter telescope defines the energy and direction in the laboratory system of one particle. If there are only two particles in the final state of the reaction, this determines the kinematics of the entire process. Then the relation between cross section and counting rate can be expressed in terms of quantities fixed by the telescope:

$$dC = N_T\, dz\ \sigma' \frac{d\Omega'}{d\Omega}\ d\Omega\ N(k) \frac{dk}{dT}\, dT\ \eta(x,y)\, dx\, dy$$

where $\frac{d\Omega'}{d\Omega}$ is the solid angle transformation from c. m. to laboratory at constant k

$d\Omega$ is a laboratory solid angle element

$\frac{dk}{dT}$ gives the change of photon energy with particle energy at constant angle

dT is an element of particle energy accepted by the telescope.

The counting rate is therefore given by a six-fold integral:

$$C = N_T \int \sigma' \frac{d\Omega'}{d\Omega}\ N(k) \frac{dk}{dT}\ \eta(x,y)\, dx\, dy\, dz\, d\Omega\, dT$$

The purpose of a telescope experiment is to determine an average cross section,

$$\overline{\sigma'} = C \Big/ N_T \int \frac{d\Omega'}{d\Omega}\ N(k) \frac{dk}{dT}\ \eta(x,y)\, dx\, dy dz\ d\Omega\ dT$$

The six-fold integral now depends only on experimental parameters and relativistic kinematic relations, and may be evaluated. The limits of x, y, and z are fixed by the target size and beam size; the limits of Ω and of T are given by the angular and energy acceptance of the telescope. A program has been made for the Datatron automatic digital computer to calculate the integral for a general telescope and for any two-body reaction. The experiments reported in this thesis were of an exploratory nature, however, and an approximate evaluation is accurate enough for their discussion.

If the finite size of the target is not important, the integration over x, y, and z gives $\int n(x, y)dx\, dy\, dz = \overline{\ell}$, the effective target length. Furthermore, if $N(k)\, d\Omega'/d\Omega dk/dT$ does not vary greatly within the limits of integration an average value may be used. Then approximately

$$\overline{\sigma'} \approx c \Big/ N_T \overline{\ell}\, \frac{Q B(K)}{k}\, \frac{d\Omega'}{d\Omega}\, \frac{dk}{dT}\, \Delta\Omega\, \Delta T \qquad (1)$$

where $\Delta\Omega$ and ΔT are the angular and energy intervals accepted by the telescope. This formula was used to analyze the counting rates of the experiments reported here.

C. Comparison of Telescope and Spectrometer

Many high energy reactions can be studied either with a counter telescope or with a magnetic spectrometer. At this laboratory both

techniques have been used to study π^o photoproduction (11, 14) and π^+ photoproduction (15, 16). A spectrometer experiment on K mesons has been carried out; the experiments of this thesis were attempts at similar work with telescopes. This section discusses the relative merits of the two systems.

Counter telescopes of almost arbitrary size can be built. With not unreasonably large counters it is possible to obtain a considerably greater solid angle than is convenient with magnetic spectrometers. The telescopes for K detection typically subtended about 0.04 steradians; this compares with 0.007 steradians for the K spectrometer. A large solid angle is naturally of great advantage in low yield experiments, but it has the disadvantage of giving high counting rates in the individual counters. To bring the rate of accidental coincidences down to a level comparable to that with spectrometers, considerably faster electronic analyzing equipment must be used. The basic telescope coincidence circuit used for much of the K work had a resolving time of 30 mμ sec, compared to 0.1 or 0.2 μsec for the K spectrometer circuits. Pulse height analysis on a fast time-scale requires fast gate circuits, amplifiers, and oscilloscopes that are not needed in most magnetic spectrometer work.

While counter telescopes often have a large angular acceptance, their energy acceptance can become quite small for high-energy particles. Consider for example a telescope containing a two inch stopping counter. This counter by itself would stop 62 Mev K mesons. In a typical experiment one might place enough absorber in front of

the counter to study 100 Mev K mesons. The energies accepted would then be between 88 and 113 Mev - a 25 Mev interval. For 200 Mev K mesons the interval is 18 Mev; for 300 Mev it is 12 Mev. In contrast, a magnetic spectrometer maintains $\Delta P/P$ constant for various momenta. If $\Delta P/P$ is 0.1, as is typical, the acceptance intervals for 100, 200, and 300 Mev K's are 18, 35, and 49 Mev. This serves, in some measure, to make up for the smaller solid angle of spectrometers.

The most serious disadvantages of counter telescopes are caused by the necessity for stopping the particles being studied. The amount of absorber required quickly becomes excessive. For example, stopping a 400 Mev pion requires 27 cm of copper absorber. The momentum of this pion is 522 Mev/c; it could easily be analyzed with the medium-energy spectrometer at this laboratory. The trouble with using such thick absorbers is that nuclear absorption and scattering take place. About 90 $^{o}/_{o}$ of the pions entering 27 cm of copper are absorbed, assuming geometrical cross sections. Absorption and scattering not only drastically reduce the counting rate but also make the experimental results uncertain, since it is difficult to correct accurately for these effects. It is this consideration that limits the use of telescopes to energies below about 300 Mev for pions and 500 Mev for protons. Worlock (11) discusses proton absorption in detail; for pions, a mean free path of 12.1 cm in copper absorber has generally been assumed.

Counter telescopes are considerably smaller and more easily handled than are magnetic spectrometers. Their small dimensions are a great advantage in the study of short-lived particles. The magnet used in a recent K experiment had a path length of 165 inches, in which typically 75 °/o of the mesons decayed before being counted. A telescope might have a path length of 16 inches, in which only about 10 °/o would decay.

Minor advantages of telescopes include their low cost (compared to large magnets) and their lack of pole-tip surfaces to cause scattering problems.

D. Experimental Layout

Figure 6 shows the experimental area of the synchrotron. Once each second electrons are accelerated inside the synchrotron and are then allowed to strike a tantalum radiator. The resulting photon beam lasts for about 20 milliseconds and leaves the machine through a lead collimator. The beam then passes through various targets, sweeping fields, and lead scrapers. The first experiment reported here was done at the front table (location A, figure 6) using a polyethylene target. The subsequent experiments used the liquid hydrogen target (location B). The photon beam finally hits an ionization chamber which monitors the intensity of the beam, and is then stopped in a lead "beam catcher."

It is particularly important in counter telescope experiments to provide shielding from particles produced elsewhere than in the

Figure 6

Experimental Area of Synchrotron Laboratory

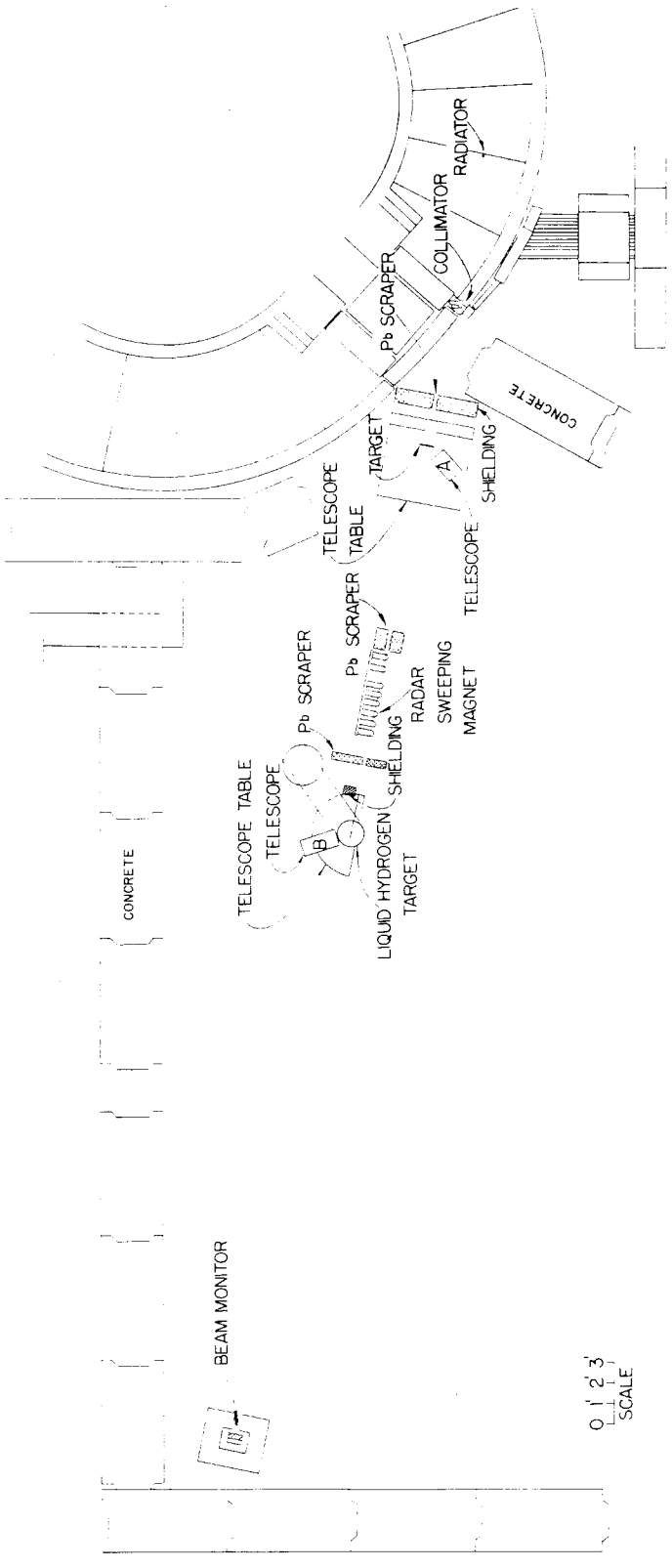
RADIATOR
COLLIMATOR
Pb SCRAPER
CONCRETE
TARGET
SHIELDING
TELESCOPE
TELESCOPE TABLE
A
Pb SCRAPER
RADAR
SWEEPING
MAGNET
Pb SCRAPER
SHIELDING
TELESCOPE TABLE
TELESCOPE
B
LIQUID HYDROGEN
TARGET
CONCRETE
BEAM MONITOR
0 1' 2' 3'
SCALE

target. The elaborate series of scrapers and sweeping magnets shown in figure 6 gave a clean, well defined beam, no part of which struck the metal fittings of the targets. It was further found necessary to prevent the telescope counters from seeing directly the lead scraper hole located in front of the target; lead shielding was provided to accomplish this. At least two inches of lead were also placed along the sides of the counter telescopes to reduce the background still further.

III. SCINTILLATION TELESCOPE EXPERIMENT

A. Introduction

This telescope experiment was designed to test whether or not K mesons are produced in photon reactions. A simple four-counter telescope was set up in the hope that a K meson pulse height peak would be found. It quickly became clear that the K cross section was quite low; proton and pion peaks obscured whatever K's might have been present. Further identification was needed, and was obtained by requiring the particles to stop in a thick scintillator which then gave delayed pulses from K decay. Signals from the counter were photographed and analyzed in detail. A number of delayed pulses indicated that K mesons were indeed produced by photons, and gave an approximate figure for their yield from a CH_2 target. The height of the delayed pulse provided information about the decay mode. The proportion of τ decays relative to K_L decays (K's giving a single charged decay product) agreed with that found elsewhere. The measured lifetime also agreed with the accepted value.

Considerable uncertainty in the K meson yield resulted from the difficulty of distinguishing true decay pulses on the necessarily fast time scale. Certain afterpulses and reflections of the decay signal made the tedious film analysis somewhat subjective. Because of these drawbacks this experiment was finally abandoned in favor of different techniques.

This work has been reported in a letter to the Physical Review (17).

B. Equipment

Since a liquid hydrogen target was not yet available, this experiment used a polyethylene target 0.325 inches thick. Figure 7 is a diagram of the telescope arrangement. The sizes of the counters and absorbers were as follows:

Counter 1:	3 1/4" x 2 3/16" x 0.512"	Liquid counter
Counter 2:	3 1/4" x 2" x 0.490"	Plastic counter
Counter 3:	3 1/4" x 2 1/4" x 0.875"	Liquid counter
Counter 4:	4" x 3" x 0.250"	Plastic counter

Absorber A: 9/16" copper plus 3/4" aluminum

Absorber B: 1/16" copper plus 3/4" aluminum

Absorber C: 1/4" copper

The plastic counters were made from a polystyrene-base scintillator obtained from the University of California Radiation Laboratory at Livermore. The liquid counters were boxes with 1/16" lucite walls, filled with a solution of 3 grams p-terphenyl scintillator and, for the first part of the experiment, 10 milligrams diphenylhexatriene shifter per liter of phenylcyclohexane. Each counter was wrapped in 0.0008" and 0.005" aluminum foil and was viewed by an RCA type 6655 photomultiplier tube.

Particles were required to give pulses in counters 1, 2, and 3, but no pulse in 4. Absorbers B and C were chosen to give good peak separation, while absorber A was chosen so that the telescope accepted K's between 136 and 145 Mev. The solid angle subtended by the

Figure 7

Top View of Scintillation Counter Telescope

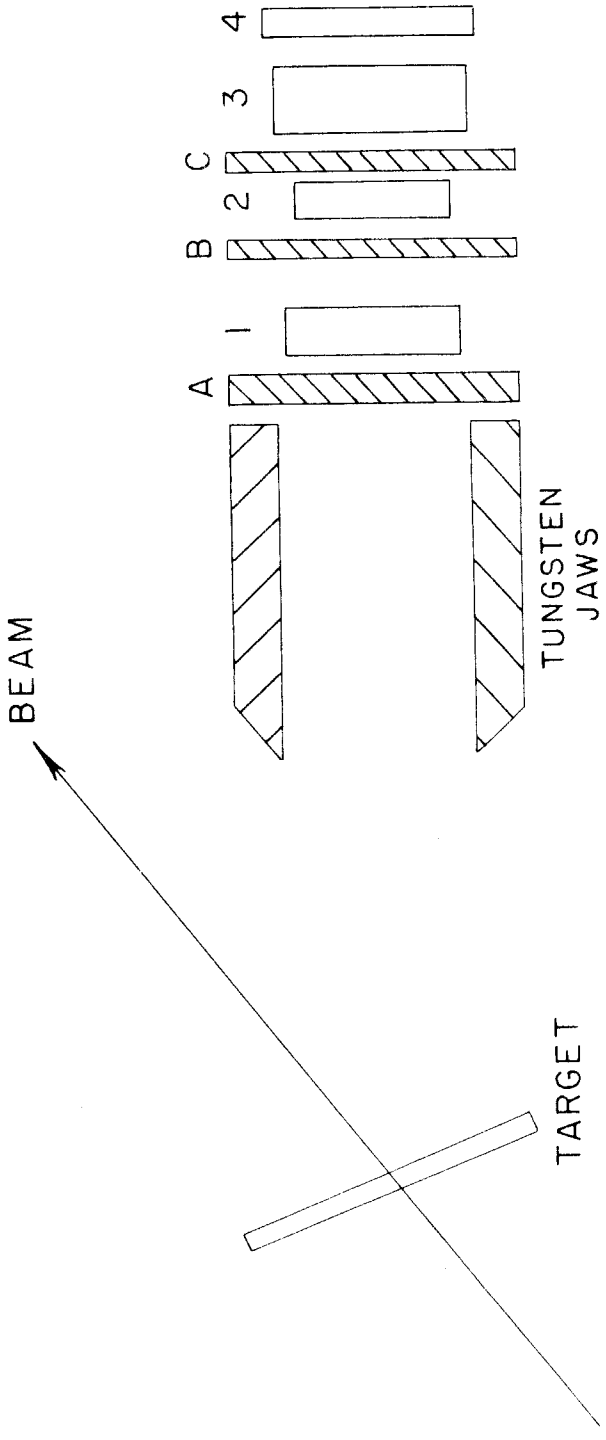
4
3
C
2
B
1
A
TUNGSTEN
JAWS
BEAM
TARGET

telescope was 0.04 steradians; the angular acceptance was 10 degrees.

Figure 8 shows the electronic system used. Negative signals from all four counters were inverted in the bias diode circuit, which could also discriminate against very small pulses. The signals were amplified and then entered a bias discriminator circuit, which produced standard pulses if the signals exceeded a preset level. The discriminator pulses passed to a coincidence-anticoincidence circuit; counters 1 and 2 each drove two discriminator channels so that upper and lower limits could be set to give a pulse height window. When an appropriate coincidence took place the coincidence circuit gated a 20 channel pulse-height analyzer to accept a signal from counter 1 or counter 2. The analyzer thus displayed as much of the pulse spectrum as was passed by the windows on the dE/dx counters.

A Tektronix type 517 oscilloscope was used to look for K meson decays. Fast pulses from the ΔR counter were clipped, amplified with Hewlett-Packard distributed amplifiers, and then delayed for about 400 mμsec with RG/63 cable to allow time for the coincidence circuit to initiate the sweep. The delay cable was connected directly to the oscilloscope deflection plates, giving a pulse about 8 mμsec wide which was displayed near the start of a 160 mμsec sweep. The sweeps were photographed on 16 mm Tri-X film with an f/0.95 lens. Frequent calibrations of the oscilloscope sweep speed were made with a 50 megacycle oscillator and frequency meter.

Figure 8

Electronic System for Scintillation Telescope Experiment

The following electronic symbols are used throughout this thesis:

A	Amplifier, Model 552; Maximum Gain 2500; Rise Time 70 mμsec
BD	Bias Diode Circuit, Model 1
GDC	Gated 6-channel Discriminator, Model 1, and 6-channel Coincidence-anticoincidence circuit; Resolution Time 0.2 μsec
H	Hewlett-Packard Distributed Amplifier, Model 460 A or 460 B; Maximum Gain 20 db or 15 db; Rise Time 2.6 mμsec
KS	20 Channel Pulse Height Analyzer ("Kicksorter")
O	Oscilloscope, Tektronix Model 517
S	Scaler, Model 2

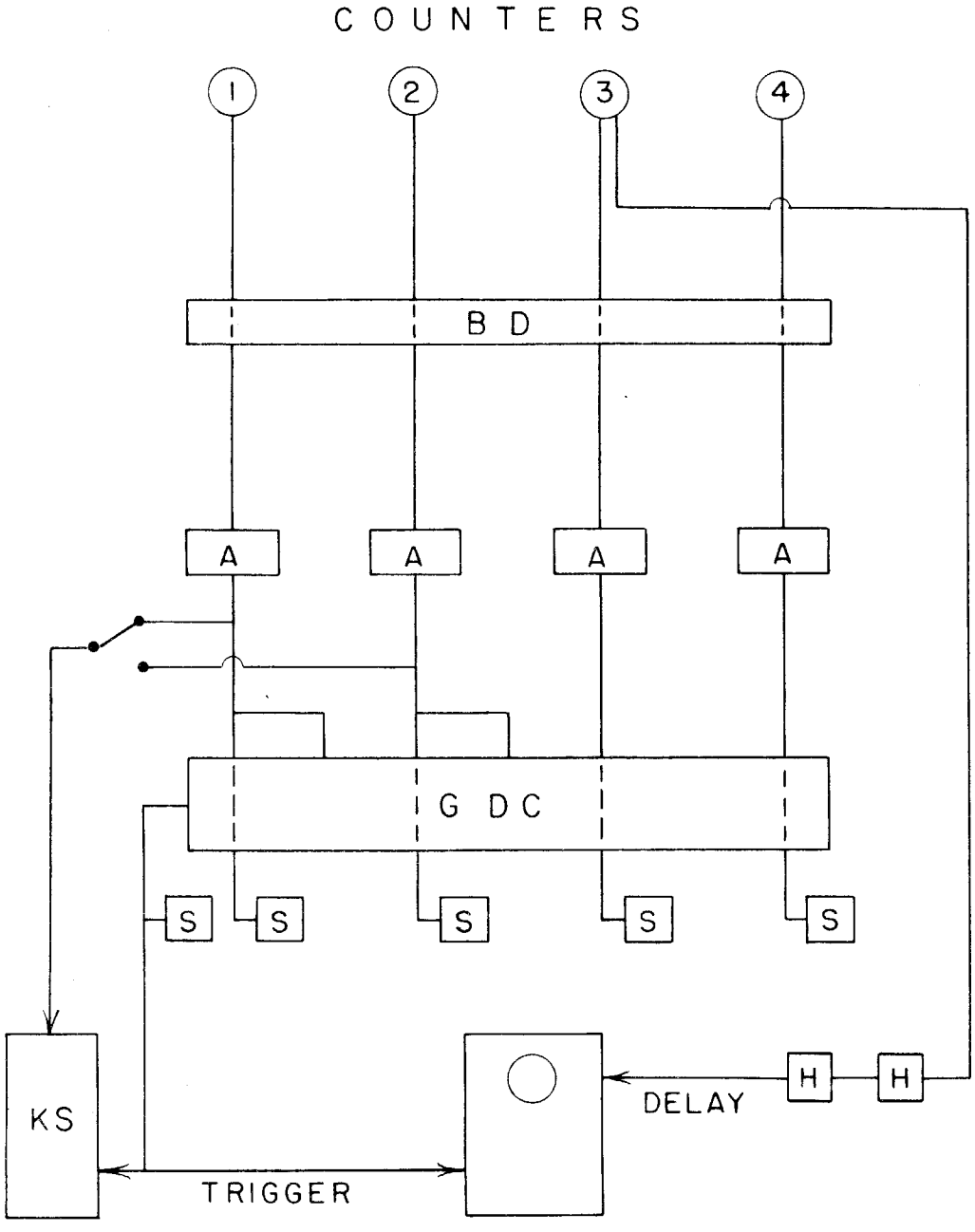
COUNTERS
1
2
3
4
B D
A
A
A
A
G DC
S
S
S
S
S
KS
TRIGGER
DELAY
H
H

C. Results

Preliminary runs, showing that no K meson peak was distinguishable on the analyzer, indicated that the production cross section was less than 10^{-30} cm^2/steradian. K meson runs from the CH_2 target were taken with the telescope set at $37\frac{1}{2}$ degrees, using the equipment for detecting decay pulses. A number of pion runs also were taken at 90^o from an aluminum target, with the dE/dx windows set to accept pions. Occasionally a carbon target was used, but the data were not nearly accurate enough for a CH_2-C subtraction to be made. Most runs were made with a maximum photon energy of 1100 Mev; a few backgrounds were taken at 800 Mev.

Figure 9 shows oscilloscope traces for various types of event. 9a is simply the pulse from a particle stopping in counter 3, followed by some wiggles and afterpulses. These wiggles, presumably due to small reflections and ringing excited by the fast signals, were always present to some degree and often made film scanning quite subjective. Parts b, c, and d of figure 9 show pion decay, K_L decay, and τ decay respectively.

The pion runs indicated that the experiment could indeed identify particles by lifetime. The films showed frequent double pulses from the ΔR counter, with the second pulse fairly constant in size, corresponding to the 4. 2 Mev energy of the muon from pion decay (as in figure 9b). The pulse separations were consistent with a single lifetime. Figure 10 is an "integral lifetime" plot of all the suitable pion runs. The points give a lifetime of 23.5 ± 1.7 mμ sec

Figure 9

Oscilloscope Traces from ΔR Counter

Sweep speed is 20 mμsec/cm

a Particle stopping in counter, followed by wiggles.

b Pion stopping and decaying:
second pulse: 4.2 Mev

c K stopping and decaying:
second pulse: 16 Mev

d stopping and decaying:
second pulse: 60 Mev

A

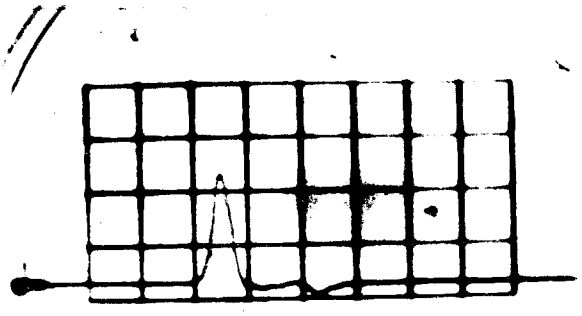

B

C

D

Figures 10 and 11

Integral Lifetime Plots for Pions and K Mesons

Vertical scale is total number of counts with life $\geq$ value on horizontal scale.

Lines show measured lifetimes.

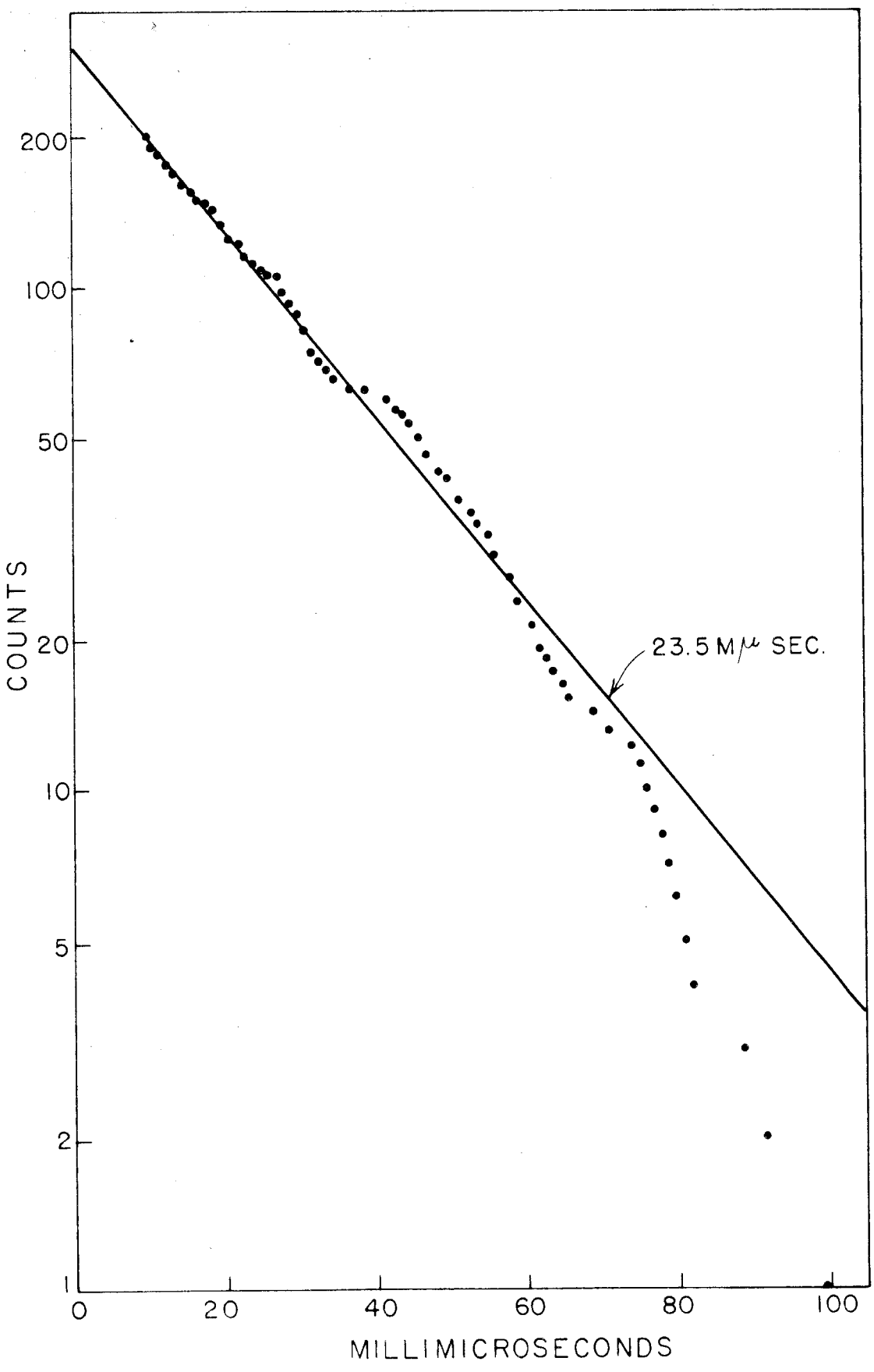
200
100
50
20
10
5
2
1
COUNTS
23.5 Mμ SEC.
0
20
40
60
80
100
MILLIMICROSECONDS

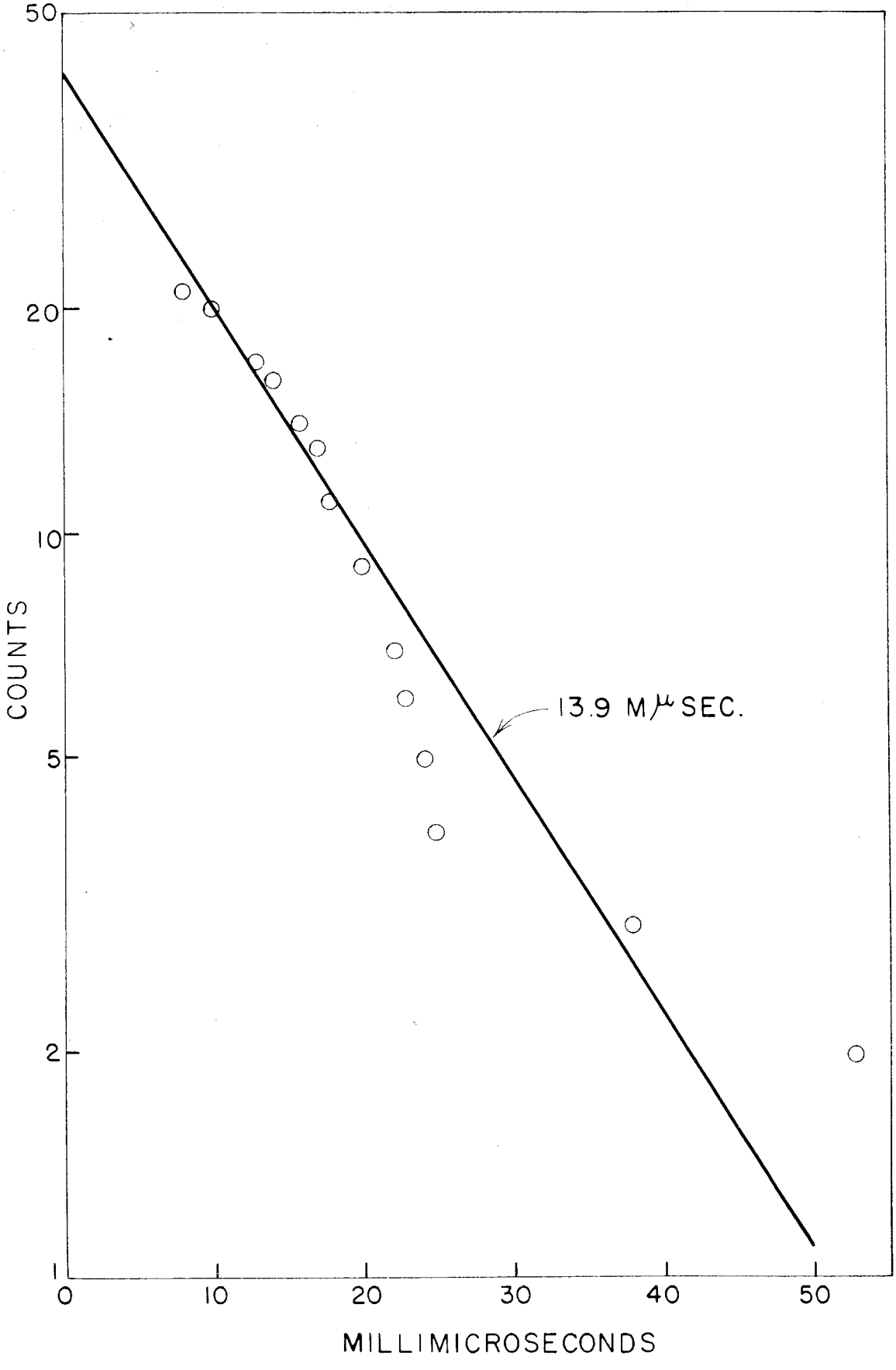
50
20
10
5
2
1
COUNTS
13.9 MμSEC.
0
10
20
30
40
50
MILLIMICROSECONDS

as calculated by the arithmetic mean method of Peierls (18).

Next it was important to determine whether K mesons could really be observed. Films from about 7000 Bips of running yielded 21 double pulse events with the second pulse several times larger than that from pion decay. Figure 9c shows such a K meson event. Figure 11 is an integral lifetime plot for these events; the life is 13.9 ± 3.0 mμsec, which compares well with the accepted K lifetime of 12.4 mμsec (19). Twelve of the events included second pulses too large to be caused by single charged decay products, as in figure 9d. These counts presumably showed the τ decay mode. The lifetime for them was 12.9 ± 3.7 mμ sec. At the time of this experiment only one other τ lifetime measurement had been made; it gave 11.7 mμ sec (20). The equality of the τ and K_L lifetimes was interesting in connection with the question of parity conservation.

Once an identification of K mesons was established, a quantitative measure of their yield was attempted. Films from CH_2 target runs at $37\frac{1}{2}^{o}$ were closely scanned for double pulses. Traces from 3531 Bips were relatively free of the wiggles and afterpulses mentioned above, and gave 78 double pulses. An integral lifetime plot of these pulses was graphically resolved into K meson and pion components. This analysis indicated that 40 K's were seen with a contamination of 14 pions as well as 24 spurious counts with small separation due to the afterpulses. Pulses closer than 10 mμ sec were not clearly resolvable, but extrapolation to zero time gave a total of 89 K mesons. Of the 40 mesons seen, 6 showed the τ decay

mode. Subtracting the τ's leaves 76 K_L's, or K mesons having a single charged decay product.

The pulse height spectrum of the primary signals from particles decaying in the ΔR counter gave further confidence that all double pulses were not caused by pions. The distribution was roughly rectangular and extended to an upper limit about twice that for the pion runs, corresponding to the fact that a stopping K can lose up to twice the energy in ΔR as can a pion.

The efficiency for seeing K_L decays was found from a Monte Carlo calculation on the Datatron automatic digital computer. This calculation gave the range distribution in the ΔR counter of secondaries from K mesons stopping at random positions and decaying in random directions, including the fact that some secondaries pass through the veto counter and veto the entire event or through the dE/dx counters and raise the pulse height above the acceptance window. This range distribution gave a secondary pulse height distribution; the observed pulse heights followed this distribution within the limitation of poor statistics. An efficiency of 31 $^{o}/o$ resulted from requiring a secondary pulse large enough to eliminate most pion decays and spurious signals. Figure 12 shows the calculated distribution. Note that many K counts were lost because small pulses had to be eliminated.

The efficiency for distinguishing τ decays was estimated at 50 $^{o}/o$, which would indicate that the observed ratio of τ to K_L decay modes is about 5 $^{o}/o$. The ratio measured from K's produced in

Figure 12

Distribution of Energy Loss in ΔR Counter for K Decay Particles.

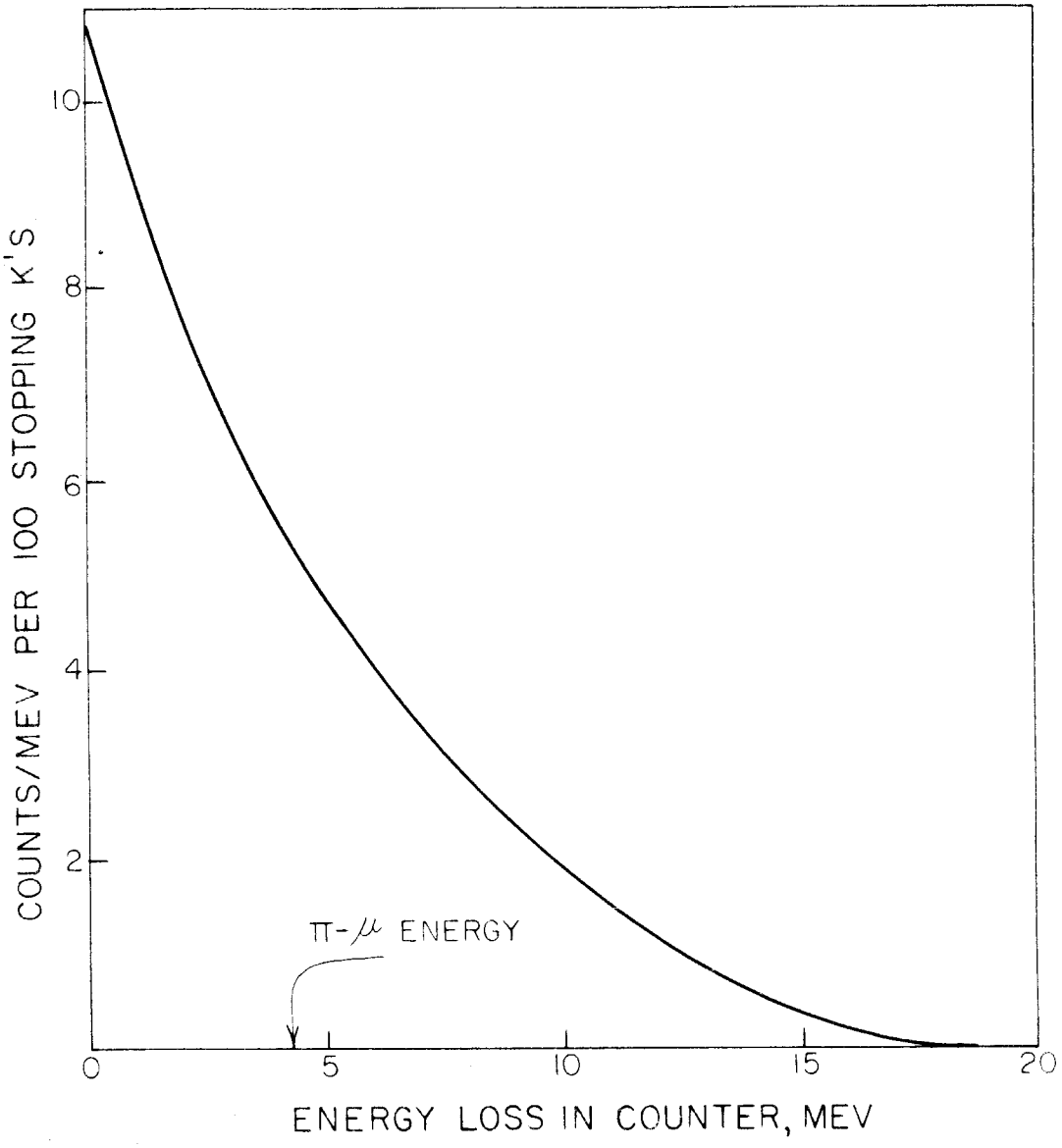
COUNTS/MEV PER 100 STOPPING K'S
10
8
6
4
2
π-μ ENERGY
0
5
10
15
20
ENERGY LOSS IN COUNTER, MEV

nucleon-nucleon collisions has been reported as 6.0 °/o (21) and 7.4 °/o (22). Until quite recently, the present experiment was the only one to observe τ's from photoproduction. Peterson (23) has now seen one in photographic emulsion exposed at this laboratory.

Several corrections are required for the number of K_L mesons. The camera could photograph only one sweep per machine pulse, while there were occasionally two or three counts per pulse. Overall there were 79.8 °/o as many photographs as counts. A correction of 20 °/o is required for nuclear absorption of K mesons in the telescope. This corresponds to an interaction cross section of 10 millibarns per nucleon, as reported by groups studying K mesons in nuclear emulsion (24). The proportion of K's having the K_L decay modes was taken as 91 °/o (22). Decay in flight, so that no K was counted, gave a 10 °/o loss. If the mesons result from the reaction

$$\gamma + P \longrightarrow K^+ + \Lambda^\circ$$

and if all the protons in polyethylene are assumed to be free, the kinematics of the reaction are fixed. For this experiment the photon energy is 1057 Mev and the center of mass K angle is 100 degrees. Equation 1 then provides a value for the cm cross section of 2.7×10^{-31} cm^2/steradian.

The probable error associated with this figure is difficult to determine. From statistics alone the observed K counts have a probable error of 16 °/o. The calculated efficiency for seeing K_L events may be in error by 20 °/o because of the subjective film

analysis. No effort was made to correct for the fact that most of the protons in CH_2 are not free. The single counting rate in the ΔR counter was low enough for accidental second pulses to be negligible; the sweep lasted 160 mμsec and virtually all of the second pulses were within 60 mμsec of the first pulse. The data were actually taken during two separate series of runs. These runs analyzed independently gave cross section values of 3.5 and 1.8×10^{-31} cm^2/steradian. In view of all these considerations, the cross section from this experiment was taken to be $(2.7 \pm 0.9) \times 10^{-31}$ cm^2/steradian, per proton of the CH_2 target.

It is perhaps meaningless to compare this value from a target of complex nuclei with the results of Donoho and Walker (1) from a hydrogen target. However, interpolation between their 1060 Mev results gives a cross section of $(1.62 \pm 0.34) \times 10^{-31}$ cm^2/steradian, so that there is no large disagreement in numerical values.

Had it not been for the low counting rate and tedious film analysis, this experiment would have been shifted to the liquid hydrogen target where yields are more significant. The use of larger counters and improved electronics (such as a modern traveling-wave oscilloscope for pulse display) might have given a successful experiment, providing information about the K lifetime and decay modes as well as the cross section. However, as later experiments show, background problems at the hydrogen target are so severe that even improved techniques fail to give clear separation of K mesons.

IV. CERENKOV TELESCOPE EXPERIMENT

A. Introduction

One great disadvantage of the preceding experiment was the fact that every particle stopping in ΔR and having the correct dE/dx pulse height was recorded. This gave thousands of photographs, only a few of which showed double pulses. The principal innovation in the second telescope experiment was the use of a thick Cerenkov counter to stop the K mesons. This was supposed to give no signal from the incoming mesons but only from their fast decay products, thus discriminating against all events without decay. The counter was made quite thick—10 cm of water—so that the energy acceptance and counting rate were $4\frac{1}{2}$ times as large as for the previous experiment.

Unfortunately, there were large numbers of both prompt and random Cerenkov counts which almost completely obscured any delayed counts from K decay. The use of a large stopping counter which was most sensitive to the fast electrons present in great numbers around the synchrotron beam led to unreliable and unreproducible results, particularly since no fast coincidence between the counter and the rest of the telescope could be required. Another "tag" on the K's was provided by detecting the decay particles in a separate counter located beside the stopping counter. This system identified K's fairly well and gave a figure for their yield, but it reduced the counting rate most drastically.

By the time these conclusions were reached, Donoho and Walker had investigated K's of medium energy and the interest had

shifted to lower energies. The Cerenkov experiment was not well suited to low K energy, and, in view of the difficulties just mentioned, was discontinued.

B. Equipment

The Cerenkov stopping counter was a lucite box 14 cm x 9 cm x 10 cm in size, filled with water and viewed by an RCA type 6810 photomultiplier. The inside surfaces of the box were painted white to minimize the effect of scintillation in the lucite and to give good light reflection. The production of Cerenkov light in water requires an energy of at least 73, 253, or 458 Mev respectively for pion, K meson, or proton. Incoming particles of these energies had residual range much greater than 10 cm of water, and so would trigger the telescope veto counter. The charged mesons from $K_{\mu 2}$ or $K_{\pi 2}$ decay, however, have energies of 152 and 109 Mev, enough to cause a slightly delayed Cerenkov pulse. Such a Cerenkov stopping counter was used by Fitch and Motley (25) to identify and to time K decays.

Figure 13 shows the telescope configuration adopted in this work. The telescope was set up to look at particles from the liquid hydrogen target which had recently become available. Counters 1 and 2 were the dE/dx scintillators of the previous experiment. 4 was the stopping counter, and 5 was a large veto counter; it was a lucite box $4\frac{1}{2}'' \times 6\frac{1}{2}'' \times \frac{1}{2}''$ with 1/16" lucite walls filled with scintillator liquid and viewed by a 6810 phototube. The need to guard against spurious counts from electrons led to the inclusion of a veto Cerenkov counter 3.

Figure 13

Top View of Cerenkov Counter Telescope

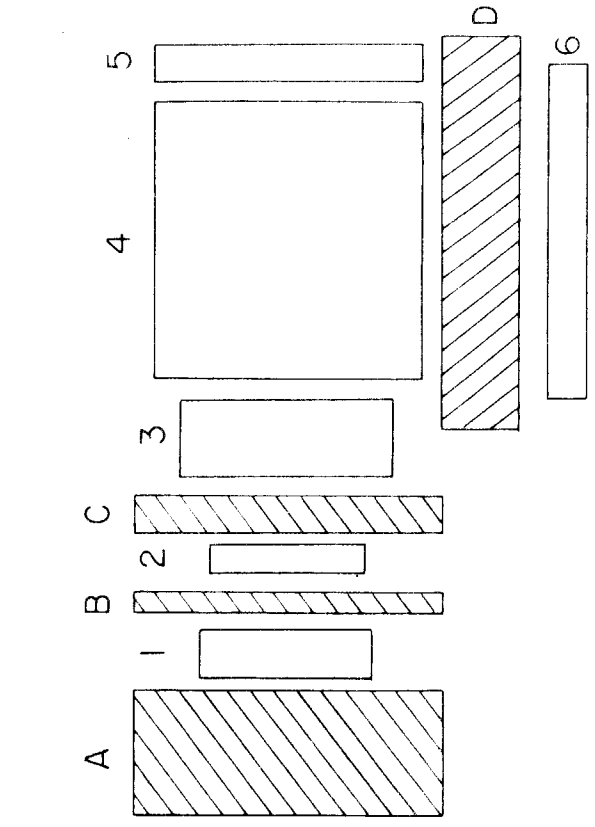
A
B
C
D
1
2
3
4
5
6

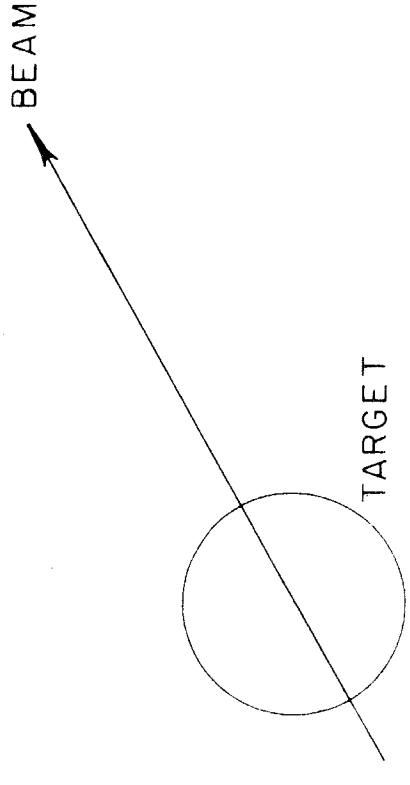
BEAM
TARGET

This was a water-filled box with 1/16" lucite walls, 2 3/4" x 3 3/4" x 1 3/4" in size with a 6810 tube. This counter reduced the background counting rate by about a factor of two.

A final effort to identify K's involved the use of counter 6 to look for decay products emerging from the stopping counter. This side counter was the same size as the veto counter 5. The counting rate was reduced to a level only about ten times the expected K rate by this counter.

The absorbers most often used were

A 1 1/2" polyethylene

B 3/8" copper

C 7/16" aluminum

while an absorber D of about 1 inch of copper or lead was used with the side counter 6. These counters and absorbers constituted a telescope which accepted K mesons between 120 and 164 Mev and subtended a solid angle of 0.04 steradian. It was set at angles of $37\frac{1}{2}$, 34, and 30 degrees during the course of the experiment.

Figure 14 shows the electronic system used with this telescope. Because it was feared that accidental coincidences might lead to false counts, fast Garwin-type coincidence circuits (26) were placed between counters 1 and 2 and between 2 and the veto Cerenkov counter 3. The Garwin outputs were amplified and sent to coincidence and veto channels respectively on the slow discriminator-coincidence system. Counters 4 and 5 also went to coincidence and veto channels. The resolving time of the slow circuit (0.2 μsec) was long enough to

Figure 14

Electronic System for Cerenkov Telescope Experiment

The following electronic symbol is used, in addition to the symbols of figure 8:

G Garwin-type Coincidence Circuit, Model 210; Resolution Time 30 mμsec

50

COUNTERS

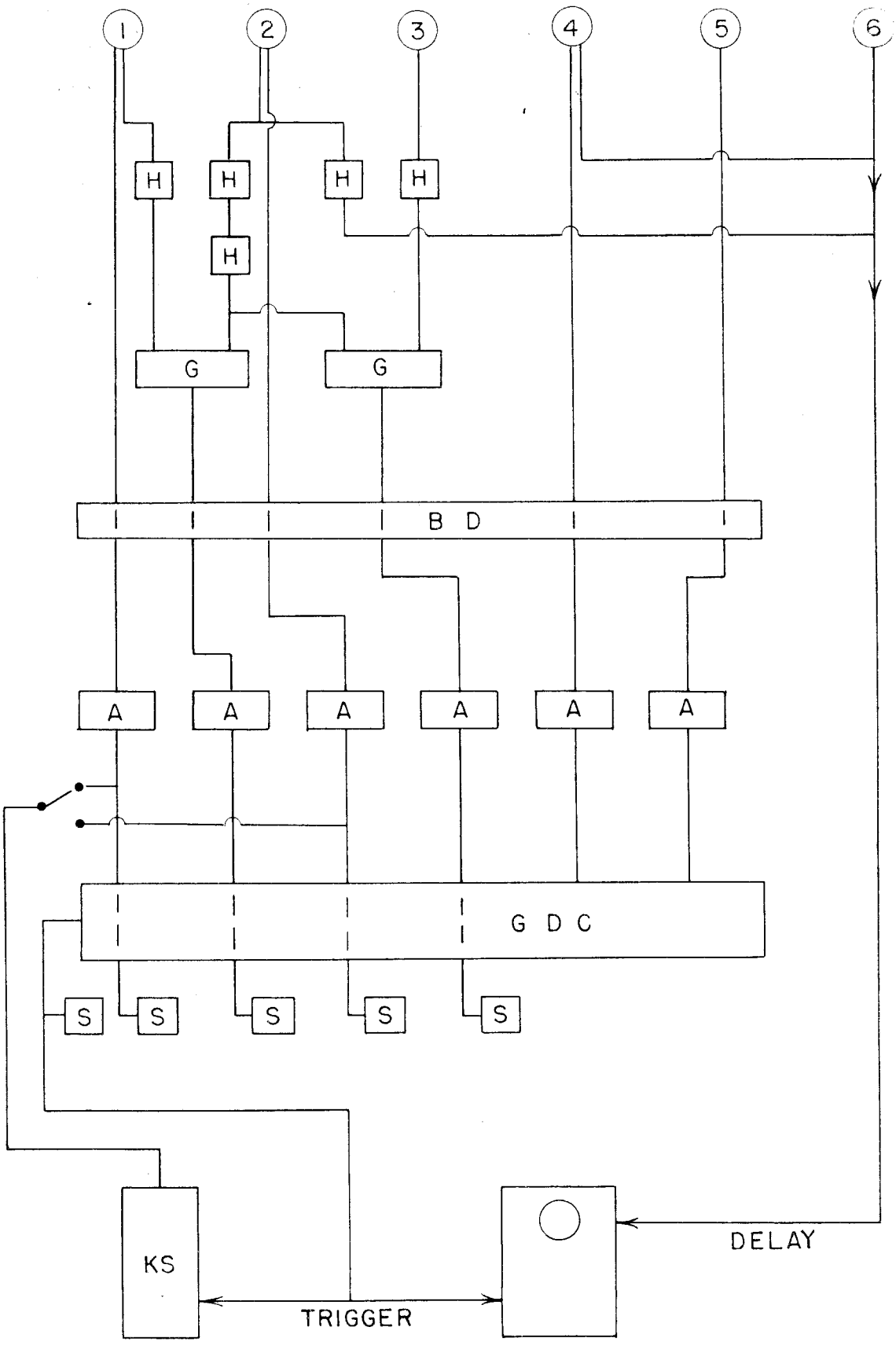

accept a delayed decay count from counter 4, so that an output signal from it indicated a particle stopping and decaying in this counter. This signal gated the 20 channel analyzer to accept a pulse from either dE/dx counter, and also initiated a fast oscilloscope sweep. Displayed on the oscilloscope were the counter 4 pulse, a pulse from counter 2 (to give a time reference, since entering K particles gave no signal in 4), and the pulse from the side counter 6 on the occasions when that counter was used. The large ΔR in this experiment prevented pions and protons from showing separate dE/dx peaks. Therefore no pulse height windows were set in counters 1 and 2, although a lower bias eliminated some pions.

C. Results

Quantitative results from this experiment required a knowledge of the Cerenkov counter efficiency, which was estimated as follows. Cosmic ray μ mesons, identified by their minimum dE/dx in a scintillation counter, showed what pulse height a very fast particle made passing through the 10 cm Cerenkov counter. These signals were corrected for the lower velocity of the $K_{\mu 2}$ and $K_{\pi 2}$ decay mesons, using the fact that Cerenkov light emission varies as $(1 - 1/\beta^2 n^2)$ where β is the relative particle velocity and n the index of refraction for the counter material. A minimum pulse height requirement was empirically set to reject most spurious pulses. To exceed this bias a muon from $K_{\mu 2}$ decay had to pass through 5 cm of water, while a pion from $K_{\pi 2}$ had to pass through 9 cm. It should be mentioned that this

bias corresponded to signals from only about four electrons at the photocathode, so there were large statistical variations in pulse amplitude and shape. Once the required range for decay products was known, the Datatron calculation used earlier showed that $K_{\mu 2}$'s were seen with 43 °/o efficiency, while $K_{\pi 2}$'s were seen with 10 °/o efficiency. The overall efficiency for K mesons was 27 °/o, assuming the usual distribution of decay modes. This figure indicates that the telescope should have registered about 9 K counts per hundred Bips for a reasonable cross section of 1.7×10^{-31} cm^2/steradian.

The most conspicuous feature of the experiment was that its counting rate was much higher than this. The great majority of counts showed prompt coincidences (within the few millimicrosecond resolving time of the oscilloscope trace) between the Cerenkov and dE/dx counters. Since the Cerenkov signal released only a few electrons from the phototube cathode there were considerable statistical variations in pulse shape, making the separation of delayed from prompt counts somewhat indefinite. Probable causes of the prompt Cerenkov signals were interactions in the counter which produced secondaries fast enough to give light, and fast particles which entered the counter but scattered or otherwise missed the veto counter. Other less likely causes were scintillation in the lucite counter walls, and proton or pion bremsstrahlung in the water.

The situation was further complicated by the presence of a considerable background of randomly timed Cerenkov pulses, presumably due to electrons striking the counter. An excess of very late

Cerenkov pulses indicated that some of the counts were caused by fast electrons from $\pi - \mu - e$ decay. Subtracting the estimated background left a lifetime plot which appeared to have a component with the K meson life, as shown in figure 15a. This type of result was not reproducible, however, and it should be noted that the sum of a uniform background and a prompt peak can give a curve showing the same features. This is illustrated in figure 15b.

The side counter 6 was installed as a final attempt to overcome the background problems of this telescope. The efficiency of the system was estimated as follows. In the first place, glycerol replaced water in counter 4; because of the large index of refraction, mesons from $K_{\mu 2}$ and $K_{\pi 2}$ decay had to pass through only 3.6 and 4.9 cm of glycerol respectively to be counted. A Cerenkov efficiency of 100 °/o was taken for decays this far or farther from the side counter, and 0 °/o for closer decays. This efficiency was then multiplied by the solid angle subtended by the side counter at the center of this "active volume," which was 11 °/o of a sphere for $K_{\mu 2}$'s and 10 °/o for $K_{\pi 2}$'s. The overall efficiency for seeing K mesons was then 4.7 °/o. Had the data warranted more accuracy, a Datatron efficiency calculation would have been made as for the next experiment.

The results of 475 Bips of running gave 15 events with delayed side counter-Cerenkov counter coincidences. The delays were consistent with the K lifetime. Together with the above figure for counter efficiency and the usual corrections for absorption and decay in flight, this indicates a cross section of 3.4×10^{-31} cm^2/steradian,

Figure 15

a Integral Lifetime Plot for Cerenkov Pulses
Line shows known K lifetime.

b Similar Curve Generated by Adding Uniform Background to Prompt Peak

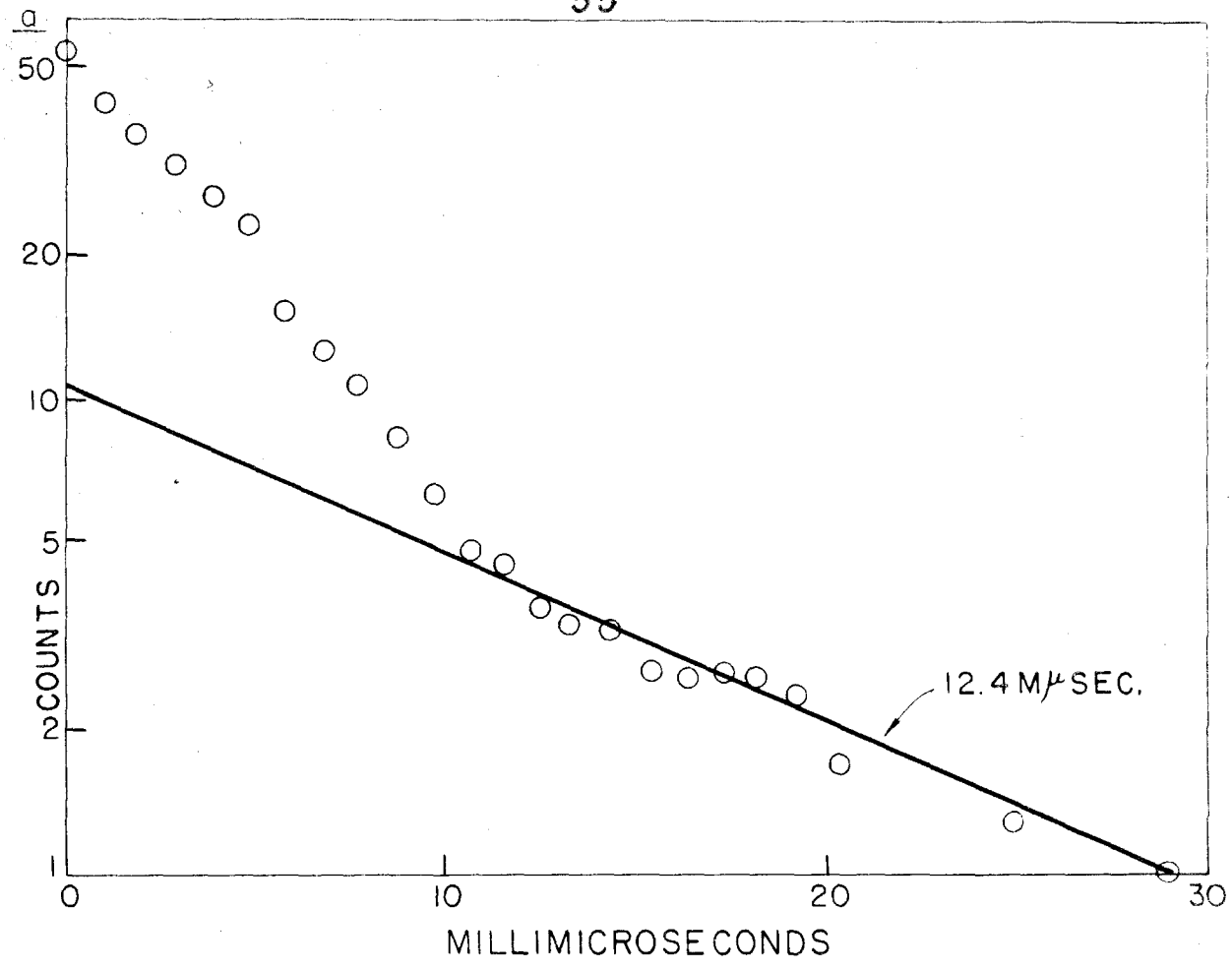
a
50
20
10
5
2
1
COUNTS
0
10
20
30
MILLIMICROSECONDS
12.4 MμSEC.

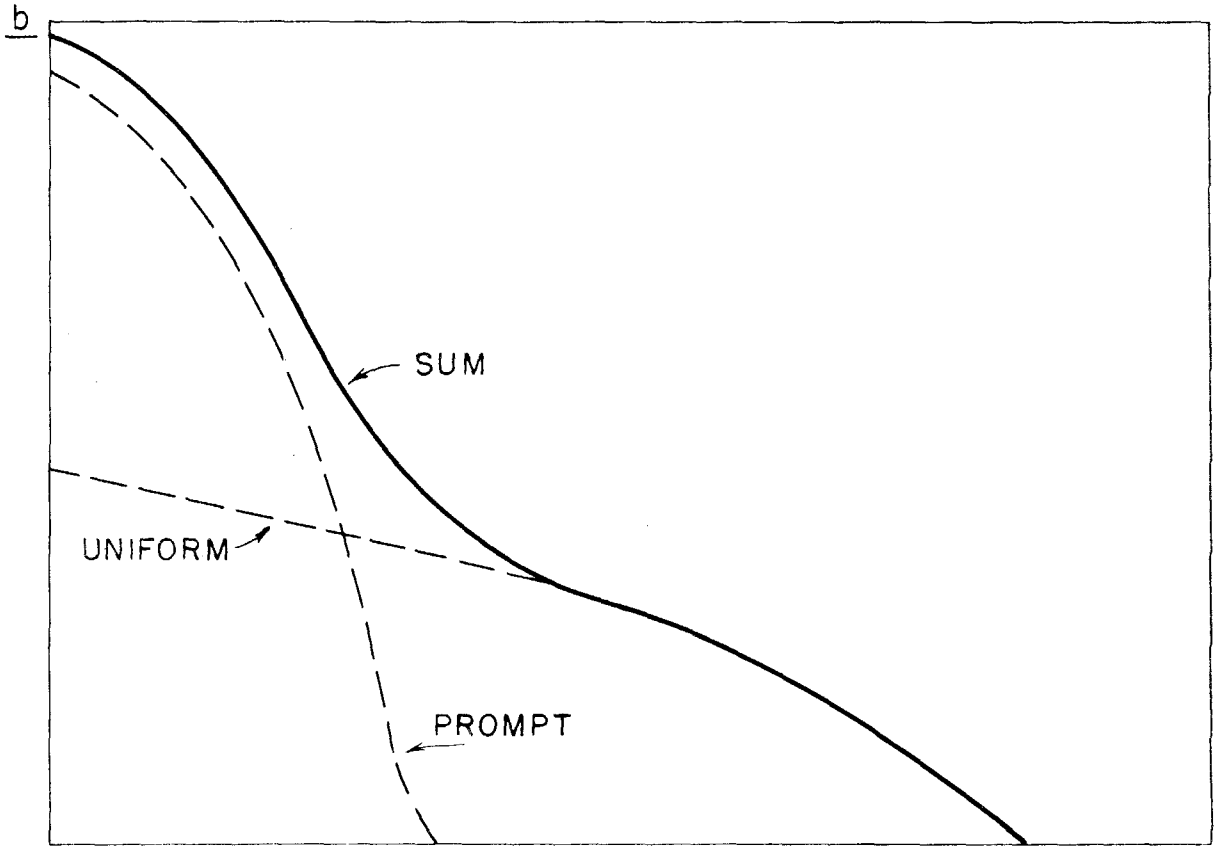
b
SUM
UNIFORM
PROMPT

at 88° in the cm system and 1020 Mev photon energy. Because of poor statistics, uncertainty in the efficiency estimate, and particularly because of the questionable results and curious effects found in later side-counter experiments, this cross section should not be believed to better than $\pm$ 50 $^{o}/o$.

V. SIDE COUNTER EXPERIMENT

A. Introduction

The telescope to be described here was designed for the study of low energy K mesons—down to about 60 Mev. It embodied the promising features of the two preceding experiments: a thick scintillator to stop the mesons, and a side counter system to observe their decay products. The use of a scintillation ΔR counter permitted a fast coincidence to be required between it and the rest of the telescope; the lack of such a coincidence allowed the troublesome random counts in the Cerenkov telescope experiment. Furthermore, development of the $dE/dx + \Delta R$ pulse addition system permitted the use of a stopping counter twice as thick as that used in the original scintillation telescope work. The system did have the drawback that K decay could cause a large ΔR signal, thus smearing the K peak up into the protons. It was hoped that requiring a slightly delayed side counter coincidence would nevertheless permit clear identification of K mesons.

The telescope gave very good pion and proton peaks, and demonstrated the usefulness of the $dE/dx + \Delta R$ idea. Unfortunately, however, there was a large background of prompt side counter coincidences, presumably due to particles scattered from the telescope, which obscured the pulses from K decay. While the electronics could probably have been improved to give better discrimination against these prompt pulses, this might have meant discarding all the K's which decayed in less than 10 mμsec or so. Together with the low

counting rate of the side counter arrangement, this would have been a prohibitively low rate experiment. The system was finally abandoned in favor of a more efficient experimental method.

B. Equipment

In order to permit the study of low energy K's and to get a reasonable solid angle for the side counter system, a completely new set of counters was constructed for this experiment. Figure 16 shows the telescope arrangement. The counter sizes were:

Counter 1:	3 3/8" x 2 3/4" x 0.243"
Counter 2:	3 3/4" x 3 3/16" x 0.995"
Counter 3:	3 3/8" x 2 3/4" x 0.243"
Counter 4:	5" x 4 1/4" x 1.912"
Counter 5:	5 1/2" x 4 1/2" x 0.490"
Counter 6:	6 1/2" x 4 1/2" x 0.490"
Counter 7:	6 1/2" x 4 1/2" x 0.490"

All were plastic scintillators except 2, which was a lucite Cerenkov counter; all were wrapped in 0.0008" and 0.005" aluminum foil and viewed by RCA 6810 photomultipliers. During the course of the experiment two absorber settings were used:

Absorber A:	1/8" copper	29/32" copper
Absorber B:	1/32" copper	1/32" copper
Absorber C:	5/32" copper	5/32" copper

Absorbers D and E were each about 1/2" lead.

Figure 16

Top View of Side Counter Telescope

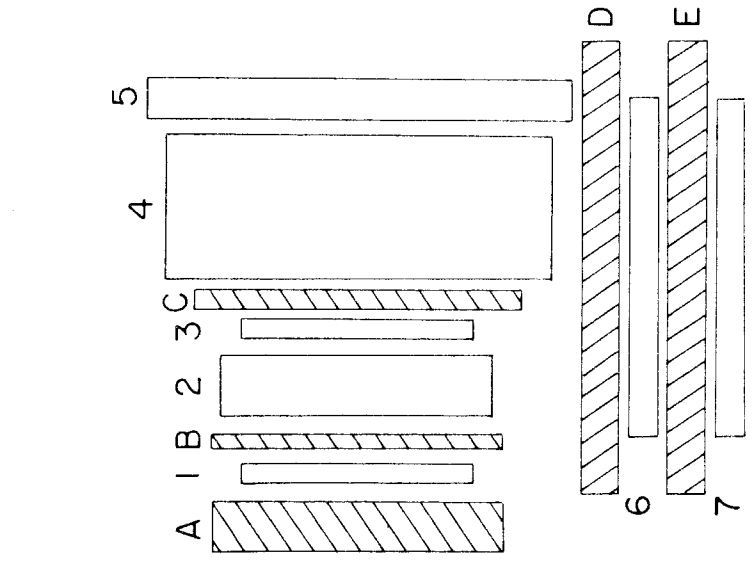
A
I
B
2
3
C
4
5
D
6
E
7

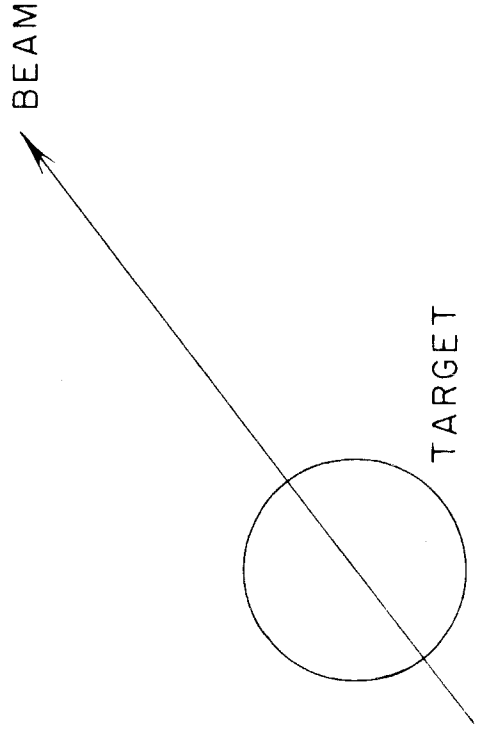
BEAM
TARGET

Counters 1 and 3 were standard dE/dx counters, made somewhat thinner than usual so that low energy K's could penetrate the telescope. 2 was a Cerenkov counter to veto fast electrons. The stopping counter 4 was made quite large so that K decay particles had a long path length before they left the counter. Coincident signals from both side counters 6 and 7 were intended to indicate the passage of the decay product. Two counters were used because accidental pulses from a single counter might have indicated misleading coincidences. The telescope subtended a solid angle of 0.044 steradians; depending on the absorbers used, it accepted K's from 84 to 109 or from 134 to 153 Mev.

Figure 17 shows the electronic system incorporating the dE/dx + ΔR scheme. Signals from dE/dx counters 1 and 3 were fed to a Garwin coincidence circuit, as were signals from 3 and the veto Cerenkov counter 2. The Garwin outputs went to a coincidence and a veto channel respectively on a 50 mμsec coincidence circuit. (This circuit provided for pulse height biases in the various channels, and will henceforth be called the "bias coincidence circuit"). Signals from the ΔR counter and the veto counter 5 went to other coincidence and veto channels. The bias coincidence circuit thus gave an output when an incoming particle stopped in the ΔR counter. This signal caused the gated coincidence circuit to generate a 50 mμsec wide pulse which was used to open two fast gate circuits.

One of these gates passed a signal which was the dE/dx + ΔR pulse formed by adding, in a carefully controlled ratio, outputs

Figure 17

Electronic System for Side Counter Experiment

The following electronic symbols are used, in addition to the symbols of figures 8 and 14:

Ad	Addition Network
At	Attenuator, Tektronix Model B-170A
B	Berkeley-type Coincidence Circuit, Model 13: Resolution Time 10 mμsec
BC	Bias Coincidence Circuit Model 2; Resolution Time 50 mμsec
FG	Fast Gate, Model 15
GC	Gated Coincidence Circuit, Model 2; Resolution Time 50 mμsec

COUNTERS

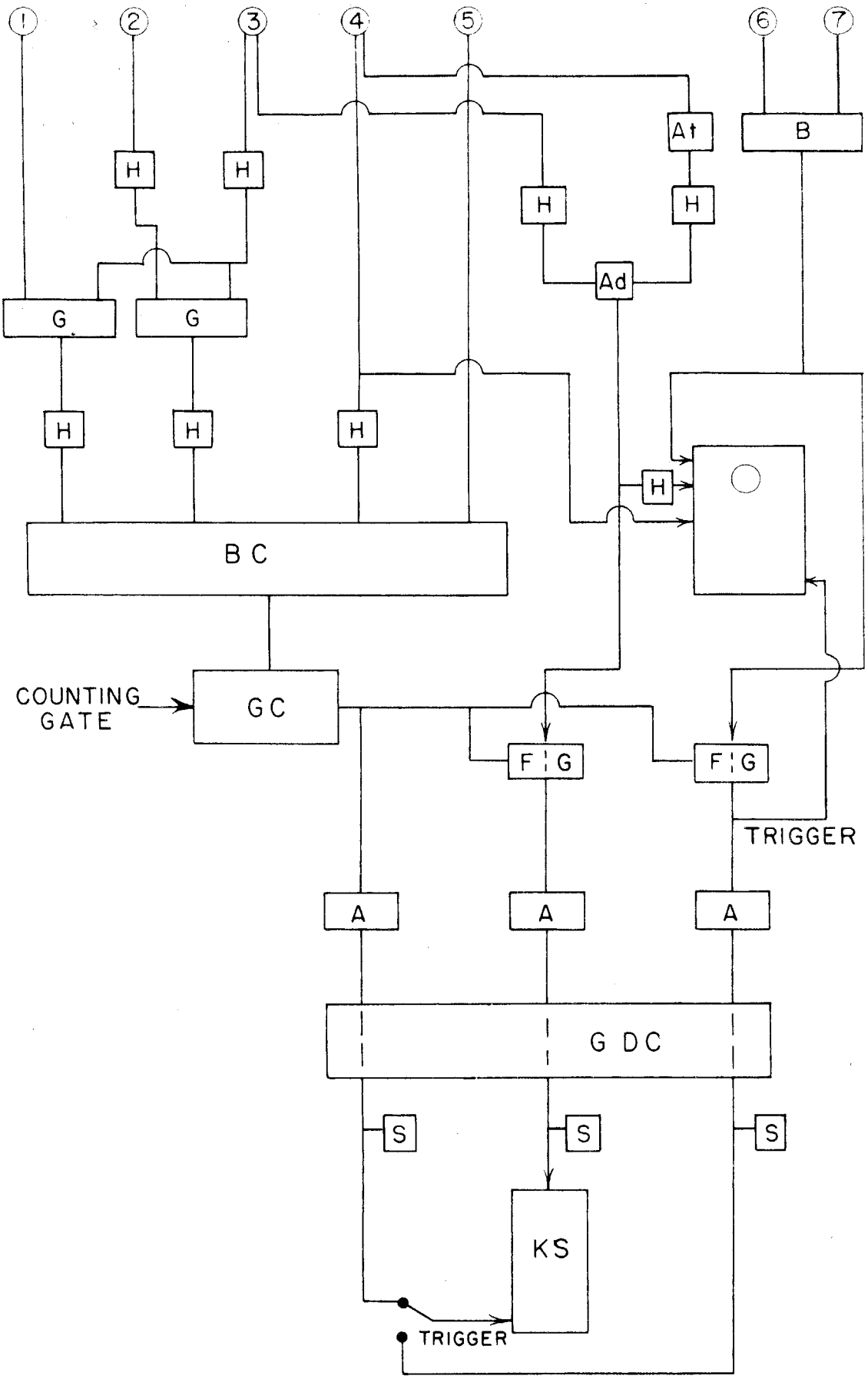
1
2
3
4
5
6
7
H
H
H
H
At
B
Ad
G
G
H
H
H
H
BC
COUNTING GATE
GC
F G
F G
TRIGGER
A
A
A
G DC
S
S
S
KS
TRIGGER

from counters 3 and 4. After passing through the gate this signal was amplified and displayed on the pulse height analyzer and on a fast oscilloscope.

The other fast gate passed an output pulse from a Berkeley-type coincidence circuit (27) between side counters 6 and 7. Thus a side counter coincidence within 50 mμsec after a particle stopped in the telescope would give an output from the gate. This signal was used to trigger the oscilloscope sweep and pulse height analyzer. It was hoped that the analyzer would show a K peak. Three pulses were displayed on the oscilloscope. First, a pulse from counter 4 gave a time reference. Second, a slightly delayed pulse from the side counter coincidence circuit supposedly indicated the passage of a K decay product. Third, the $dE/dx + \Delta R$ pulse indicated whether the incoming particle was in the right part of the pulse height spectrum to be a K.

C. Results

This experiment was intended to count only those K mesons decaying in the K_L mode; particles from Υ decay had too little energy to penetrate the lead absorbers between the side counters. For K mesons stopping at random positions in the ΔR counter and decaying in random directions, a Monte Carlo Datatron calculation gave the fraction of decay particles which passed through the side counters, and gave their range distribution within the stopping counter. 10.9 % of the K_L decays were counted if there was no pulse height bias in this counter. For a reasonable photoproduction cross section this

indicates a counting rate of about 1 per 100 Bips. The use of side counters obviously gives a low rate experiment. Additional counters to surround counter 4 more completely could have improved this situation at the expense of more complicated electronics.

The observed counting rate was about 10/100 Bips, showing a large background of unwanted events. For each count the oscilloscope trace told both the $dE/dx + \Delta R$ pulse height and the delay of the side counter signal (relative to the stopping signal in ΔR). Plotting both delay and pulse height should be a very sensitive way to separate K's from background. Figure 18a is such a plot, containing the points from 1900 Bips of running; 18b is a pulse height spectrum showing the region where K mesons should lie.

Several facts are obvious from the figure, which is typical of all the data in this experiment. First, most of the side counter pulses were "prompt," within the resolving time of the equipment, rather than delayed as K counts should be. Moreover, the resolving time was so long that it was impossible cleanly to eliminate the prompt counts. Finally, there was no pronounced tendency for delayed counts to be located in the K meson pulse height region.

Two telescope settings were used in the course of this work; they accepted K's at 110° in the cm system from 1005 Mev photons, and at 90° from 1035 Mev photons. Runs above and below threshold were made for both settings. All runs showed the same pattern as figure 18a; there were a few delayed counts amid a number of prompts. For no telescope setting did an integral lifetime plot show the K life,

Figure 18

a Side Counter Delay and dE/dx + ΔR Pulse Height Plot

b dE/dx + ΔR Pulse Height Spectrum

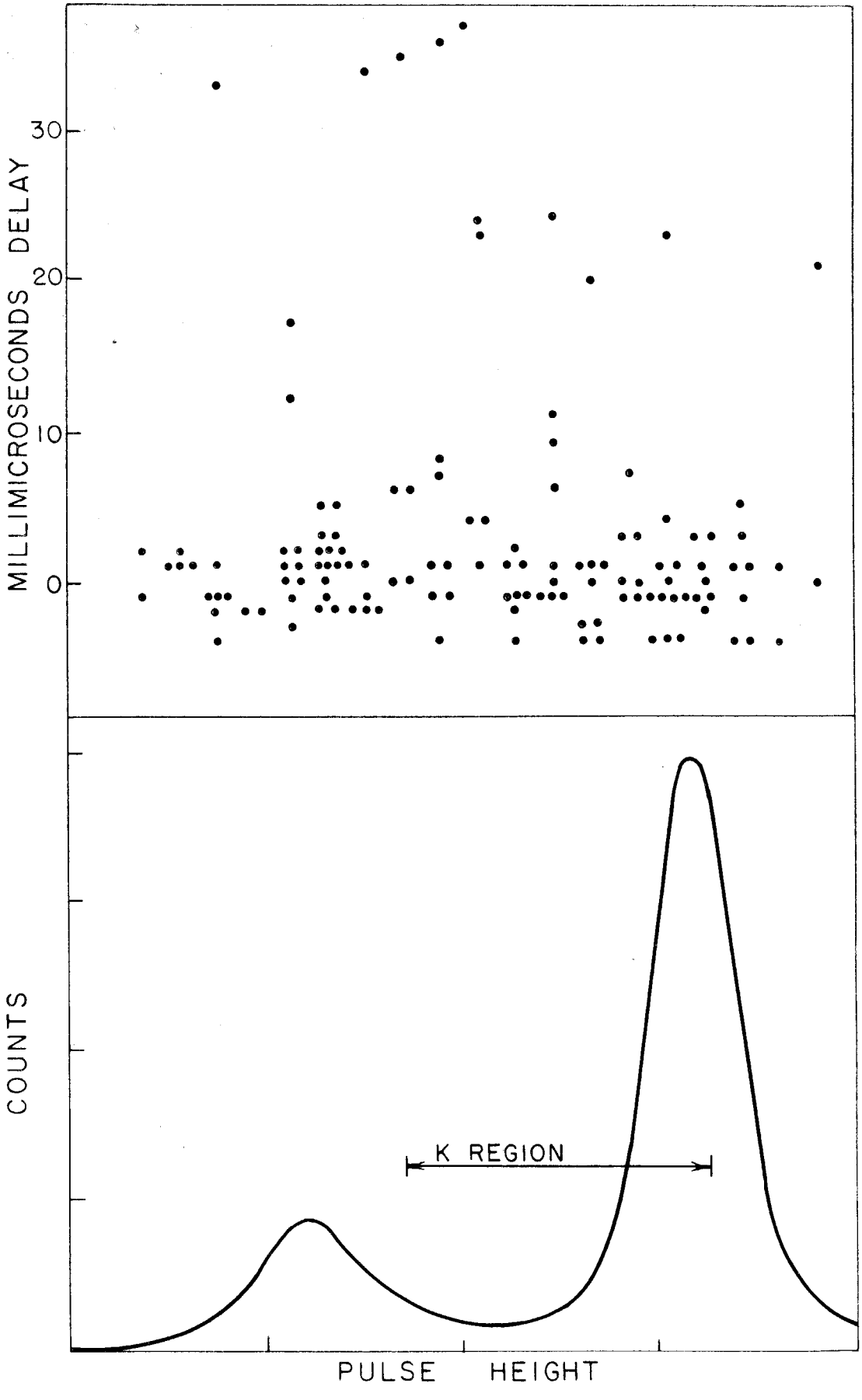
MILLIMICROSECONDS DELAY
30
20
10
0
COUNTS
K REGION
PULSE HEIGHT

or indeed any single lifetime.

Two methods were used to estimate a cross section from these meager data. In the first method all counts above threshold with delay greater than 5 mμsec and an appropriate pulse height were assumed to be K's. A correction was made for the lost counts during the first 5 mμsec; the results were cross section values of 0.9×10^{-31} cm^2/steradian at 110° (cm), and 1.1×10^{-31} at 90°. The second method consisted of assuming that any difference in counting rate above and below threshold in the K pulse height region was due entirely to K mesons. This yielded a cross section of about zero at 110° and 1.3×10^{-31} cm^2/steradian at 90°. All these values are smaller than the cross sections of Donoho and Walker, who found about 1.2 and 1.7×10^{-31} cm^2/steradian at the two angles.

An interesting question is the nature of the prompt coincidences, which could be caused either by two particles from a reaction in the hydrogen target, with one particle entering the telescope and the other penetrating the side counters, or by a particle passing through the telescope, scattering or reacting in counter 4, and hitting the side counters. The first cause was investigated by putting more shielding between the target and the side counters; the prompt coincidences were not greatly affected. A more critical test was made by turning the side counter system 90°, so that it faced the target. The coincidences decreased significantly. This showed that the particles passing through the side counters did not come from the target but rather from within the telescope. Increasing the side

counter absorbers (D and E) decreased the prompt coincidences fairly effectively. Unfortunately, thicker absorbers could not be used in practice because the mesons from K decay could not get through.

Pions scattered in counter 4 could cause prompt counts which would not all appear in the pion channels of a plot like figure 18a, since scattered pions with a long path in the ΔR counter could give a large $dE/dx + \Delta R$ signal. Known photoproduction cross sections indicate that about 100 pions per Bip passed through the telescope with too little energy to trigger the veto Cerenkov counter. Counter 4 contained 2.2×10^{23} carbon nuclei per cm^2; an estimate of the 90^o scattering cross section from carbon is 5 millibarns/steradian (28). These figures show that as many as 15 pions/100 Bips might be scattered into the side counters, which subtended 10.9 $^o/o$ of a sphere as seen from counter 4.

A recent K meson experiment at Cornell (5) also made use of side counters. There, however, the counter system was located behind an analyzing magnet and was exposed only to particles in a narrow momentum interval. In the present experiment particles of all energies which could reach counter 4 had a chance to scatter through the side counters, which caused the intolerable background problem.

VI. LAMBDA TELESCOPE EXPERIMENT

A. Introduction

The final effort to achieve an efficient K meson experiment involved two telescopes, to count simultaneously the K and the proton from Λ decay. For a fixed K energy and angle the Λ direction is determined; the protons tend strongly to emerge near this direction, so that a proton counter of reasonable size could be much more efficient than the side counter system of the preceding experiment. Moreover, this plan did not require fast time resolution since there was no question of distinguishing prompt from delayed counts but only of separating out accidentals.

However, the problem of identifying Λ decay protons was quite difficult, and was never satisfactorily solved. The difficulty was caused by the large energy spread of the protons, typically ranging from 100 to 300 Mev. Conventional systems for particle identification, whether counter telescopes or magnetic spectrometers, have small energy acceptances which do not begin to cover this range. A series of counters sandwiched between absorbers to stop the protons might have been satisfactory, but would have required detailed and tedious pulse analysis to determine which particles were really protons. Instead, a simple system of counters was set up here, without the range requirements of a real counter telescope. It was hoped that the background from events other than K-Λ coincidences would either be small, or that it would be composed of fast particles on the Λ side which could be eliminated by requiring pulses at least as large as

those from 300 Mev protons. Unfortunately the background was large and was not eliminated by pulse height analysis.

B. Equipment

Throughout this work the K telescope was the same as for the previous experiment; it consisted of counters 1 through 5 arranged as in figure 16. Several Λ telescope configurations were tried. The most satisfactory is shown in figure 19. The counter sizes were:

Counter 6: 3 1/4" x 2 1/4" x 0.490"

Counter 7: 4" x 2 5/8" x 2"

Counter 8: 6 1/2" x 4 1/2" x 0.490"

Counter 9: 6 1/2" x 4 1/2" x 0.490"

Scintillation counters 6 and 8 were supposed to give large dE/dx signals when a proton passed through, with no accompanying pulse from the lucite Cerenkov counter 7. Absorbers D and E were usually thin (1/2" CH_2 or 1/8" copper), and were intended chiefly to keep the individual counter rates reasonably low. Counter 9 detected those particles which went through absorber F; this absorber was frequently varied in an effort to estimate the range and energy of particles striking the Λ telescope.

Figure 20 is a diagram of the electronics used with these counters; the K system was the same as shown previously (figure 17). As in that figure, the bias coincidence circuit sent a pulse to the gated coincidence circuit whenever a particle stopped in the ΔR counter.

Figure 19

Top View of Lambda Telescope

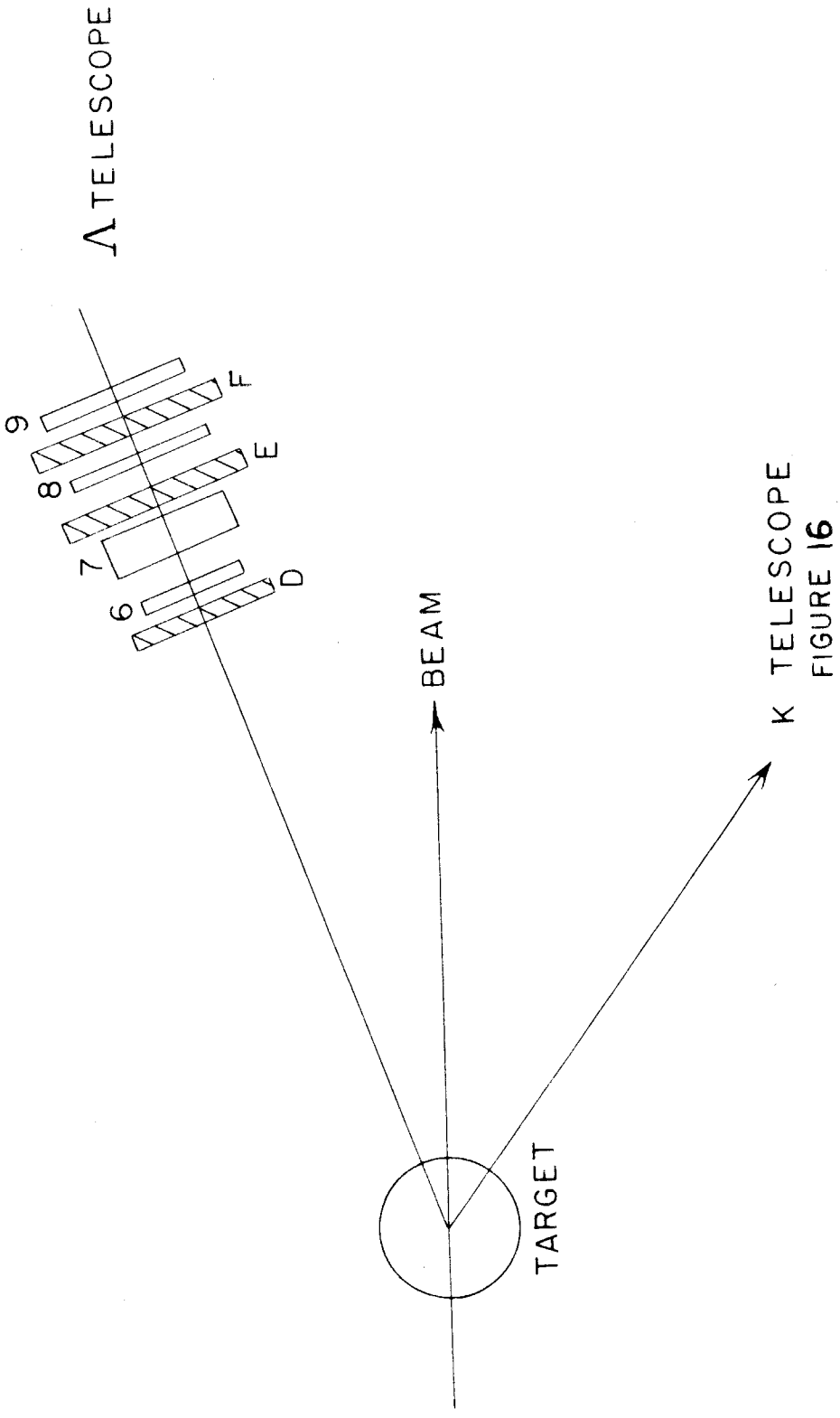

FIGURE 16

Figure 20

Electronic System for Lambda Telescope Experiment

The symbols are the same as in figures 8, 14, and 17.

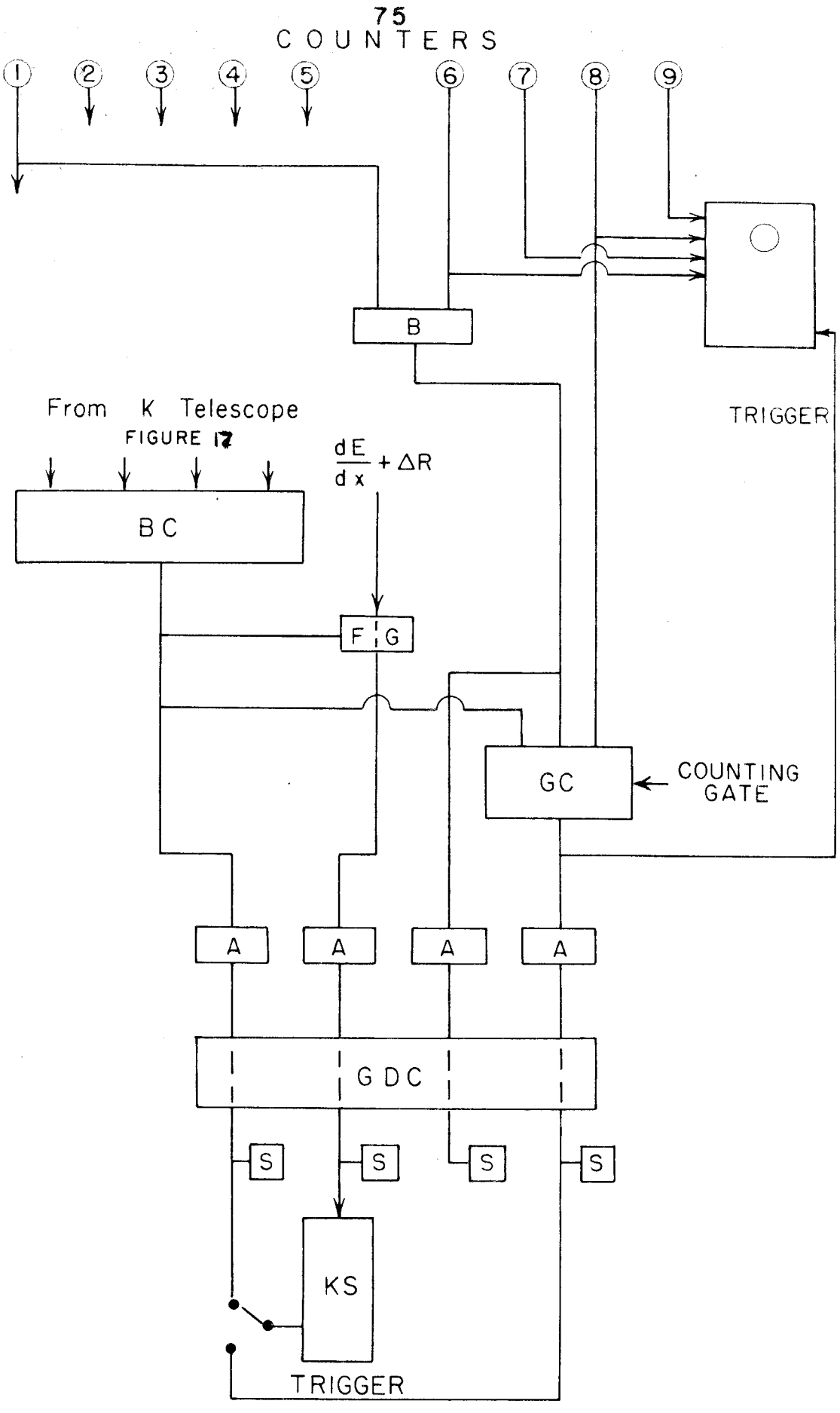
75
COUNTERS
1
2
3
4
5
6
7
8
9
B
TRIGGER
From K Telescope
FIGURE 17
dE/dx + ΔR
BC
F
G
GC
COUNTING GATE
A
A
A
A
GDC
S
S
S
S
KS
TRIGGER

For this experiment, the bias coincidence circuit also opened the fast gate which passed the dE/dx + ΔR pulse.

Signals from the front counter of the K telescope (no. 1) and from the front counter of the Λ telescope (no. 6) went to a fast Berkeley-type coincidence circuit. Output signals from this circuit, as well as signals from Λ counter 8 went to the gated coincidence circuit. When this circuit recorded pulses from the bias coincidence circuit (indicating a particle stopping in the K telescope), from the Berkeley circuit (indicating coincident particles in counters 1 and 6), and from counter 8 (indicating a particle penetrating the Λ telescope), it generated a signal which triggered both the pulse height analyzer and the oscilloscope.

Displayed on the 50 $m\mu$ sec/cm oscilloscope sweep were five pulses: the dE/dx + ΔR pulse and the pulse from each of the four counters in the Λ telescope. For events showing a dE/dx + ΔR pulse height appropriate for K mesons, an analysis of the Λ counter pulses was supposed to tell whether the coincident particle was a proton from Λ decay.

C. Results

The anticipated counting rate was the product of the K telescope rate and the efficiency for seeing Λ decay protons. The K rate was the same as in the preceding experiment (without side counters), about 7 counts per 100 Bips for a reasonable cross section. The Λ telescope subtended 0.033 steradians and was set at 18°, which is the angle at which Λ's emerge if a 144 Mev K is produced

at 34°. 68 °/o of the Λ 's were assumed to decay into protons and charged pions (29). It was then estimated that the Λ telescope caught about 40 °/o of the protons. This percentage was found from a numerical folding of the Λ angular distribution (determined by the K telescope resolution), the proton angular distribution from Λ decay, and the angular acceptance of the Λ telescope. The number may be in error by as much as $\pm$ 50 °/o; a Datatron program to compute it accurately was written but was not used before the experiment was abandoned. The above figures indicate a K-Λ rate of about 2 per 100 Bips.

It soon became clear that the counting rate was considerably higher than this. There were about 40 events in 100 Bips with three Λ scintillator pulses in coincidence with a particle stopping in the K telescope; for perhaps 10 of these counts there was no Λ Cerenkov signal. The nature of these events was extensively investigated.

In the first place, at least 80 °/o of the counts came from the liquid hydrogen; empty target runs gave quite low backgrounds. That the counts were not accidentals was checked by delaying various coincidence signals. The rate was not strongly dependent on the Λ telescope angle, as K-Λ counts would have been; there was no significant change between 18° and 45°. The rate decreased by about half when the synchrotron energy was lowered from 1080 to 900 Mev.

Studies were made with various absorbers at F on the Λ side. One arrangement allowed 100 Mev protons (the least energetic from Λ decay) barely to reach counter 9. This eliminated only low

energy particles; high energy pions could still count. Another absorber arrangement just stopped 200 Mev protons before counter 9. A third arrangement just stopped 300 Mev protons (the most energetic from Λ decay). It was hoped that a detailed analysis of pulse heights for the three counters would indicate the type of particle that was causing all the coincidences.

It was found that about 2/3 of the Λ scintillator counts appeared to come from pions, and 1/3 from protons. Pions were usually accompanied by a proton count in the K telescope, although occasionally a second pion was seen. Protons in the Λ counters were almost always accompanied by a pion on the K side. Once or twice per 100 Bips the Λ counters indicated a proton while the K telescope apparently showed another proton. These presumably were the desired K-Λ coincidences. A quantitative count of these events was not possible, because proton identification in the Λ counters was never really clear.

The large number of background counts was due to the production of pion pairs, with charged pions and recoil protons being counted in the Λ and K telescopes. Using the pion pair cross sections given by Bloch (30), one can predict a counting rate of the same order of magnitude as that observed. The fact that the counts were not strongly dependent on Λ telescope angle but were sensitive to changes in photon energy also indicated that pion pairs were being observed. Since fast pions were readily identified by the Λ counters, this work pointed the way toward the pion pair experiment to be described in the second half of this thesis.

VII. CONCLUSION

This thesis has reported a number of efforts to measure the photoproduction of K mesons with counter telescopes. Several new techniques have been described: the use of $dE/dx + \Delta R$ signals to separate particles, the use of a Cerenkov counter to veto fast electrons, the use of a Cerenkov or scintillation counter system to detect meson decays, and the use of fast time and amplitude analysis to distinguish different particles. These techniques gave tentative figures for the yield of K mesons. However, for the beam energies available at this laboratory the cross section for K production is far smaller than for pions, and there are many more photons able to produce pions than K's. Consequently all the K experiments were obscured by pion phenomena, as well as by electromagnetic interactions from the large number of electrons and photons present near the synchrotron beam. No system of particle identification was found that could cleanly eliminate the background.

It would be fair to say that these experiments showed conventional counter telescopes to be devices of limited usefulness in experiments with high energy photon beams. For low yield reactions they do not provide clear particle identification, while for high yields their potentially greater counting rates are not needed. However, recent advances in high speed electronics (such as the traveling-wave oscilloscope, fast photomultiplier tubes, and fast transistor circuitry) may well modify this pessimistic conclusion.

PRODUCTION OF PION PAIRS BY 1 BEV PHOTONS

I. INTRODUCTION

The study of pion photoproduction has been a chief concern at all laboratories where high-energy photon beams are available. Yields of single pions from nucleons have been extensively measured at energies up to 1 Bev (11, 14, 31). For the higher energies in this range the experimental results (as well as their theoretical interpretation) are complicated by the presence of multiple pion production. Two pions can be produced by a photon with energy above 321 Mev, three pions above 512, four above 725, and five above 958. In the case of double pion production from protons, with which this thesis is concerned, three reactions are possible:

$$\gamma + P \longrightarrow P + \pi^+ + \pi^-$$
$$\longrightarrow P + \pi^\circ + \pi^\circ$$
$$\longrightarrow N + \pi^+ + \pi^\circ$$

This thesis describes an experiment to investigate the first reaction by observing the proton and one charged pion.

Early experimental results on single pion production revealed a resonant state with angular momentum 3/2 and isotopic spin 3/2, which dominated the process near 300 Mev. Other resonances at higher energy have been discovered more recently. Thus far the results for double pion production have been too incomplete to disclose any similar features. An attempt at interpreting such results as have

been obtained can be made by assuming that one pion and the recoil nucleon are temporarily joined in the 3/2, 3/2 resonant state. The present experiment was intended largely as a test of this "isobar model."

The first observation of negative pions from a hydrogen target (which can only result from multiple production) was made with the California Institute of Technology 500 Mev synchrotron beam. Peterson and Henry (32) found π^- stars in nuclear emulsion, and Sands, Bloch, Teasdale, and Walker (33) used a magnetic spectrometer to identify the mesons. Since the reaction was observed near threshold, the counting rate was quite low, but it was found that the π^-/π^+ ratio was on the order of a few percent.

Friedman and Crowe (34) at Stanford measured the yield of negative pions and their energy spectra for bremsstrahlung energies up to 600 Mev. They found the spectra peaked at low π^- energy, in fair agreement with the threshold theory of Cutkoski and Zachariasen (35).

More recent experiments at Cornell (36) have utilized a diffusion cloud chamber, in which both charged pions and the recoil proton were seen. On the basis of some hundred events, the total cross section is observed to rise steeply between 450 and 550 Mev to a value of about 80 μbarns; above 550 Mev it slowly falls. The π^- tends to have less energy than predicted by a purely statistical distribution; the proton and π^+ have more energy. The angle and energy distributions are reasonably consistent with those predicted by a doubly charged 3/2, 3/2 isobar, but the statistics are poor.

Bloch and Sands (30) at this laboratory used a magnetic spectrometer to observe negative pions produced by 650, 800, and 1000 Mev bremsstrahlung, the pions emerging at 60° and 120° in the laboratory. Elliott (37) has extended these measurements to 35°, and has in addition detected the coincident positive pion at several angles. In the experiments the differential cross section shows no large angular dependence, and seems roughly independent of photon energy from 600 to 1100 Mev. Furthermore, the π^+ mesons appear to be isotropic in the cm system. Neither this isotropic distribution nor the energy spectrum of the π^- is in close agreement with two phenomenological models which have been considered – namely, the isobar model and the density of states or statistical model.

The production of pions in nucleon-nucleon or pion-nucleon reactions has been investigated at Brookhaven (38, 39). Detailed calculations have been made for these experiments on the basis of an excited nucleon isobar (40, 41, 42). Production of pions by pions gives the same final state as pair photoproduction–a nucleon plus two pions. The fair success of the isobar model for these reactions is therefore of interest in the present experiment.

The measurement of π^- energy and angle and of photon energy, as by Bloch, does not fix the kinematics of pion pair production. The reaction involves 9 kinematic parameters, taken to be the photon energy, the energy and angle to the beam of each of the three outgoing particles, and the azimuth of two of the particles relative to the third. These are related by one energy and three momentum equations; five

parameters must therefore be measured to fix the reaction. Experiments which do this, such as the Cornell cloud-chamber measurements and the counter work of Elliott, have so far suffered from either a tedious analysis process or a low counting rate. The present experiment held promise of avoiding these drawbacks.

Here the reaction kinematics were fixed by using a counter telescope to measure the proton energy and angle, another telescope to give the angle of one pion, and the "photon difference" method to find the photon energy. Since protons must emerge at foreward angles in the lab while pions can emerge at any angle, a proton telescope can be quite efficient. The counting rate in this experiment was several times the corresponding rate for detecting both pions (with an equal photon difference interval). This advantage was of course accompanied by the disadvantage of poor energy and angular resolutions. Nevertheless, the resolutions were not so wide as to obscure the details of the distinctive distributions predicted by various models.

This experiment evolved out of the search for K-Λ coincidences, as reported in the first half of this thesis. It began as an exploratory attempt to confirm that the coincidences seen there were indeed caused by pion pairs. Its final result was a proton angular distribution which could in principle determine the validity of the isobar model for pair production by 1 Bev photons.

II. EXPERIMENTAL TECHNIQUES

This experiment counted pion pairs by detecting charged particles simultaneously in two separate counter telescopes. One of these telescopes was a five counter array in which protons were stopped and were separated from pions by pulse height analysis in two dE/dx counters. The other was a three or four counter system which identified fast pions by requiring them to make minimum pulse-height signals, to emit Cerenkov light in a lucite counter, and to penetrate a considerable thickness of absorber. The first telescope fixed both the angle and energy of the protons, but since pions did not stop in the second telescope their energy was undetermined. Knowledge of this energy was not required to specify the reaction kinematics.

Figure 21 shows a top view of both telescopes in position at a liquid hydrogen target. The telescopes are in the same plane, so that the azimuthal angle of the pion is 180° from the proton. Four more kinematic quantities suffice to fix the reaction: photon energy, proton angle and energy, and pion angle.

Table I gives the size of the various counters, the thickness of the absorbers, and the solid angle and energy acceptance of the telescopes. Each counter was wrapped in 0.0008" and 0.005" aluminum foil and was viewed by a 6810 photomultiplier. It will be noted that two different telescope configurations and four absorber arrangements were used. The different telescopes result from the fact that the experiment was set up and operated on two separate occasions; both the telescopes themselves and the electronic equipment were refined

Figure 21

Top View of Proton and Pion Telescopes

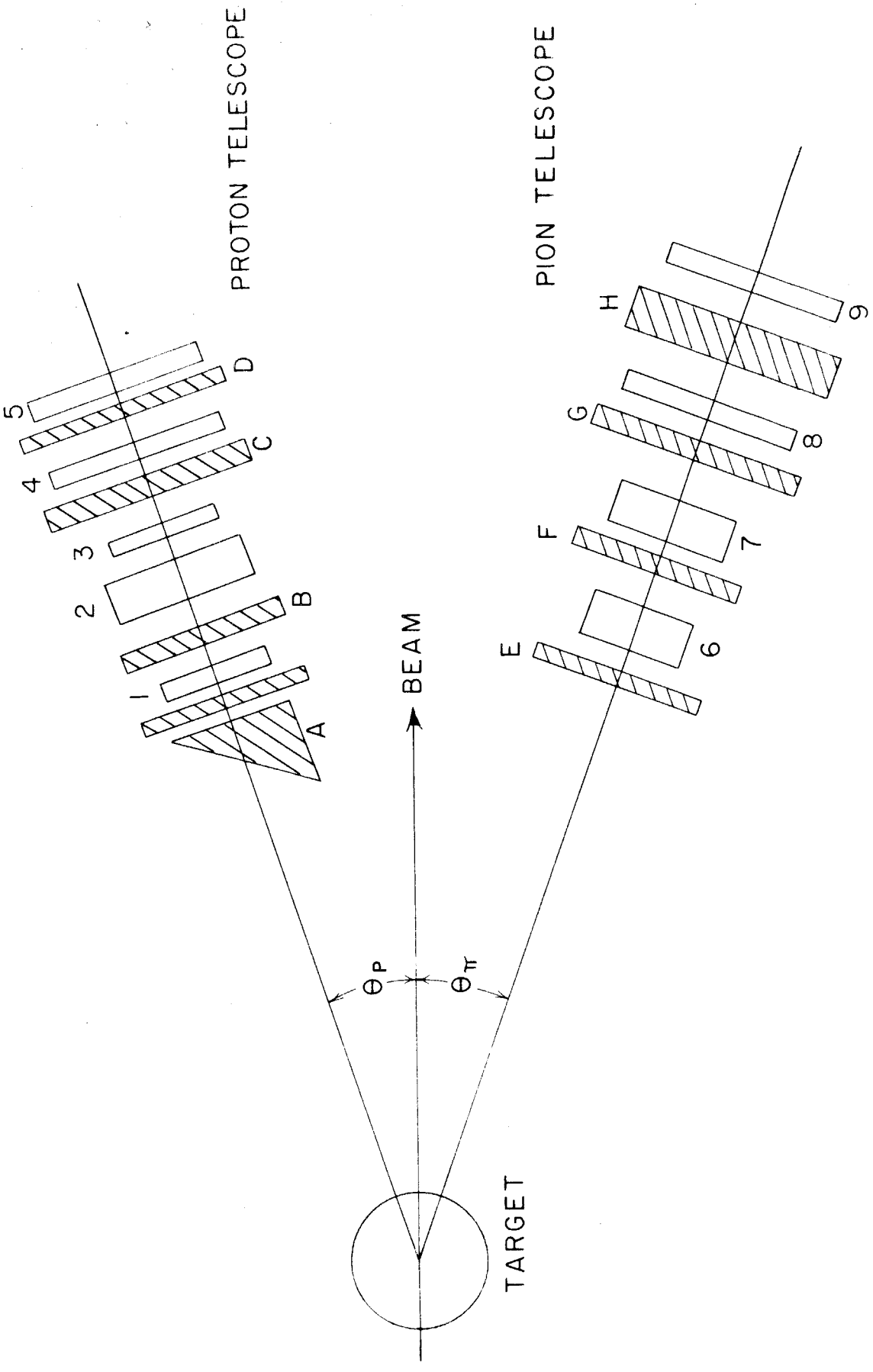
PROTON TELESCOPE
PION TELESCOPE
BEAM
TARGET
θ_p
θ_π
A
B
C
D
E
F
G
H
1
2
3
4
5
6
7
8
9

Table I

	First Runs	Second Runs	Third Runs	Fourth Runs
Counter 1	3 3/8" x 2 3/4" x 0.243" P		3 3/8" x 2 3/4" x 0.243" P	
Counter 2	3 3/4" x 3 3/16" x 0.995" L		3 3/4" x 3 3/16" x 0.995" L	
Counter 3	3 3/8" x 2 3/4" x 0.243" P		3 3/8" x 2 3/4" x 0.243" P	
Counter 4	5" x 4 1/4" x 1.912" P		6 1/2" x 4 1/2" x 0.490" P	
Counter 5	5 1/2" x 4 1/2" x 0.490" P		5 1/2" x 4 1/2" x 0.490" P	
Counter 6	3 1/4" x 2 1/4" x 0.490" P		4" x 2 5/8" x 2" L	
Counter 7	4" x 2 5/8" x 2" L		3 1/4" x 3" x 0.490" P	
Counter 8	6 1/2" x 4 1/2" x 0.490" P		6 1/2" x 4 1/2" x 0.490" P	
Counter 9	6 1/2" x 4 1/2" x 0.490" P		none	
Absorber A	0.5" CH_2	2.636 cm Cu	2.147 cm Cu	0.365 cm Cu+Pb wedge
Absorber B	0.078 cm Cu	1.820 cm Cu	1.027 cm Cu	1.027 cm Cu
Absorber C	0.405 cm Cu	0.405 cm Cu	1.524 cm Cu	1.524 cm Cu
Absorber D	0	0	0.615 cm Cu	0.615 cm Cu
Absorber E	0.5" CH_2	0.5" CH_2	0	0
Absorber F	0	0	0.5"CH_2	0.5"CH_2
Absorber G	1/8" Pb	1/8" Pb	1 1/2" Cu	1 1/2" Cu
Absorber H	1" Pb	1" Pb	-	-
Proton Energy T_P	123	243	240	200-303
ΔT_P	32	20	21	23-17
Proton Solid Angle	0.0412	0.0412	0.0282	0.0282
Pion Solid Angle	0.0183	0.0183	0.0217	0.0217

Wedge Height 4"
Width 3"
Thickness 0" to 2"

P = Plastic Scintillation Counter
L = Lucite Cerenkov Counter

and improved during the interval between runs.

Counters 1, 3, 4, and 5 constituted an ordinary range telescope, 1 and 3 being dE/dx counters and 5 the veto counter; particles had to stop either in counter 4 or absorber D. For the first runs D was omitted and 4 was a thick stopping counter. 2 was a lucite Cerenkov counter, set to veto fast electrons. The factors involved in the selection of absorbers A, B, C, and D have been described in the first part of this thesis. Here it need only be said that D adjusted ΔR and hence the energy acceptance, C served to separate the proton and pion dE/dx peaks, and B and A fixed the energy of the accepted protons, with A being thick enough to shield counter 1 yet thin enough to avoid producing spurious counts from stars.

The pion telescope essentially contained two scintillation counters and a lucite Cerenkov counter. Fast pions produced minimum pulses in the scintillators as well as a Cerenkov signal. The threshold of the Cerenkov counter was measured by placing it in front of a telescope counting pions of known energy. Pions down to 100 Mev were found to be counted quite efficiently; the pions observed in this experiment had energies generally above 200 Mev. The absorbers before the first scintillator and Cerenkov counter (absorbers E and F) were held to a minimum in order to avoid gamma-ray conversion as much as possible. Fast electrons from conversion could be indistinguishable from fast pions. Absorber G was quite thick, so that low-energy electrons could not penetrate it and give a minimum pulse in 8. Absorber H and counter 9 were used during the earlier runs in attempt

to get information about the pion range. This range was so large, however, that absorption in H together with the low counting rate prevented accurate pion energy measurement. This last absorber and counter were abandoned in the later runs.

The use of a wedge-shaped absorber A requires explanation. With the telescope set to count 250 Mev protons, its angular width caused considerable smearing of the angular distribution being measured. Reaction kinematics show, however, that a 10° angle change is in some ways equivalent to a 100 Mev proton energy change. For example, if the photon energy is 1 Bev and the pion angle $33\frac{1}{2}^{\circ}$, then 300 Mev protons are kinematically possible at all angles out to 37° while 200 Mev protons are possible out to 47°. The wedge, positioned as in figure 21, allows the outer side of the telescope to count 200 Mev protons and the inner side 300 Mev. Thus, in the example, if the telescope center were set at 42° both sides (and so the entire telescope) would count protons; at 43° neither side would count. The calculated angular distributions to be presented later show that the wedge effects a similar sharpening of angular resolution at all angles studied in this experiment.

A different electronic system was used for the two times at which the experiment was run. Figures 22 and 23 show the systems. The first arrangement was similar to that used in earlier K meson experiments in that the sum of dE/dx and ΔR signals was used to separate proton and pion peaks. As in figure 22, coincidence signals were formed between the proton dE/dx counters and between the Cerenkov and a dE/dx counter. These went to a coincidence and a

Figures 22 and 23

Electronic Systems for Pion Pair Experiment

The following electronic symbol is used, in addition to those of figures 8, 14, and 17:

· SO Slow oscilloscope, Tektronix Model 541

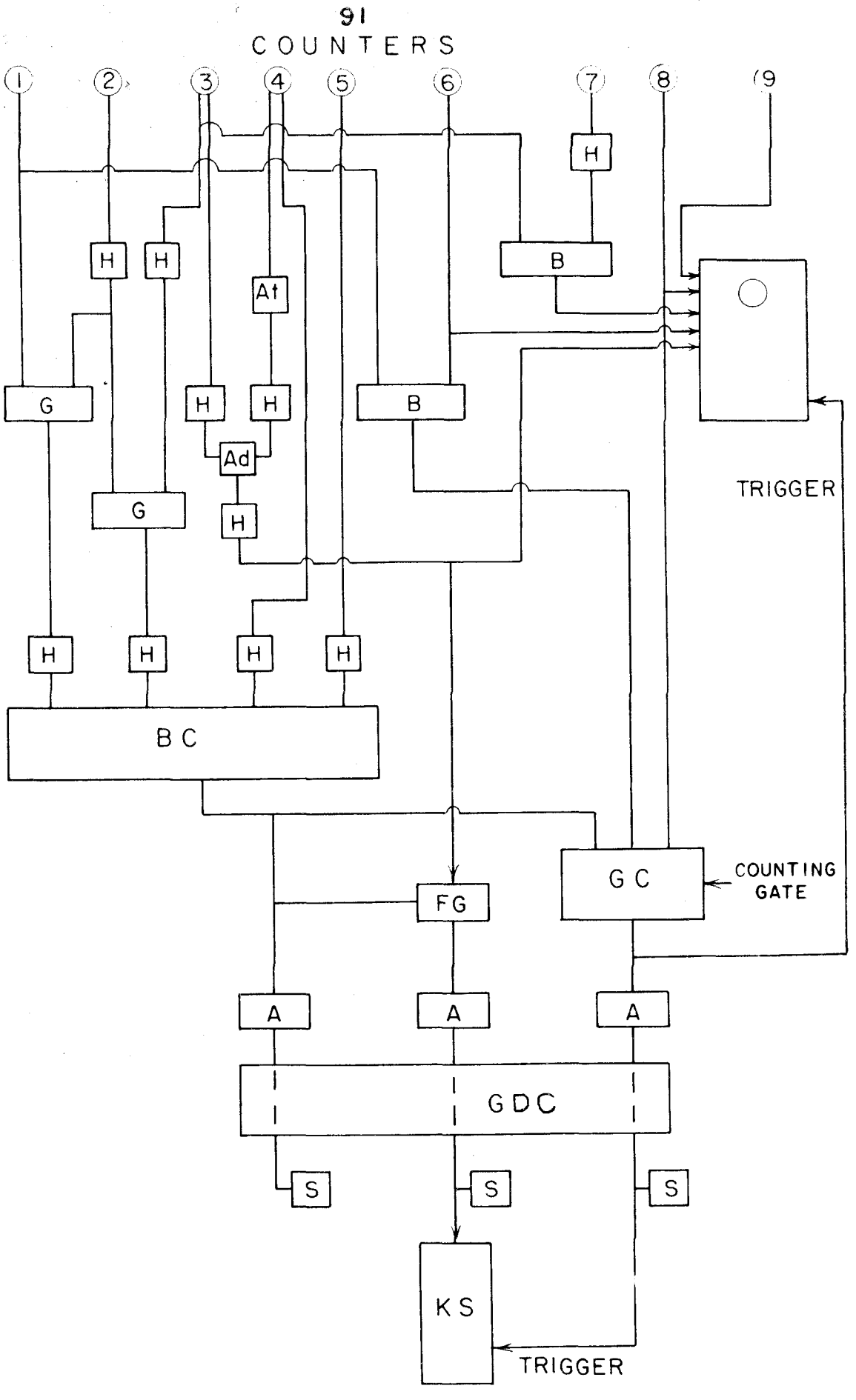
COUNTERS
1
2
3
4
5
6
7
8
9
H
H
H
At
B
G
H
H
B
Ad
G
H
H
H
H
H
BC
TRIGGER
GC
COUNTING GATE
FG
A
A
A
GDC
S
S
S
KS
TRIGGER

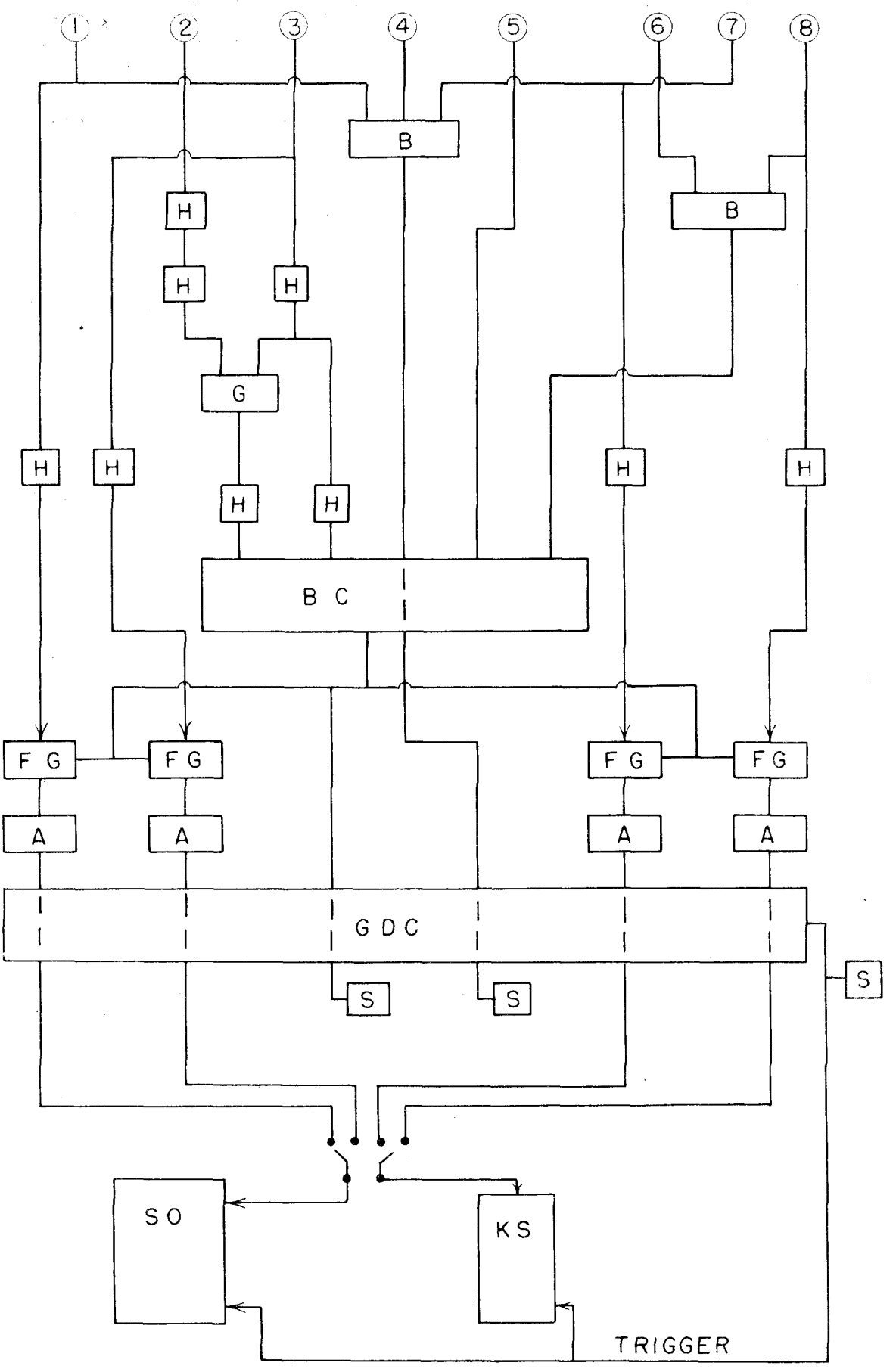
COUNTERS
1
2
3
4
5
6
7
8
B
B
H
H
H
G
H
H
H
H
H
H
B C
F G
F G
F G
F G
A
A
A
A
G D C
S
S
S
S O
K S
TRIGGER

veto channel, respectively, of the "bias coincidence circuit" described earlier. Signals from the thick ΔR counter and the veto counter also went to coincidence and veto channels. An output from the bias coincidence circuit then indicated a particle stopping in the proton telescope. This signal, together with one from counter 7 and an output from a fast coincidence circuit between pion counter 6 and proton counter 1, served to indicate a coincidence between the two telescopes. When such a coincidence occurred, a gated coincidence circuit triggered a fast oscilloscope and the pulse height analyzer. The analyzer displayed the combined $dE/dx + \Delta R$ pulse, which also appeared on the oscilloscope. The oscilloscope further showed the signals from pion counters 6, 8, and 9, as well as a fast coincidence signal from counters 3 and 7. An automatic 16 mm camera recorded the oscilloscope traces.

A pion pair was counted whenever analysis of the film indicated that (1) the dE/dx signal was of the right height to be a proton rather than a pion, (2) there was a definite 3 - 7 coincidence signal, showing that a fast particle triggered the Cerenkov counter 7 in coincidence with the proton telescope, and (3) the pulses from counters 6 and 8 were both small, indicating that the fast particle had sufficient range to be a pion rather than merely an electron. The counts selected in this manner constituted about 80 $^{o}/o$ of those accepted by the electronics, although this proportion got as low as 65 $^{o}/o$ for the highest counting rate runs. These numbers show the need for careful film analysis.

The second system, shown in figure 23, avoided this tedious analysis by placing more stringent electronic requirements on the

various pulses. Here there was no need for dE/dx + ΔR signal addition. Good proton peaks were obtained from both dE/dx counters 1 and 3. A fast coincidence (10 mμsec) was required between proton counters 1 and 4 and pion counter 7, and between pion counters 6 (the Cerenkov counter) and 8. These coincidence signals were fed to the bias coincidence circuit, as were pulses from counter 3, from counter 5, and from the 2 - 3 coincidence circuit, with the latter two signals going to veto channels. The bias coincidence circuit thus gave an output when a particle stopped in the proton telescope and, simultaneously, a fast penetrating particle traversed the pion telescope. This output opened four fast gates, which passed the signals from proton dE/dx counters 1 and 3 and pion scintillators 7 and 8. These four signals were amplified and sent to slow discriminator-coincidence circuits, where accurate pulse height biases could be set. Small pulses from either 1 or 3, indicating pions, were biased out; pulses from the other counter were displayed on the analyzer where protons again could be distinguished from pions. This use of two dE/dx signals guarded against mesons which, because of stastical fluctuations, gave unusually large pulses in one of the counters. Similarly, minimum pulses in 7 and 8 could be required. Any of the counters could be examined on a slow oscilloscope as well as with the analyzer. Signals satisfying both coincidence and pulse height requirements indicated a pion pair.

The number of accidental counts depended of course on the resolving time of the coincidence equipment. The fast oscilloscope in the first electronic arrangement or the fast 1-4-7 circuit in the

second guaranteed that the coincidence between the telescopes occurred within 10 mμsec or less. However, the general analysis of accidentals in terms of single counter rates is very difficult for systems as complex as these. Experimental tests were therefore made by putting extra cable lengths in various signal leads. This was done, in the system of figure 23, for the signal from counter 7 to 1-4-7 circuit, for the signal from 6 to the 6-8 circuit, for the signal from 3 to the bias coincidence circuit, and for the signal from the 6-8 circuit to the bias coincidence circuit. In none of these tests was a single accidental pion pair count recorded. The tests were run long enough to insure that the accidental rate was less than 5 $^{o}/_{o}$ of the true rate.

An investigation was made of events other than multiple pion production which could conceivably trigger both telescopes and give a misleading count. The most dangerous reaction would be single π^{o} production, with the proton being counted properly and one π^{o} γ-ray converting to give a pion-like count in the pion telescope. Two arguments were made against false counts from this source. First, the kinematics of π^{o} production show that the pions are emitted at backward angles – from 60^{o} to 110^{o} – for the proton energies and angles studied here. The counting rate from this source would therefore increase as the pion telescope was moved backward from its usual position near 30^{o}. No such increase was found. Second, and more conclusive, the rate would increase if more converter were placed in front of the pion telescope. (The telescope normally had only 1/2" of CH_2 in front, which, together with the first counter,

formed less than 1/10 radiation length.) A 1/4" lead converter (1.2 radiation lengths) produced no measurable increase in counting rate. This test showed that single π^o production, elastic photon scattering, or any other process yielding proton plus photon was not interfering with the reaction being studied.

Another source of false counts could be K-Λ production, with the K appearing like a proton and the pion from Λ decay counting in the pion telescope. Arguments against this can be made on the basis of kinematics and the known K cross section. In the first place, the energy of a K counted in the proton telescope would be 200 Mev. K's of this energy cannot be made at angles beyond 32^o by 1080 Mev bremsstrahlung, whereas counts in this experiment were found out to 45^o or 50^o. K's cannot be made at all by 900 Mev photons, while the experimental rate at 900 was about half that at 1080. Finally, a reasonable K cross section of 2×10^{-31} cm^2/steradian would give at most 4 K's per hundred bips through the proton telescope. An estimate of the efficiency of the pion telescope for seeing the Λ pion (remembering that this pion can emerge at any angle, and that the Λ direction is well foreward of the pion telescope angle) would be 2 %. Since only 68 % of the Λ's give charged pions, the coincidence rate might be 0.05 per 100 Bips, or less than 5 per cent of the pion pair rate.

During the earlier series of runs the arrangement of collimators, scrapers, etc. was the same as for the preceding K-Λ telescope experiments. The usual 3" liquid hydrogen target was used. A separate target was built for the later runs. This was a 2" cup of

liquid hydrogen, insulated by styrofoam (but not by vacuum) and kept filled from a pressurized Dewar. It was quite similar to a target developed at Cornell (43). The experiment was located just behind the primary scraper, quite close to the synchrotron. Anticipated troubles from stray magnetic fields and background radiation at this location did not materialize, but the empty target unfortunately gave about 50 $^{o}/_{o}$ more background counts than did the other liquid target. Actual counting rates will be given in a later section.

III. DERIVATION OF CROSS SECTIONS

The derivation of cross-sections from yields for three-body reactions (such as pion pair photoproduction) differs greatly from the well-known two-body calculation, and will be described before the experimental results are given. Let $\sigma(k, T_p, \theta_p, \theta_\pi)$ be the laboratory cross section for the production of a pion pair by a photon of energy k, with the proton having energy T_p and direction θ_p, and with one pion having direction θ_π. Note that k, T_p, θ_p, and θ_π completely determine the kinematics of the coplanar reaction. Specifically, the pion energy is given by

$$E_\pi = \left(HJ^2 \pm G\sqrt{J^4 - M_\pi^2 (H^2 - G^2)} \right) \Big/ (H^2 - G^2)$$

where

$$G = k \cos\theta_\pi - P_p \cos(\theta_p + \theta_\pi)$$

$$H = E - E_p$$

$$J^2 = kP_p \cos\theta_p - E(E_p - M_p)$$

Figures 24a and b show the relevent kinematic parameters in the laboratory and cm systems. The energy and angle of the second pion, if required, follow directly from energy and momentum conservation.

In analogy with the 2-body calculation, consider a beam containing $Q\, B(E_o, k)\, dk/k$ photons per Bip striking a target element dx dy dz, with the z-coordinate along the beam. $Q\, B(E_o, k)\, dk\, n(x, y)\, dx\, dy/k$ photons strike the target element, n(x, y) being the spatial distribution of the beam at the target. If the target has N_t nucleons per unit volume, or $N_t\, dz$ per unit area, the counting rate is

Figure 24

Kinematics of Coplanar Pion Pair Production

a Laboratory System, Total Energy E

b Center of Mass System, Total Energy E'

c Isobar Model: Laboratory System

d Isobar Model: Center of Mass System

e Isobar Model: Isobar Rest System

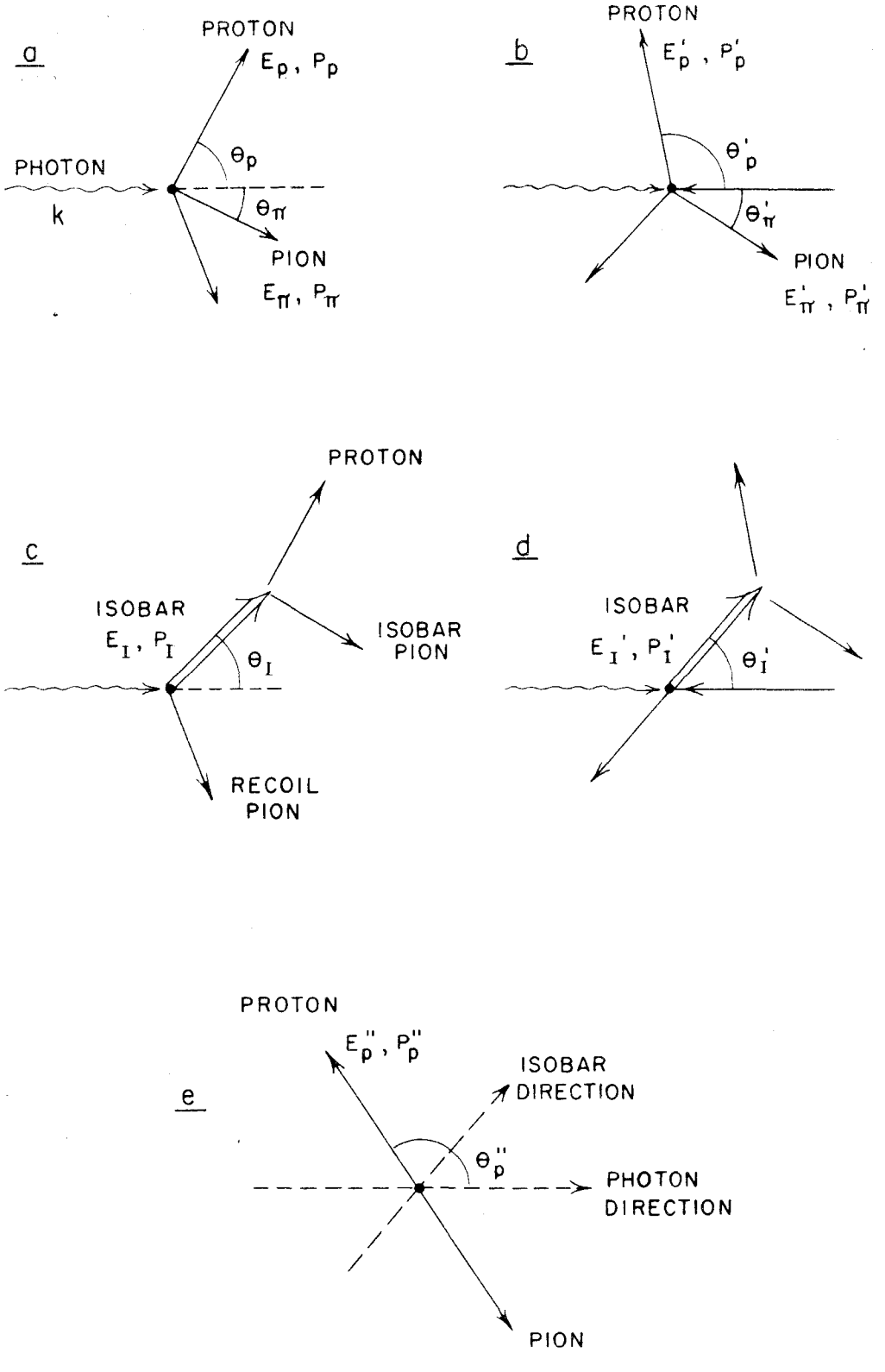
a
PROTON
E_p, P_p
θ_p
PHOTON
k
θ_π
PION
E_π, P_π
b
PROTON
E'_p, P'_p
θ'_p
θ'_π
PION
E'_π, P'_π
c
PROTON
ISOBAR
E_I, P_I
θ_I
ISOBAR
PION
RECOIL
PION
d
ISOBAR
E_I', P_I'
θ_I'
e
PROTON
E''_p, P''_p
ISOBAR
DIRECTION
θ''_p
PHOTON
DIRECTION
PION

$$dC = \frac{Q B(K)}{K} dK \; \eta(x,y)\, dx\, dy\, N_T\, dz\, \sigma(K, T_p, \theta_p, \theta_\pi)\, dT_p\, d\Omega_p\, d\Omega_\pi$$

for protons emerging in the energy range dT and in the solid angle $d\Omega_p$, accompanied by a pion in the solid angle $d\Omega_\pi$. The total counting rate is given by a nine-fold integral:

$$C = \int \frac{Q B(K)}{K} \eta(x,y)\, N_T \sigma \; dx\, dy\, dz\, dK\, dT_p\, d\Omega_p d\Omega_\pi \qquad (2)$$

where the limits of integration are given by the target size, the telescope sizes and energy acceptance, and the maximum photon energy.

As for two body reactions, this integral can be simplified, assuming certain approximations to be valid. If the finite size of the target is not important, the integration over x, y, and z gives $\int n(x, y)\, dxdydz = \bar{l}$, the effective target length. If $Q\, B(E_o, k)\sigma/k$ does not vary greatly within the integration limits of T_p, Ω_p, and Ω_π,

$$C \approx N_T\, \bar{l}\; \Delta T_p\, \Delta\Omega_p\, \Delta\Omega_\pi \int_o^{E_o} \frac{Q B(E_o, K)}{K} \sigma \; dK \qquad (3)$$

where ΔT_p, $\Delta\Omega_p$, and $\Delta\Omega_\pi$ are the energy and angular intervals accepted by the telescopes, and E_o is the maximum photon energy.

Pion pair results have commonly been expressed as yield "per equivalent quantum," defined as

$$\sigma^*(E_o, T_p, \theta_p, \theta_\pi) = \int_o^{E_o} \frac{B(E_o, K)}{K} \sigma(K, T_p, \theta_p, \theta_\pi)\, dK \qquad (4)$$

so that the counting rate is

$$C \approx N_T \bar{I} \Delta T_p \Delta\Omega_p \Delta\Omega_\pi Q \sigma^* \qquad (5)$$

The difference in yield for two settings of E_o can be used to find the actual cross section, by the method of photon differences. With fixed values of T_p, θ_p, and θ_π the definition of yield per equivalent quantum gives, for $E_2 > E_1$:

$$\sigma^*(E_2) - \sigma^*(E_1) = \int_o^{E_2} \frac{B(E_2,K)}{K} \sigma dK - \int_o^{E_1} \frac{B(E_1,K)}{K} \sigma dK$$
$$= \int_o^{E_2} \frac{R(K)}{K} \sigma dK$$

The resolution function $R(k) = B(E_2,k) - B(E_1,k)$ consists mostly, but not entirely, of photons with energies between E_1 and E_2. If the cross section σ were small below E_1, one could use the thin-target bremsstrahlung spectrum measured by Donoho, Emery, and Walker (13) to get

$$\int_o^{E_2} \frac{R(K)}{K} \sigma dK \approx \frac{B_o \Delta K}{\bar{K}} \sigma$$

where $B_o = 0.9$ is the value of B for $2E_o/3 < k < E_o$. Therefore,

$$\sigma(K, T_p, \theta_p, \theta_\pi) \approx \frac{K}{B_o \Delta K} [\sigma^*(E_2) - \sigma^*(E_1)] \qquad (6)$$

with $\Delta k = E_2 - E_1$ and $\bar{k} = (E_1 + E_2)/2$.

Unfortunately the cross section can be quite large below 900 or 920 Mev, the values of E_1 used in this experiment. Sands (44) has calculated more accurately the solution of the integral equation 4. He finds

$$\sigma(K=E_o, T_p, \theta_p, \theta_\pi) = \frac{E_e}{B_o}\left\{\frac{d\sigma^*(E_o)}{dE_o} + \frac{1}{B_o}\int_o^{E_o} \frac{\partial^2 B(E_o,K')}{\partial E_o\, \partial K'}\, \sigma^*(K')dK'\right\} \quad (7)$$

The first term is the same as the approximate expression 6. The other term is a correction which can be estimated from the appropriate data.

IV. OPERATION AND RESULTS

Five distinct series of measurements were made in the course of this experiment. Because of the exploratory nature of the work, the first two sets of runs were intended to identify the observed reaction as pion pair photoproduction. The subsequent runs were designed to measure the reaction cross section, and in particular to test the validity of the isobar model.

The experimental arrangement as previously described contained four adjustable kinematic parameters – the angle and energy settings of the proton telescope, the angle of the pion telescope, and the maximum photon energy in the synchrotron beam. Since all measurements were made for photon, proton, and pion in the same plane, a single angle specifies the proton direction and another angle the pion direction.

In the first series of runs, the yield of 122 Mev protons at 30° in coincidence with pions at 30° was measured as the peak photon energy was set successively at 1080, 920, 750, and 600 Mev. The next runs were made with the same proton telescope settings, but with the maximum photon energy left at 1080 Mev and with the pion angle set successively at 30°, 48°, and 70°. The third set of runs was taken with pion angle $33\frac{1}{2}^{\circ}$, proton energy 244 Mev, and proton angle 20°, 30°, 40°, and 50°. During these runs the maximum photon energy was alternated between 1080 and 920 Mev, so that the method of photon differences could give a definite cross section.

Because the data from this third set of runs appeared inconsistent with the attempted interpretations, the 30° and 40° points were measured again, using modified telescopes, the pressure-fed target, and the second of the electronic systems described earlier. The final runs were similar in that again the pion angle was $33\frac{1}{2}^{\circ}$ and several proton angles were measured; the peak photon energy was 900 or 1080 Mev. During these runs the wedge-shaped absorber was placed in the proton telescope, to narrow the effective angular resolution.

Experimental data were taken for a total of 30, 000 Bips; 18, 400 of these were used in the "wedge runs." Because the pressure-fed target gave an appreciable background when empty, it was necessary to run almost 5000 Bips without hydrogen. Several thousand Bips were also used in aligning the equipment, calibration runs, etc.

Table II lists the kinematic parameters of each measured point, and gives the corresponding counting rate and yield per equivalent quantum. The yields were calculated from equation 5, using the values of angular and energy acceptance of table I. $N_t\bar{l}$ was taken to be 3.06×10^{23} protons/cm^2 for the liquid target, and 2.09×10^{23} for the pressure-fed target. Q for standard temperature and pressure was obtained from the work of Gomez on the Cal Tech ion chamber (12); these values were increased by 11.1 % for the effect of atmospheric temperature and pressure. This corresponds to an average temperature of 25°C and a pressure of 745 mm. Hg. More detailed corrections were not warrented by the accuracy of the data. A correction for nuclear absorption in the proton telescope was made,

Table II

E_o Mev	T_p Mev	θ_p^o	θ_π^o	COUNTS / 100 BIPS Full target	COUNTS / 100 BIPS Empty target	σ^* cm^2/Mev sterad^2 x 10^{-32}
1080	123	30	30	78.40±3.96		9.06 ± .81
920	123	30	30	88.80±4.22		9.02 ± .79
750	123	30	30	58.33±4.42		5.08 ± .56
600	123	30	30	13.50±2.60		1.00 ± .23
1080	123	30	48	63.45±4.07		7.33 ± .73
1080	123	30	70	70.75±4.20		8.17 ± .78
1080	243	20	331/2	16.80±1.30	2.00 ± 1.00	4.06 ± .45
920	243	20	331/2	11.25±1.19	1.50 ± 0.87	2.36 ± .36
1080	243	30	331/2	12.70±1.13	1.50 ± 0.87	3.07 ± .38
920	243	30	331/2	6.12±0.78	1.00 ± 1.00	1.24 ± .31
1080	243	40	331/2	6.58±0.74	1.00 ± 1.00	1.53 ± .33
920	243	40	331/2	2.00±0.50		.48 ± .27
1080	243	50	331/2	1.00±0.33		.27 ± .16
920	243	50	331/2	0.30±0.30		.07 ± .07
1080	240	30	331/2	5.36±0.70		2.93 ± .56
900	240	30	331/2	2.90±0.63		1.37 ± .39
1080	240	40	331/2	3.47±0.45		1.89 ± .36
900	243	40	331/2	0.50±0.25		.24 ± .14
1080	200-303	25	331/2	4.30±0.44	1.22 ± 0.37	2.24 ± .41
900	200-303	25	331/2	2.41±0.45	0.67 ± 0.33	1.10 ± .35
1080	200-303	30	331/2	3.55±0.42	0.56 ± 0.25	2.18 ± .35
900	200-303	30	331/2	1.54±0.39	0.30 ± 0.20	.78 ± .28
1080	200-303	35	331/2	2.42±0.36	0.40 ± 0.28	1.47 ± .33
900	200-303	35	331/2	1.09±0.44	0 ± 0.25	.69 ± .31
1080	200-303	39	331/2	2.82±0.36	0.33 ± 0.24	1.82 ± .31
900	200-303	39	331/2	0.29±0.20	0 ± 0.18	.18 ± .16
1080	200-303	42	331/2	1.70±0.41	0.33 ± 0.33	1.00 ± .38
900	200-303	42	331/2	0 ±0.33	0 ± 0.12	0 ± .22
1080	200-303	45	331/2	0.86±0.35	0 ± 0.33	.63 ± .35
900	200-303	45	331/2	0 ±0.23	0 ± 0.09	0 ± .16

using the standard values for absorption of protons by copper (11). This correction multiplied the counting rates by 1.11 for the 123 Mev proton points, and by 1.45 for the 243 and 240 Mev points.

Yield calculations for the runs with the wedge absorber are somewhat less accurate than for the normal telescopes. With the wedge, the proton energy acceptance varied from 23 Mev to 17 Mev across the telescope; an average value of 20 Mev was taken. The absorption correction factor varied from 1.30 to 1.72; again, an average value of 1.51 was used. Such simple calculations ignore proton angular anisotropy, which could make the average value incorrect if one part of the telescope counted much more than another. However, the limited statistical accuracy of the data precludes a more exact calculation.

The correction for pion absorption was a factor of 1.08 for the earlier pion telescope, but was 1.53 for the later telescope which included a $1\frac{1}{2}$ inch copper absorber.

Runs without liquid hydrogen in the target were made for some of the points. The empty target counting rate is also given in table II. This background has been subtracted in the calculation of yields. Average backgrounds of 12 $^{o}/_{o}$ for the liquid target and 18 $^{o}/_{o}$ for the pressure-fed target were assumed for the points where no empty runs were made, with an error of half this amount. The errors given in the table are statistical counting errors.

Cross sections can be calculated from the yields of the later runs by means of equation 7. The first term of this equation, the

same as equation 6, was evaluated directly from the data. The integral in the second term was estimated numerically, assuming that $\sigma^*(E_o)$ rises linearly from threshold to the measured value at 900 or 920 Mev, and assuming that $B(E_o, k)$ is given by $1.35\left(1 - \frac{k}{E_o} + \frac{3}{4}\frac{k^2}{E_o^2}\right)$ for $k < \frac{2}{3}E_o$ and by $B_o = 0.9$ for larger k. The reaction threshold was so high for most proton angles that this correction term was zero; for the 20^o point it was less than 0.1 % of the first term. The cross sections are listed in table III. The statistical errors are quite large, since cross section is calculated by subtracting numbers of comparable size.

It is generally of interest to express cross sections in the center of mass system of the reaction. This can be done by the transformation

$$\sigma' = \frac{dT_p}{dT_p'}\,\frac{d\Omega_p}{d\Omega_p'}\,\frac{d\Omega_\pi}{d\Omega_\pi'}\,\sigma \qquad (8)$$

Here

$$\frac{dT_p}{dT_p'}\,\frac{d\Omega_p}{d\Omega_p'} = \frac{P_p'}{P_p} \quad ; \quad \frac{d\Omega_\pi}{d\Omega_\pi'} = \frac{P_\pi'^2}{P_\pi^2}\,\frac{P_\pi(E-E_p) - KE_\pi\cos\theta_\pi + E_\pi P_p\cos(\theta_p+\theta_\pi)}{P_\pi'(E'-E_p') + E_\pi' P_p'\cos(\theta_p'+\theta_\pi')} \qquad (9)$$

where the primed quantities refer to the cm system. Table III gives the cm cross sections, as well as the cm values of proton energy and angle and of pion angle for each point. Since the proton energy was held constant in the lab as the angle was varied, each point had different

Table III

$\bar{k}$ Mev	T_p Mev	θ_p^o	θ_π^o	$\frac{\sigma}{cm^2 \times 10^{-32}}$ $Mev^{-1} sterad^{-2}$	T'_p Mev	θ'^o_p	θ'^o_π	$\frac{\sigma'}{cm^2 \times 10^{-32}}$ $Mev^{-1} sterad^{-2}$
1000	243	20	33 1/2	11.8 ± 4.0	35	73	57	1.79 ± 0.61
1000	243	30	33 1/2	12.7 ± 3.4	66	88	57	2.71 ± 0.72
1000	243	40	33 1/2	7.3 ± 3.0	110	98	57	2.00 ± 0.82
1000	243	50	33 1/2	1.4 ± 1.2	164	107	57	0.47 ± 0.40
990	240	30	33 1/2	9.5 ± 4.2	65	88	57	2.02 ± 0.89
990	240	40	33 1/2	10.1 ± 2.4	109	98	57	2.77 ± 0.66
990	200-303	25	33 1/2	7.0 ± 3.3	51	79	57	1.28 ± 0.60
990	200-303	30	33 1/2	8.5 ± 2.7	68	86	57	1.81 ± 0.58
990	200-303	35	33 1/2	4.8 ± 2.7	89	92	57	1.19 ± 0.67
990	200-303	39	33 1/2	10.0 ± 2.2	107	96	57	2.67 ± 0.59
990	200-303	42	33 1/2	6.1 ± 2.6	122	99	57	1.68 ± 0.72
990	200-303	45	33 1/2	3.8 ± 2.3	137	102	57	1.08 ± 0.65

cm energy and angle. Thus it is probably meaningless to express these cross sections in the cm system, except perhaps for comparison with future results. A true angular distribution measurement in the cm system would require the laboratory energy and angle to be varied in such a way as to keep the cm energy constant. This type of experiment will be discussed in a subsequent section.

V. INTERPRETATION OF RESULTS

A. General Discussion

Figure 25 shows the yield per equivalent quantum for the first series of runs, with a smooth curve through the points. The threshold for pion pair production, if a 123 Mev proton at 30^{o} and a pion at 30^{o} are required, is 539 Mev. The curve is drawn to go to zero at that energy.

The nature of the curve in this figure is evidence that the reaction being observed is really pion pair photoproduction. Triple pion production requires more than 700 Mev of photon energy, for the given telescope settings. The curve is not detailed enough to exclude counts from this reaction, but the yield seems to decrease smoothly toward the pair threshold. On the other hand, if the observed counts were due to single π^{o} production (with one γ-ray converting to give a pion telescope count), the threshold would be 407 Mev. The yield curve does not appear to extend to this energy.

The qualitative shape of the curve is similar to the yield of negative pions from pion pairs, as observed by Bloch (30) and others. That is, it starts with small slope at threshold, rises rapidly, and then appears to level off. Quantitative comparison with the π^{-} yields cannot be made, since the relation of pion and proton energy is undefined unless the photon energy is known (as in photon difference work). Moreover, the negative pion yields were integrated over all possible proton angles. Finally, the pion telescope in this experiment responded equally well to positive and to negative mesons, so a

Figures 25 and 26

25 Yield per Equivalent Quantum versus Maximum Photon Energy

Proton Energy 123 Mev

Proton Angle 30^{o}

Pion Angle 30^{o}

26 Yield per Equivalent Quantum versus Pion Angle

Proton Energy 123 Mev

Proton Angle 30^{o}

Maximum Photon Energy 1080 Mev

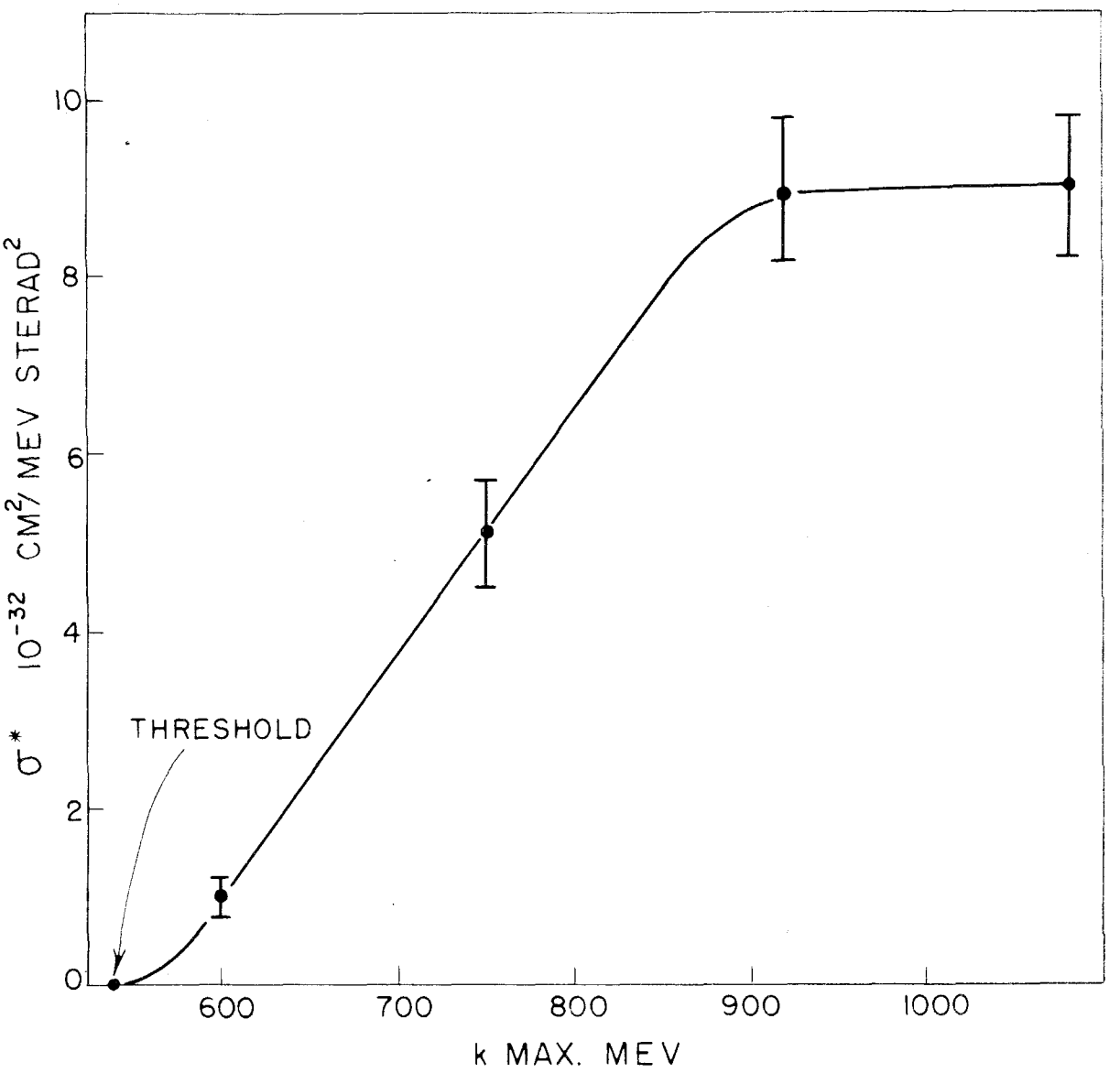
10
8
6
4
2
0
σ* 10^-32 CM^2/ MEV STERAD^2
THRESHOLD
600
700
800
900
1000
k MAX. MEV

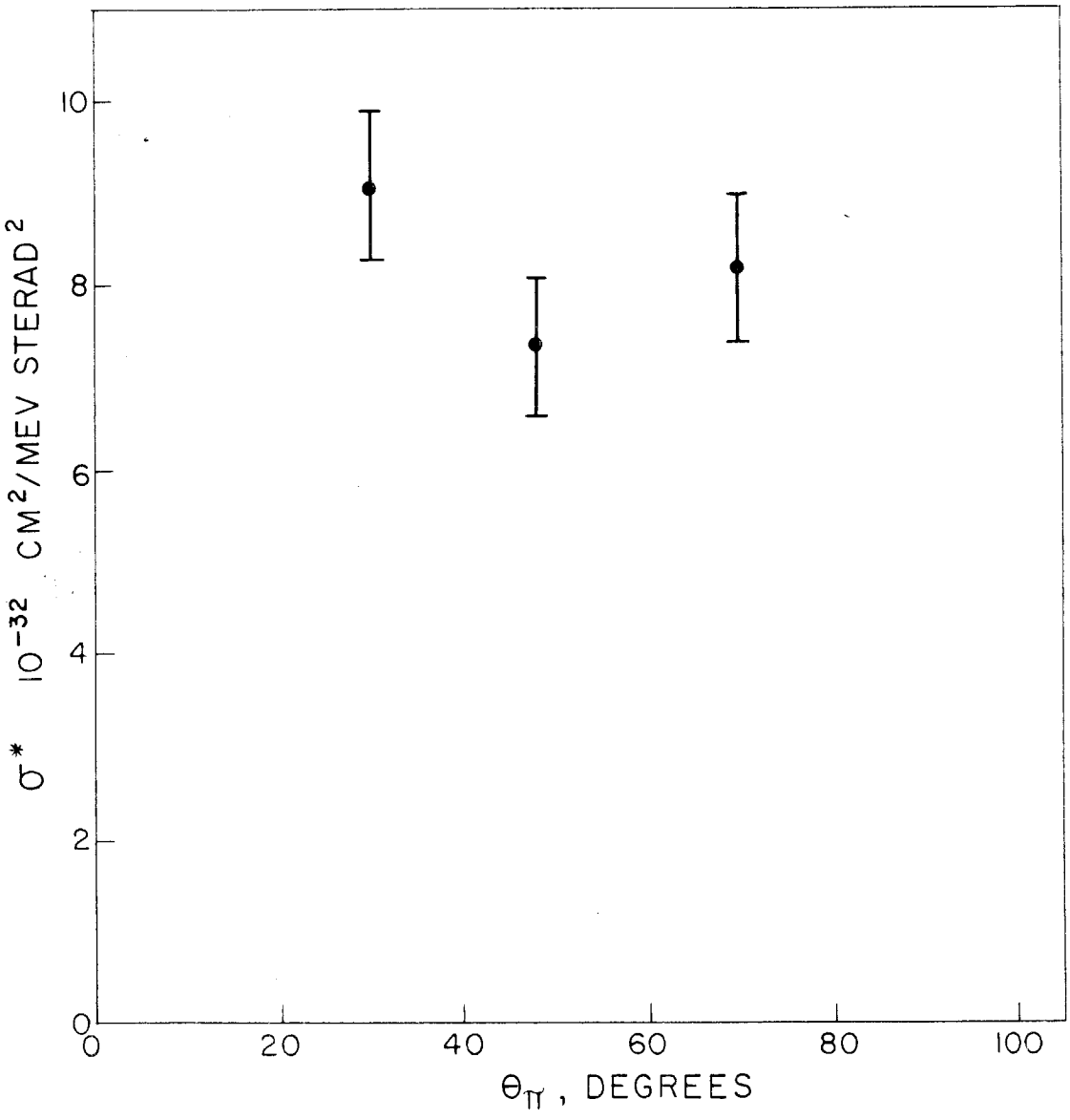
10
8
6
4
2
0
0
20
40
60
80
100
σ* 10⁻³² CM²/MEV STERAD²
θπ , DEGREES

comparison with π^- yields alone is meaningless.

Figure 26 shows the reaction yield for the second series of runs, wherein the pion telescope angle was varied. The fact that the yield does not depend strongly on angle is further evidence that the observed counts are from a three (or more) body reaction. The kinematics of pion pair production by a 1000 Mev photon allow a pion to emerge at any angle from 0° to 180°, if a 122 Mev proton at 30° is required. In single pion production, such protons would be accompanied only by pions at 95°. The fact that the yield does not rise sharply for larger angles shows that π° γ-ray conversion contributes little to the counting rate. As previously noted, more conclusive evidence against π° counts was obtained from runs with a lead converter in front of the pion telescope.

The cross sections obtained by photon differences in the later series of runs give a proton angular distribution which can be interpreted according to various models for the pair production process. Relativistic kinematic considerations indicate that the laboratory distributions should be more or less peaked near the maximum proton angle – around 40°, in this experiment – regardless of the model used. The earliest cross section measurements (243 Mev protons) showed no such peak, within the very poor statistics. The 30° and 40° points were consequently repeated, with somewhat different equipment (240 Mev protons). The 30° point came out lower and the 40° point higher than before (though within the statistical errors of the earlier measurement), so that the discrepancy with theory was not so bad. Finally a complete distribution was measured with wedge absorber to improve the proton angular

resolution. The results were again within the errors of the earlier runs, but indicated a peak near 40^{o}. Unfortunately the empty pressure-fed target gave a considerable background of counts, so that almost 20,000 Bips of running provided fairly poor statistical accuracy. Figure 27 shows the results of the three sets of runs.

Detailed comparison of these cross sections with earlier experimental results is not possible. The π^- cross sections measured by Bloch (30) and others are integrated over all possible proton angles and energies. Assuming isotropic production, Bloch estimates a total cross section of 5×10^{-29} cm^2, more or less independent of photon energy. In this experiment, if the cm angle and kinetic energy of the protons are uniformly distributed over the 4π steradians and 100 Mev or so available, and if the pion angles are then uniformly spread over all possible values (about 2π steradians), this total cross section corresponds to a cm differential cross section on the order of 1×10^{-32} cm^2/Mev sterad^2. This agrees with the values in table III. A more exact calculation of the total cross section would require an explicit model of the production process to give definite energy and angle distributions. Elliott (37) finds the π^+ meson to be isotropically distributed relative to the π^-, which supports the rough estimate just given.

B. Theoretical Considerations

The limited accuracy of the present measurements precludes serious comparison with theoretical predictions. Nevertheless, some calculations of proton angular distributions according to various models

Figure 27

Laboratory Cross Sections versus Proton Angle

Early Runs:	Proton Energy 243 Mev
	Pion Angle 33 1/2^{o}
	Photon Energy 1000 Mev
Middle Runs:	Proton Energy 240 Mev
	Pion Angle 33 1/2^{o}
	Photon Energy 990 Mev
Late Runs:	Proton Energy 200-303 Mev
	Pion Angle 33 1/2^{o}
	Photon Energy 990 Mev

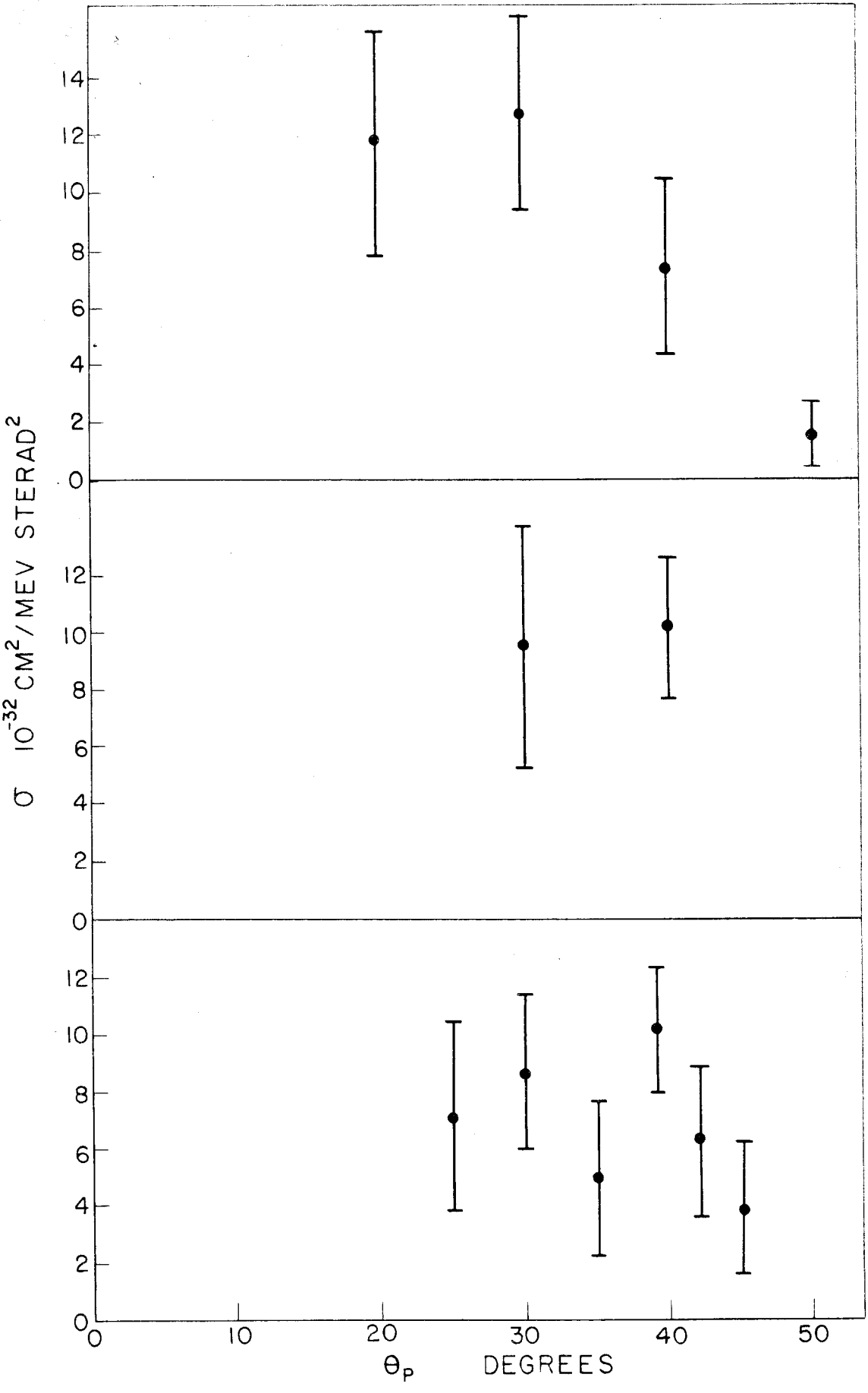
σ 10^-32 CM^2/MEV STERAD^2
θp DEGREES
0
2
4
6
8
10
12
14
20
30
40
50

will be given, largely in the hope of comparison with future experimental work.

Cutkoski and Zachariasen (35) have applied the Chew-Low meson theory to multiple production. Their calculation gives the energy and angular dependence of the two pions, but it is only valid for energies near threshold (320 Mev). There is evidence (37) that their distributions are not correct for 740 Mev photons; at 1000 Mev, as in this experiment, there is little to be learned from their calculations. A chief reason for the low energy requirement is the theory's assumption that one meson emerges in a P state and the other in an S state. The cm energies of this experiment are so large that there is no reason for this assumption to be valid.

Two simple models for double meson production at high energies will be considered: the one in which the reaction is governed only by the density of final states, and the so-called isobar model. In both these cases the proton distributions are determined solely by kinematic considerations. Neither model has been particularly successful when applied to other experimental results, but there is no more satisfactory theory for multiple production at the energies of this experiment.

1) Density of States

If the matrix element of the interaction were independent of the kinematic parameters being observed (in this case, the angular distributions of the proton and pion and the proton energy spectrum),

these distributions would depend only on the density of final states. This assumption that the matrix element is independent of the final state leads to a definite prediction for the variation of cross section with proton angle.

In the center of mass system, the density of final states is ($\hbar = c = 1$):

$$\rho = (2\pi)^{-6} \frac{(E' - E_p' - E_\pi')\, E_p'\, E_\pi'\, P_p'\, P_\pi'^2\, dE_p'\, d\Omega_p'\, d\Omega_\pi'}{P_p'(E' - E_p') + E_\pi' P_p' \cos(\theta_p' + \theta_\pi')} \tag{10}$$

where $E' = \sqrt{2kM_p + M_p^2}$ is the total energy in the cm system, and the other kinematic parameters are shown in figure 24. We use the density of states in the cm system rather than the lab because this model assumes that the interaction matrix element is isotropic in the system for which ρ is calculated; this is far more likely to be true in the cm system. For comparison with laboratory cross sections, $dE_p'\, d\Omega_p'\, d\Omega_\pi'$ must be transformed to $dE_p\, d\Omega_p\, d\Omega_\pi$. Use of equation 9 gives

$$\rho = (2\pi)^{-6} \left\{ \frac{(E' - E_p' - E_\pi')\, E_p'\, E_\pi'\, P_p\, P_\pi^2}{P_\pi(E - E_p) - K E_\pi \cos\theta_\pi + E_\pi P_p \cos(\theta_p + \theta_\pi)} \right\} dE_p\, d\Omega_p\, d\Omega_\pi \tag{11}$$

where $E = k + M_p$ is the total lab energy. The quantity in brackets has been plotted as the solid curve in figure 28. The pertinent calculations were made on the Datatron computer as a sub-routine of the isobar model program. The extent to which the curve fits the data will be discussed after the corresponding curve for the isobar model has been presented.

Figure 28

Proton Distribution from 3-Body Density of States

Proton Energy 250 Mev
Pion Angle 33 1/2°
Photon Energy 1000 Mev

Dotted line is distribution integrated over 10° aperture.

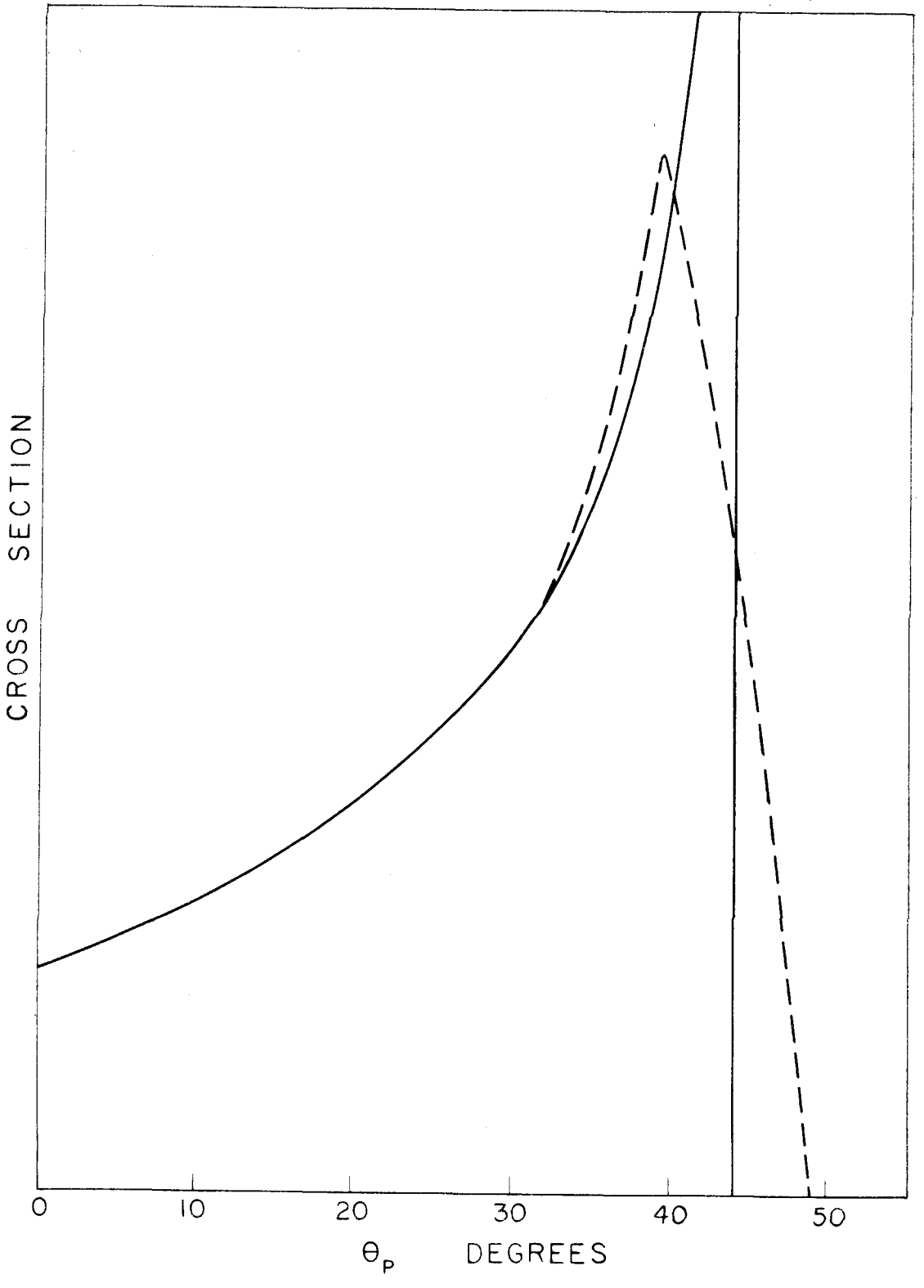
CROSS SECTION
0
10
20
30
40
50
θ_p DEGREES

It may seem surprising that the calculated cross section becomes infinitely large at the limiting proton angle. The cause of the singularity may be found by considering the derivation of equation 10. The density of states ρ is dN/dE', with the number of states dN equal to

$$(2\pi)^{-6}\ P_p'^2\, dP_p'\, d\Omega_p'\, P_\pi'^2\, dP_\pi'\, d\Omega_\pi'$$

This gives us dN/dP_π' ; ρ equals this divided by dE'/dP_π'. The latter expression is evaluated from

$$E' = [\,P_p'^2 + M_p^2\,]^{1/2} + [\,P_\pi'^2 + M_\pi^2\,]^{1/2} + [\,(-\underline{P_p'} - \underline{P_\pi'})^2 + M_\pi^2\,]^{1/2}$$

keeping P_p' fixed. At the limiting proton angle, the kinematics are such that dP_π' is equal to $-dP_\pi'$ for the other pion. Thus there is no energy change dE', so $dE'/dP_\pi' = 0$, and ρ becomes infinite.

The counting rate of course does not become infinite at the singular point. This illustrates a case in which the approximations leading from equation 2 to equation 3 are not justified. The counting rate depends on $\int \sigma\, d\Omega$ rather than $\sigma \times d\Omega$, and the integral over the angular acceptance of the proton telescope is well-behaved. This is illustrated by the dotted line of figure 28, which shows the result obtained by folding the calculated curve with a 10° angular "window," such as was used in this experiment.

2) Isobar Model

Experiments on elastic pion scattering and on single pion photoproduction have disclosed the well-known 3/2, 3/2 resonant state

of the pion-nucleon system. The model for double pion production to be considered here assumes that one pion and the recoil nucleon emerge together as a compound state or "isobar," with the other pion moving in such a way as to conserve energy and momentum. The isobar subsequently decays into a nucleon and a pion. This decay occurs in about 10^{-23} seconds, so that the isobar is still within about 10^{-13} cm. of the recoil pion; nevertheless, for the sake of calculation, the isobar decay is assumed independent of the recoil pion's presence. The following calculations show the application of this model to the present experiment.

Parts c, d, and e of figure 24 show the kinematics of the isobar reaction. Three coordinate systems are involved: the lab system, the cm system (primed), and the rest system of the isobar (doubly primed). Let q be the excitation energy of an isobar, which then acts kinematically like a particle of mass $M_p + M_\pi + q$. Earlier isobar calculations have assumed that the probability of forming an isobar with energy q was proportional to the product of two factors: first, the observed total cross section for pion scattering in the 3/2, 3/2 state at a cm energy of $q + M_p + M_\pi$; and second, the appropriate two-body phase space factor ρ for the recoil pion and isobar. ρ varies as $E_I' (E' - E_I') P_I'/E'$. Sands (45) has shown that it is more correct to multiply the observed total cross section by $(q + M_\pi)/P_\pi'$, where here P_π' is the cm pion momentum for pion scattering. He gives a curve of this product, which we call P(q). ρ P(q) is the probability of forming an isobar of energy q.

The expression $\rho\, P(q)\, dq\, d\Omega_I^{'}\, d\Omega_p^{''}$ is the probability of this isobar being emitted within the cm solid angle $d\Omega_I^{'}$, and subsequently giving a decay proton within $d\Omega_p^{''}$ in the isobar rest system. Two assumptions have been made here: the isobar is produced isotropically in the cm system, and it decays isotropically in its own rest system. The results obtained from non-isotropic distributions will be considered later.

This probability must now be expressed in terms of quantities defined by the experiment, namely dT_p, $d\Omega_p$, and $d\Omega_\pi$, all in the lab system. Two cases arise: the pion telescope can observe the recoil π or the isobar π. Since the telescope cannot distinguish between the pions, the results of these cases must be added to predict a distribution. This situation is in contrast to other experiments which use magnetic spectrometers. There the cases in which the isobar includes the negative pion (neutral isobar) or the positive pion (doubly-charged isobar) are experimentally distinguishable, and different cross sections can be calculated for each case. The inability of this experiment to distinguish the pion charge makes such a calculation meaningless here; the cross section is given by the sum of the "recoil" and "isobar" cases.

The derivation of lab cross sections will now be described. For the recoil pion case, $d\Omega_I^{'}$ is simply equal to $d\Omega_\pi^{'}$, so that

$$d\Omega_I' = P_\pi^2 E'\, d\Omega_\pi \Big/ P_\pi' (E P_\pi - K E_\pi \cos\theta_\pi)$$

The more complicated calculation for the isobar pion gives

$$d\Omega_I' = \frac{E' P_I P_\pi d\Omega_\pi}{K P_I'} \Big/ \left[E_I + E_\pi - \left(\frac{P_\pi E_I}{P_I} + \frac{P_I E_\pi}{P_\pi} \right) \cos(\theta_I - \theta_\pi) \right]$$

For either case it can be shown that

$$d\Omega_p'' = \frac{M_I P_p^2 d\Omega_p}{P_p''} \Big/ \left[E_I P_p + E_p P_I \cos(\theta_I - \theta_p) \right]$$

where $M_I = q + M_p + M_\pi$.

The calculation of proton angular distributions, as done on the Datatron computer, proceeds as follows. For a given photon energy, pion angle, and proton energy, equally spaced values of q are chosen. For each q the reaction kinematics are fixed; all the necessary lab and cm energies and angles are calculated, including the angle θ_p at which the proton emerges. $d\Omega_I'/d\Omega_\pi$ and $d\Omega_p''/d\Omega_p$ are evaluated from the preceding formulas. The product of these terms is multiplied by $\rho P(q)$ for the particular q chosen. Since the calculation is made for a specific value of proton energy rather than proton angle, $d\Omega_p$ is replaced by dT_p, using

$$d\cos\theta_p = \left\{ \left[E_I P_p - E_p P_I \cos(\theta_I - \theta_p) \right] \Big/ P_I P_p^2 \right\} dT_p$$

The expression

$$\left\{ \rho P(q) \frac{d\Omega_I'}{d\Omega_\pi} \frac{d\Omega_p''}{d\Omega_p} \frac{d\cos\theta_p}{dT_p} \right\} \Delta q \, \Delta\Omega_\pi \, \Delta T_p \qquad (12)$$

then gives the relative number of proton counts per steradian at the calculated proton angle. This number is stored in the computer as a

function of θ_p. Successive values of q are chosen, covering the entire range where P(q) is not zero. The calculation is repeated for each q, and the result shows the relative counting rate or cross section as a function of proton angle.

Figure 29a shows the angular distribution of 250 Mev protons from 1000 Mev photons for the case that the recoil pion emerges at $33\frac{1}{2}^{\circ}$; figure 29b is for the isobar pion at this angle. The sum of the two cases, which this experiment measures, is plotted in figure 30.

The most prominent feature of the proton distribution, the dip near 30°, represents the direction in which isobars tend to travel. For given q, protons of the required energy are emitted at a fixed angle to the isobar direction, and so appear both foreward and backward from the dip. The singularity at the limiting proton angle is a kinematic effect similar to that observed previously in the density of states curve. It is caused by the existence of a range of q values such that although the more energetic isobars appear at smaller angles, their extra energy ejects the proton further from the isobar direction, giving the same lab angle for all the protons. The singularity of course gives a finite value when integrated over θ_p, as shown by the dotted curve of figure 30.

In all the preceding calculations it has been assumed that isobars are produced isotropically in the cm system and decay isotropically in their rest system. Clegg (46) has suggested several non-isotropic distributions, determined by considerations of angular momentum and isotopic spin for various compound states of isobar plus

Figures 29, 30, 31

Proton Distributions from Isobar Model

Proton Energy 250 Mev

Pion Angle 33 1/2°

Photon Energy 1000 Mev

29a Recoil Pion Angle 33 1/2°

29b Isobar Pion Angle 33 1/2°

30 Sum of Recoil and Isobar Cases

Dotted line is distribution integrated over 10° aperture.

31 Anisotropic Isobar Production and Decay

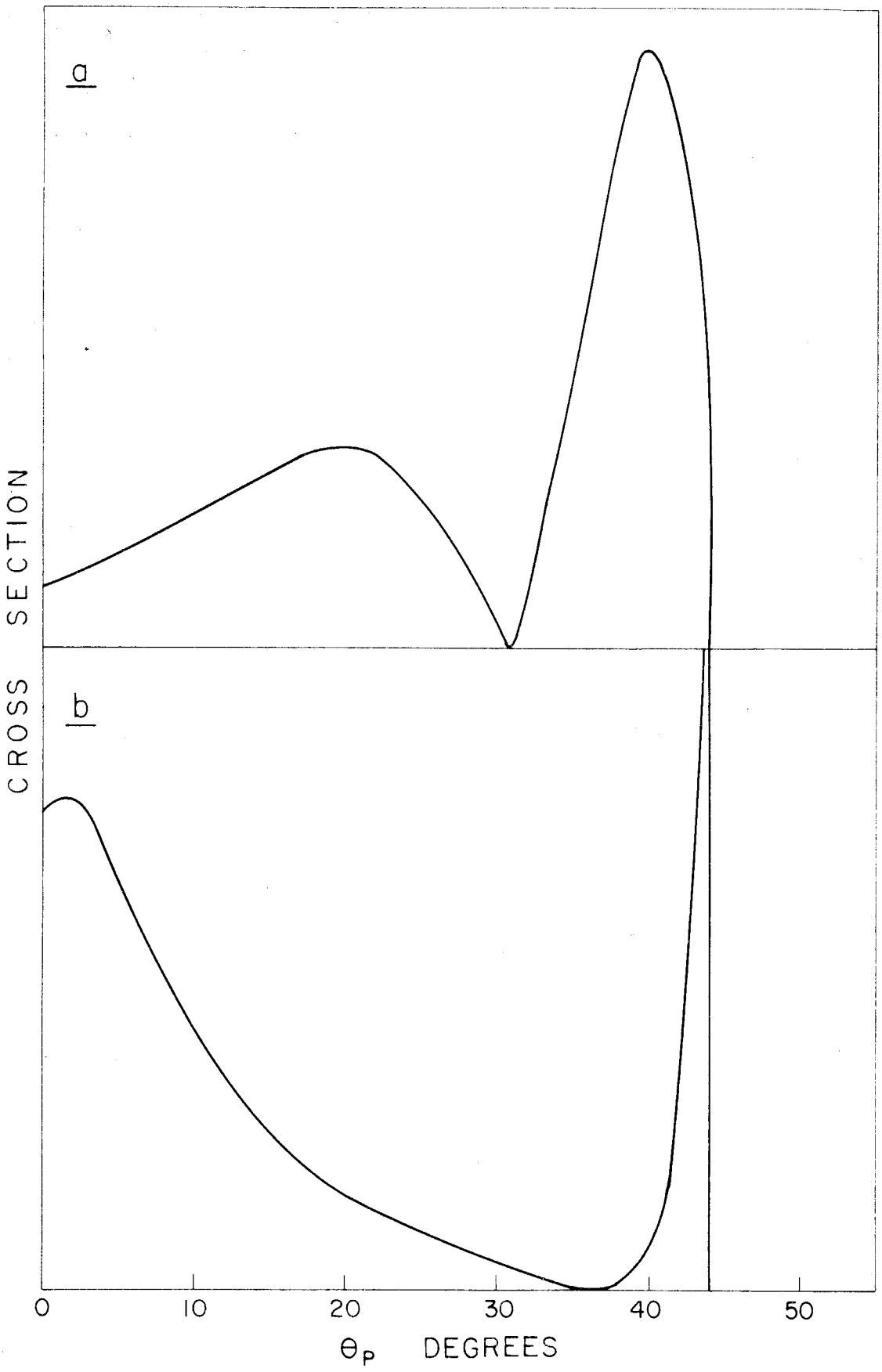
a
b
CROSS SECTION
0
10
20
30
40
50
θ_p DEGREES

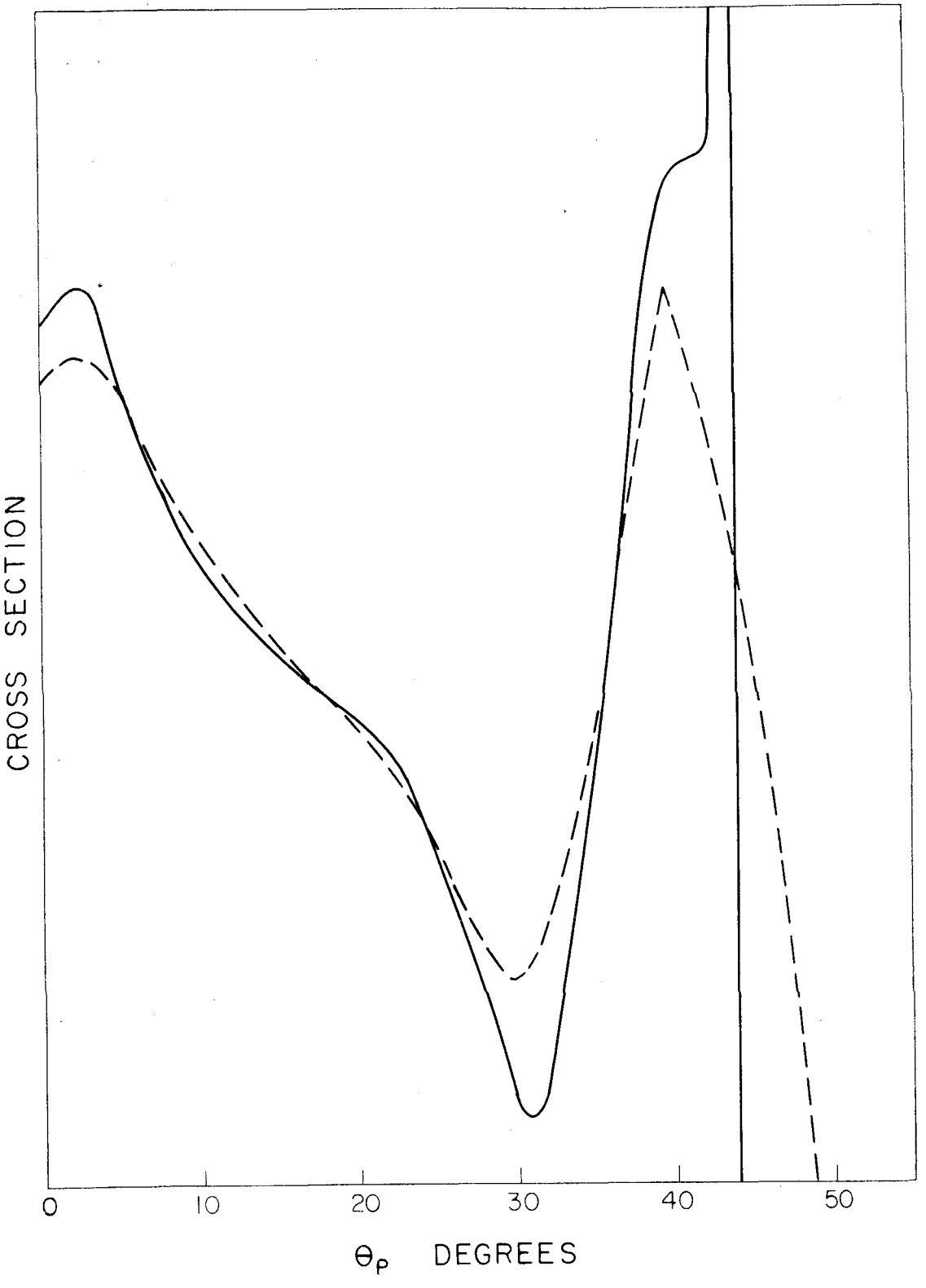
CROSS SECTION
0
10
20
30
40
50
θ_p DEGREES

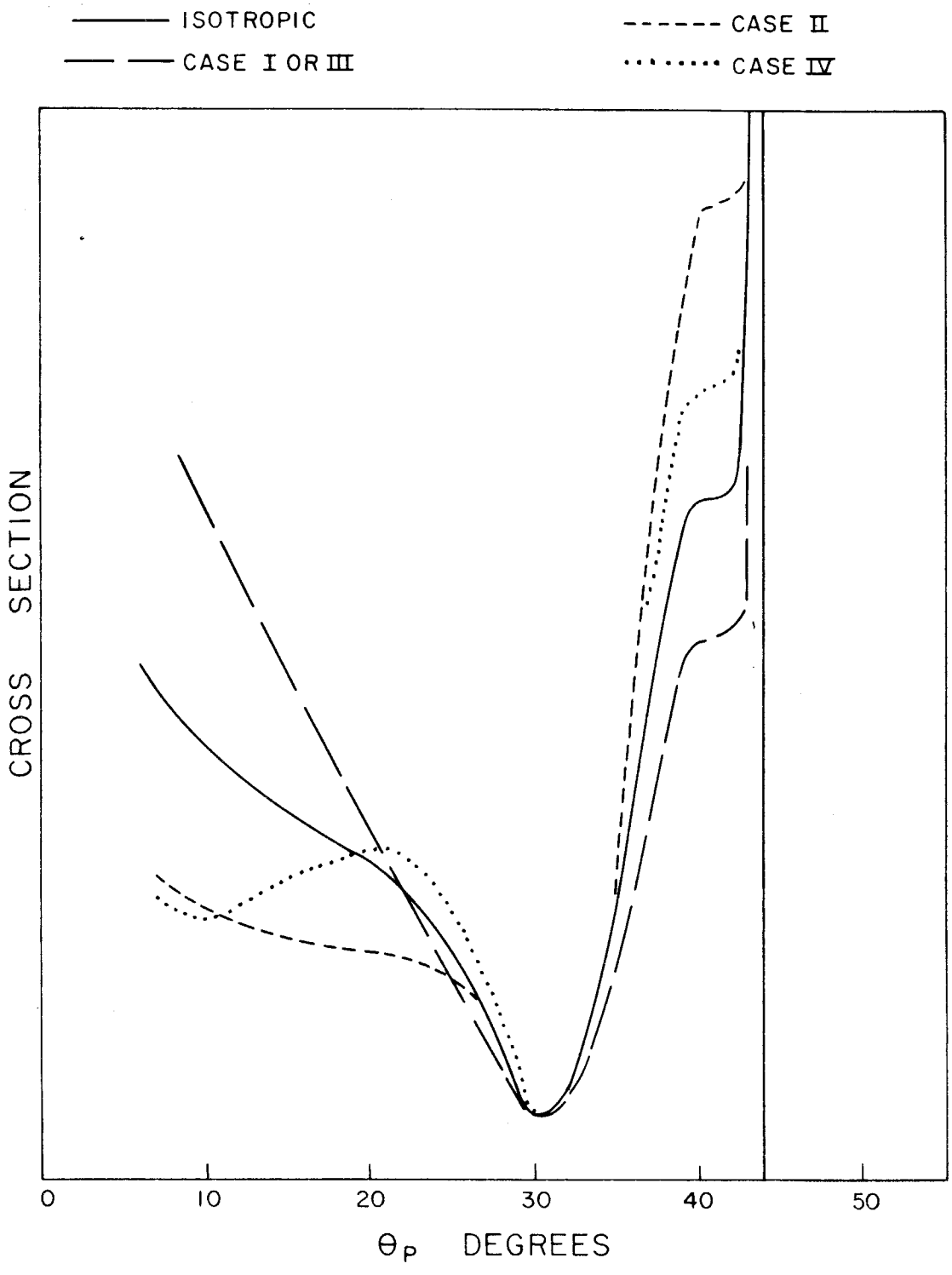
ISOTROPIC
CASE I OR III
CASE II
CASE IV
CROSS SECTION
0
10
20
30
40
50
θp DEGREES

recoil pion. He finds that the distribution of isobar decay protons is given by

$$1 + \frac{3(b-a)}{3a+b} \cos^2 \theta_p''$$

where θ_p'' is the proton angle in the isobar rest system.

Four cases are considered:

Case	Incoming photon multipole	Spin, parity of compound state	Angular distribution of isobar	a	b
I	E_1	1/2-	isotropic	$3(1-\cos^2\theta_I')$	$1+3\cos^2\theta_I'$
II	E_1	3/2-	isotropic	1	1/3
III	M_1	1/2+	isotropic	$3(1-\cos^2\theta_I')$	$1+3\cos^2\theta_I'$
IV	M_1	3/2+	$4+3\cos^2\theta_I'$	$3(1+8\cos^2\theta_I')$	$13-12\cos^2\theta_I'$

Note that cases I and III give the same distribution.

The preceding calculation of cross section vs proton angle was repeated, this time weighting θ_p'' and θ_I' according to the above distributions. Figure 31 shows the results. The distinctive peak and dip remain. The effect of non-isotropic distributions is to change the height of the peak relative to the dip, and to change the shape of the distributions at more foreward angles.

The proton distributions predicted by the two models just considered are quite distinctive. The peak and dip of the isobar model,

which contrast sharply with the smooth density of states curve, are kinematic effects and are not sensitive to the details of isobar production and decay. Good experimental distributions could certainly show which of these models (if either) is valid.

In considering the measured cross sections it must be remembered that the approximate equation 3 was used in their computation. They represent an average over the experimental intervals of proton energy and angle, pion angle, and photon angle. These intervals should therefore be folded into the calculated curves with which the points are compared. In figure 32 are shown such averaged curves. Note that the distributions from the two models are still quite distinct. The experimental points of figure 32 are those measured with the wedge absorbers, since these are the most numerous and are somewhat more accurate than the other points. The 50° point measured earlier is also shown.

As previously noted, the poor experimental statistics make it impossible to draw a definite conclusion regarding the two models of figure 32. Note that only the low 35° point prevents a fair fit with the density of states curve. On the other hand, the 30° point is the only one badly off the isobar curve. This is a significant discrepancy, since the isobar predicts such a low cross section here. Considerably more running in this angular region would be necessary to decide between the models.

Figure 32

Experimental Laboratory Cross Sections

The curves show the predictions of the two phenomenological models, averaged over the proton and pion solid angles, the proton energy interval, and the photon energy interval.

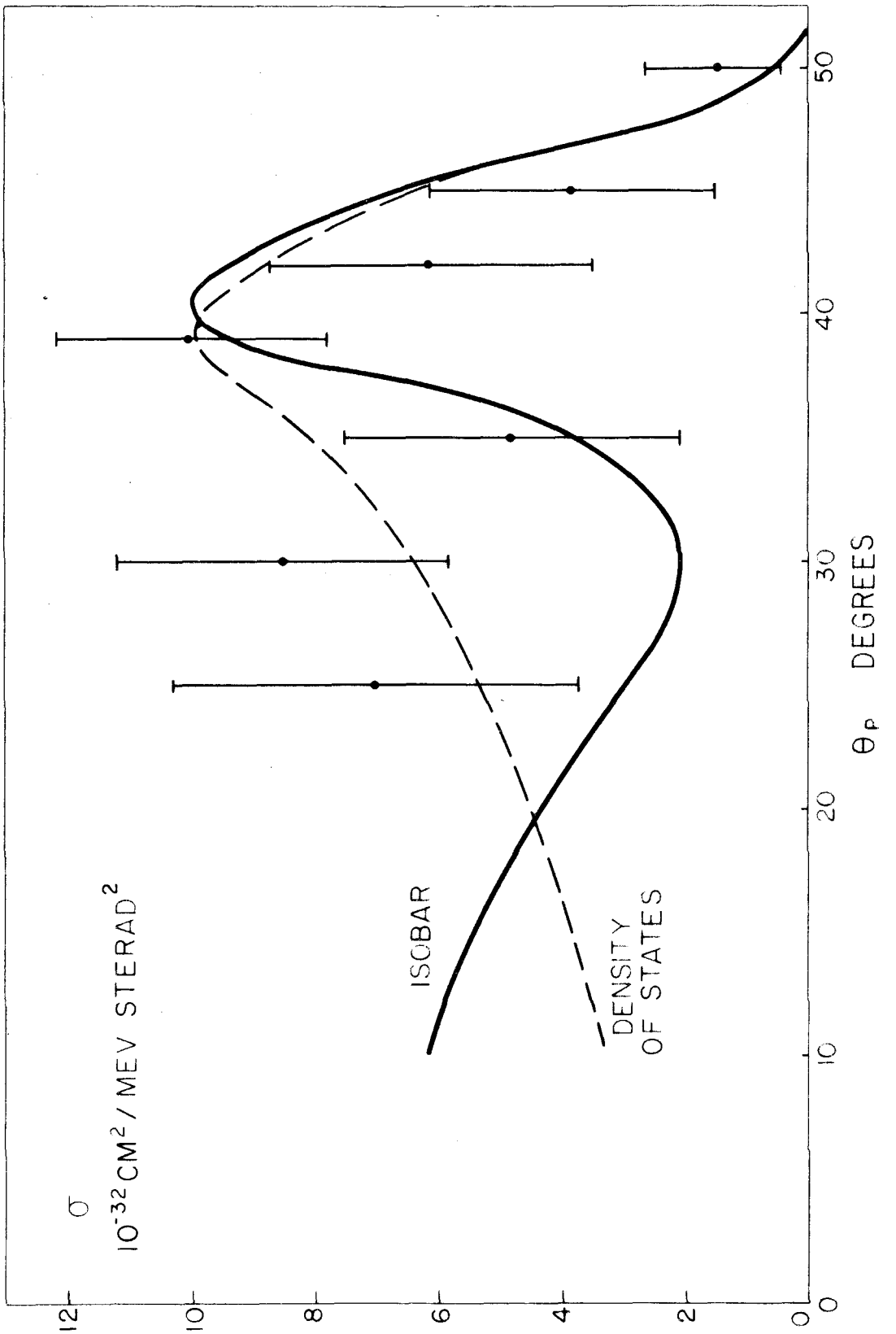
σ
10^-32 CM^2 / MEV STERAD^2
12
10
8
6
4
2
0
ISOBAR
DENSITY
OF STATES
0
10
20
30
40
50
θp DEGREES

VI. CONCLUSIONS AND SUGGESTIONS

The photoproduction of multiple pions in a hydrogen target has been studied by counting simultaneously a proton and charged pion. Yields have been measured as a function of peak photon energy, of pion angle, and of proton angle. The results in all cases are consistent with the observed reaction being coplanar pion pair production. Approximate cross sections have been obtained as a function of proton angle at about 1 Bev photon energy, 250 Mev proton energy, and $33\frac{1}{2}^{o}$ pion angle. The results are of about the right magnitude for a total cross section of 5×10^{-29} cm^2, but their poor accuracy prevents close comparison with the distribution predicted by three-body density of states or by the isobar model.

The most obvious course for future work would be to improve the accuracy of the cross sections measured in this experiment. In particular, the distribution near 30^{o} should confirm or destroy the applicability of the isobar model in this kinematic region.

It is of interest to see whether the isobar model predicts equally distinctive laboratory distributions for other energies. A standard telescope works quite well for protons between 100 and 300 Mev. Figure 33a shows the proton distributions from the isobar model for various proton energies, with the pion angle set arbitrarily at 30^{o}. Note that the dip in the curve becomes wider for lower proton energies. This would be expected from the previous explanation of the dip, namely, that it occurs near the angle at which

Figures 33, 34, 35

Proton Distributions from a Isobar Model
b Density of States

33 Photon Energy 1000 Mev
Pion Angle 30°
Various Proton Energies

34 Proton Energy 100 Mev
Pion Angle 30°
Various Photon Energies

35 Photon Energy 1000 Mev
Proton Energy 200 Mev
Various Pion Angles

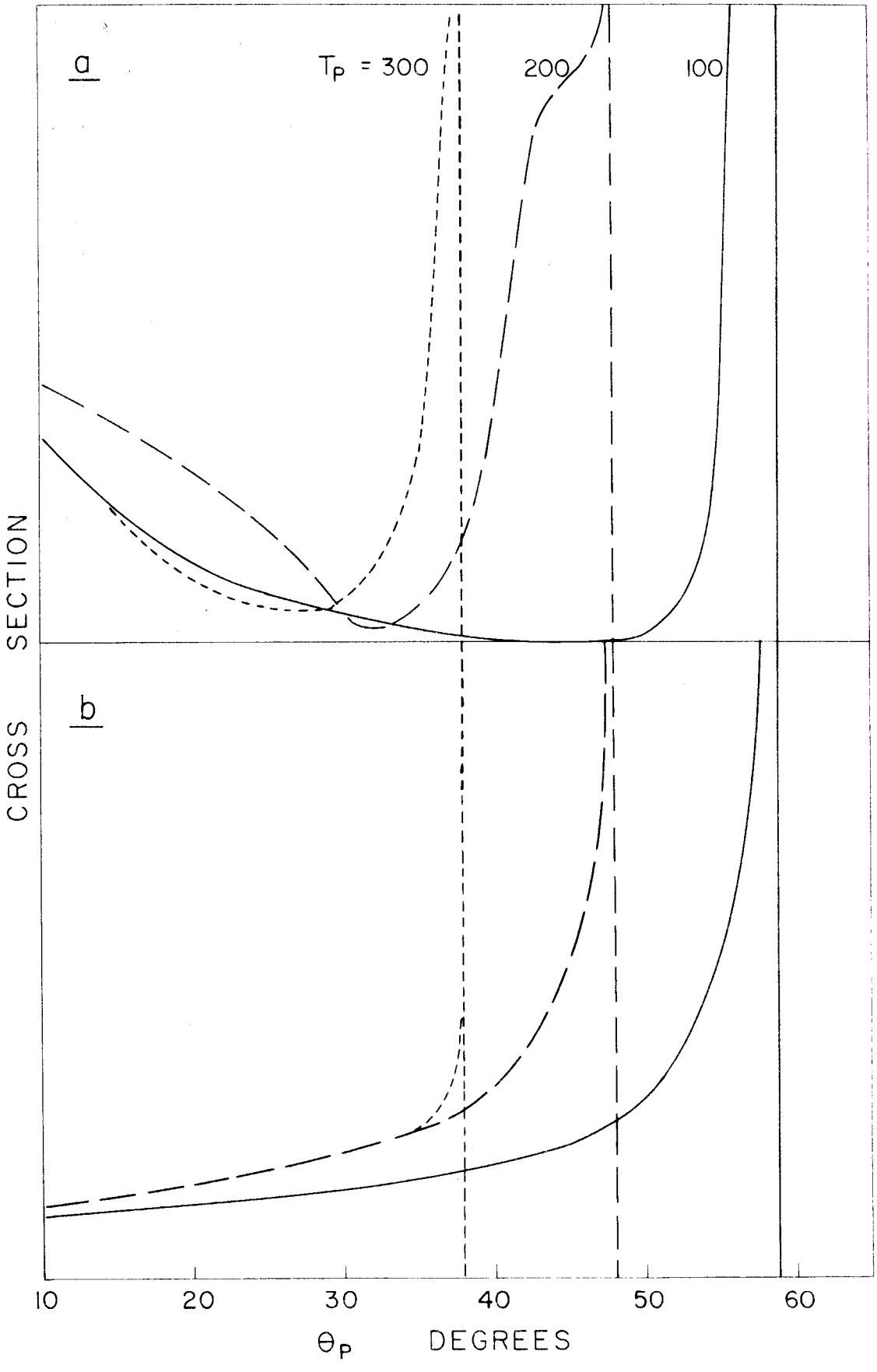
a
T_P = 300
200
100
b
CROSS SECTION
10
20
30
40
50
60
θ_P DEGREES

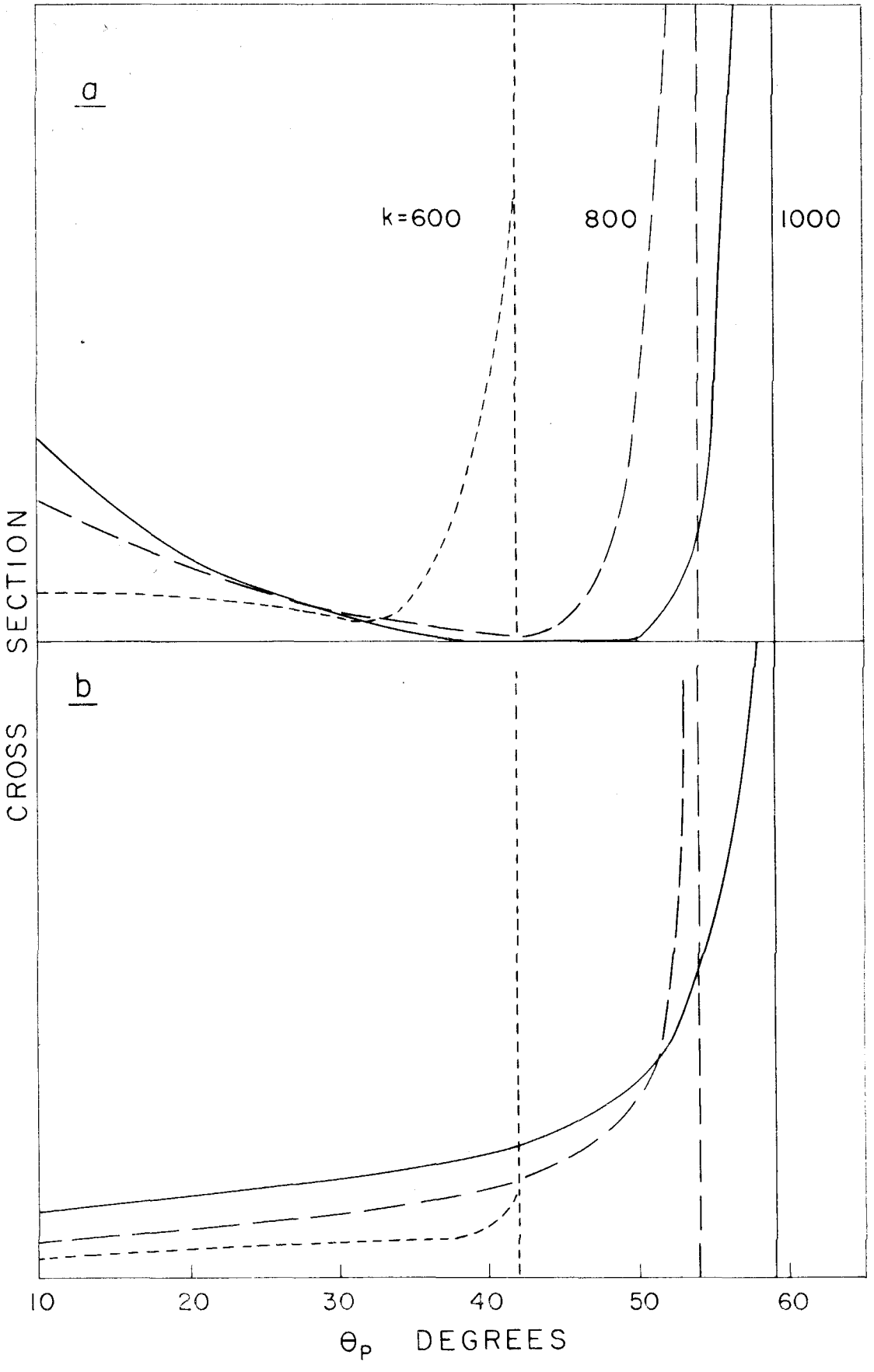
a
k=600
800
1000
b
CROSS SECTION
10
20
30
40
50
60
θp DEGREES

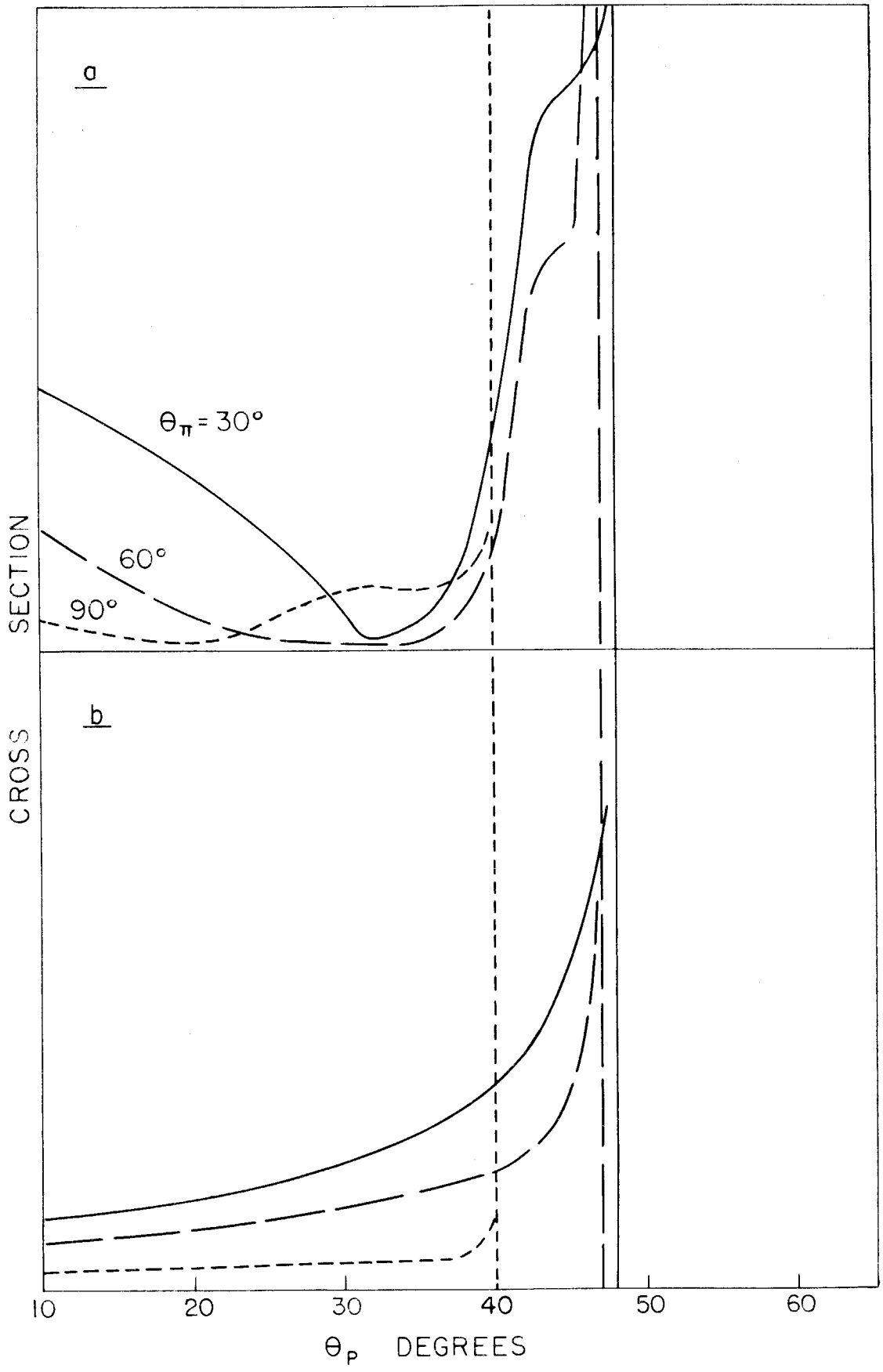
a
$\theta_\pi = 30°$
60°
90°
SECTION
b
CROSS
10
20
30
40
50
60
θ_p DEGREES

the isobars emerge. Lower energy protons appear further from the isobar direction, and the dip becomes wider. For comparison, figure 33b shows the smooth distributions given by the density of states equation.

The figure further justifies the use of wedge absorber in the proton telescope. As discussed earlier, the wedge shifts by 10^{o} the angle at which 300 Mev protons are counted relative to 200 Mev protons. If the 200 and 300 Mev curves of figure 33 are shifted left and right, respectively, by 5^{o} they approximately coincide. The effective angular resolution is greatly improved.

The behavior of the cross sections as the photon energy is changed is shown in figure 34. For the isobar model, the distribution for 100 Mev protons is not drastically affected until the photon energy is reduced below 800 Mev. Curves for higher energy protons of course are more strongly affected by photon energy because of the higher threshold. Changing the pion angle gives less interesting results. Figure 35 shows the distributions of 200 Mev protons for various pion angles. Larger angles emphasize the isobar dip, and strongly decrease the cross section for either calculation.

From an experimental point of view, measuring cross sections by means of photon differences has definite drawbacks. Not only must the synchrotron energy be constantly adjusted between various values, but also the necessary subtractions give quite large statistical errors unless each yield is quite accurately known. Two other methods could be used to fix the reaction kinematics and avoid these difficulties:

measure the pion energy in the pion telescope, or measure the angle of the second pion with another counter.

The feasability of these methods can be judged by examining their resolutions and counting rates. Counter experiments always represent a compromise between these factors of good resolution and high counting rate. It has been shown that the resolutions used in this experiment were not so large as to destroy the features of the proton distributions predicted by various models. In discussing alternative experiments, it is therefore reasonable to consider what would be required to give the same resolution as the photon difference method.

On this basis the use of another counter to find the angle of the second pion appears impractical. The pion emerges over an angular range of some 30 to 40 degrees, as the photon energy varies from 920 to 1080 Mev. This angular range often includes 180°, where no counter can be placed. It would be quite difficult to observe a large fraction of these pions; the counting rate of such an experiment would be low.

The other proposed experiment – measuring the pion energy – is somewhat more promising. The counting rate here is calculated by replacing Δk by ΔT_{π}, using

$$\left.\frac{\partial K}{\partial T_{\pi}}\right)_{T_p, \theta_p, \theta_{\pi}} = \frac{P_{\pi}(E-E_p) - KE_{\pi}\cos\theta_{\pi} + P_p E_{\pi}\cos(\theta_p+\theta_{\pi})}{P_{\pi}(E-E_p-E_{\pi})} \qquad (13)$$

This factor is on the order of 1; the resolution would be about the same as for photon differences if a pion energy acceptance ΔT_{π} equal

to Δk were used. However, a counter-absorber system accepting 100 or 200 Mev would have a large absorption correction.

A quantitative estimate of merit for the pion energy experiment, as opposed to the photon difference method, can be found. To give equally accurate cross section values the ratio of the number of Bips required is, approximately,

Photon diff. exp. /Pion energy expt. $\approx 2\beta\gamma(1+\alpha)/(1-\alpha)$. Here α is the ratio of yields at the upper and lower photon energies of the difference experiment; β is the ratio

$$\left(\frac{\partial K}{\partial T_\pi}\,\Delta T_\pi\right)\Big/\,\Delta K$$

for the two experiments; and γ is the efficiency of the pion energy telescope (considering losses by absorption, etc.) This formula assumes that the two photon difference yields are measured to equal accuracy, and that the proton and pion solid angles and proton energy intervals are the same for both experiments. Numerical values might be $\alpha \approx 1/2$ (as in this experiment), $\beta \approx 1$, $\gamma \approx 1/2$; these indicate that the photon difference experiment would have to run three times as long as the pion energy experiment to give equally good statistics. Note, however, that γ may not be known accurately if the absorption correction is large, which would decrease the advantage of the latter experiment.

The pion energy experiment has still another advantage. The numerator of equation 13 is the same as the denominator of equation 11; dk/dT_π goes to zero at the limiting proton angle and cancels the

singularity present there for fixed k. The result is a smooth proton distribution, which need not be carefully integrated over the various apertures for comparison with experimental results. Figure 36 shows these distributions for typical pion energies. Note that k changes with proton angle; the abrupt ends of the curves correspond to k exceeding 1080 Mev, the present limit of the Cal Tech synchrotron. Because of the variation of k these curves do not simply show the change of $\sigma(k, T_p, \theta_p, \theta_\pi)$ with θ_p, as do the other curves in this thesis. To measure that distribution one would have to change the pion energy for each proton angle so that k was held constant.

In all of the possible experiments discussed so far, the shape of the lab cross section distribution is largely determined by the cm to lab transformations. This fact is helpful for some purposes; for example, it makes the isobar model distributions insensitive to such details as whether isobar production is isotropic. Nevertheless, it would be more interesting to measure distributions whose physical details were not obscured by kinematic factors.

To accomplish this it is necessary to measure distributions in the center of mass system. For example, one could measure yields as a function of cm proton angle, keeping the cm proton energy and pion angle fixed. The cross sections from these yields would be converted to the cm system by equation 8.

The first consideration in this type of experiment is the range of cm angles and energies which can be reached with reasonable telescope settings. These are given by

Figure 36

Proton Distributions for Fixed Pion Energy

Proton Energy 250 Mev
Pion Angle 33 1/2°

a Isobar Model
b Density of States

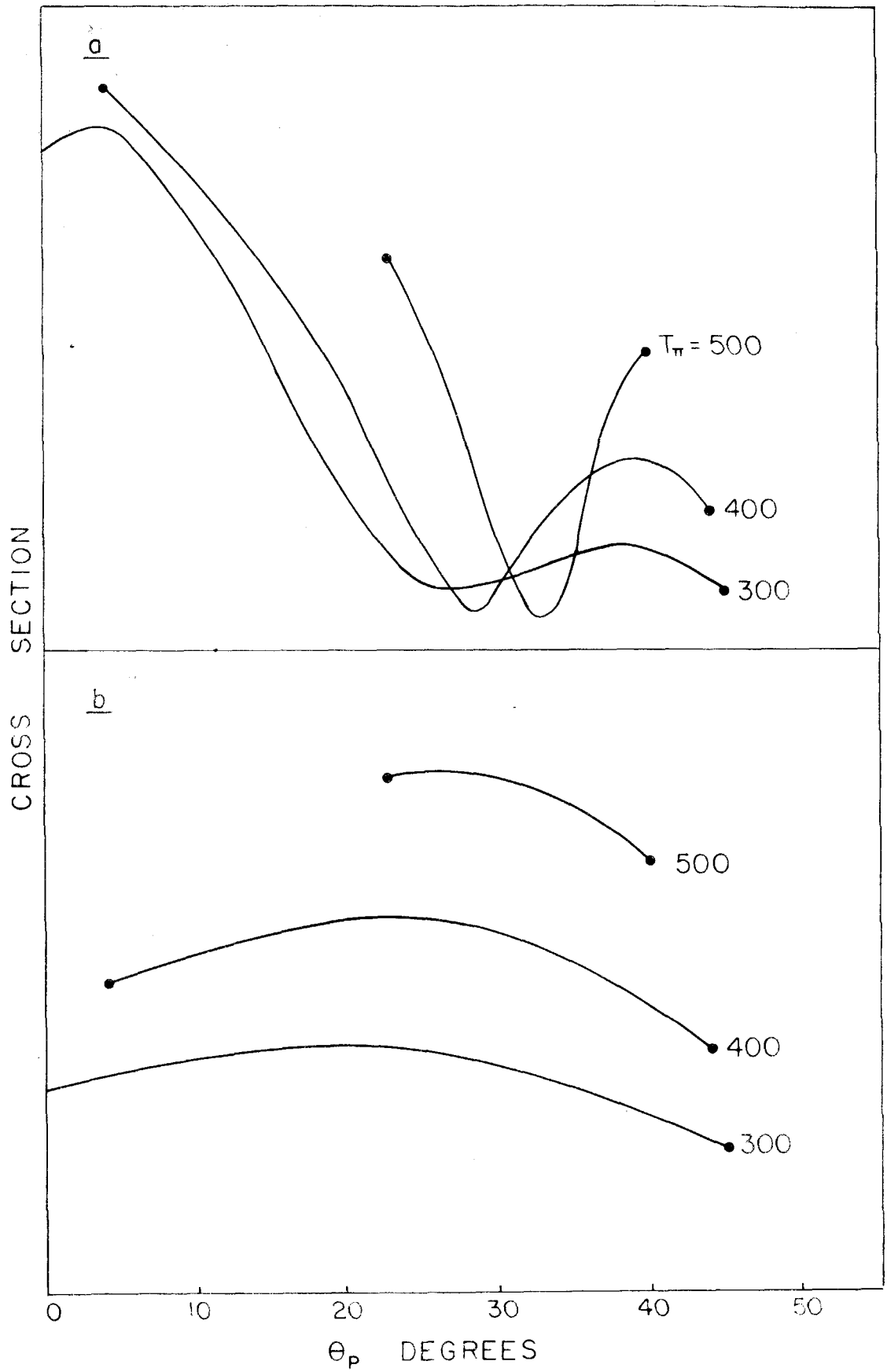
a
T_π = 500
400
300
b
500
400
300
CROSS SECTION
0
10
20
30
40
50
θ_p DEGREES

$$E_p' = \frac{E E_p - K P_p \cos \Theta_p}{E'} \qquad \text{and} \qquad \cos \Theta_p' = \frac{E P_p \cos \Theta_p - K E_p}{E' P_p'}$$

with similar equations for the pion energy and angle. If the proton telescope works well up to 300 Mev and as far forward as 20°, cm proton kinetic energies up to 120 Mev and angles from 45° to 135° can be reached. Cm pion angles can be of any value.

Distributions predicted by the cm density of states are given by equation 10. For the isobar model, $d\Omega_I'$ is equal to $d\Omega_\pi'$ for both the recoil and isobar cases. $d\Omega''_p/d\Omega'_p$ and $d \cos \theta_p'/dT_p'$ are found from the expressions previously given, with all unprimed quantities replaced by primed.

Figure 37 shows a typical proton angular distribution in the cm system, calculated from the recoil and isobar cases of the isobar model. Note that θ_π', the pion angle, gives the only fixed reference direction in the cm system if isobar production is isotropic. Proton distributions are symmetric about $\pi - \theta_\pi'$. The curves show that the distribution peaks at considerably different angles depending on whether the recoil or isobar pion is counted. For the recoil pion the peaks are sharper and closer to $\pi - \theta_\pi'$. This is to be expected from the fact that the isobar direction is $\pi - \theta_\pi'$ in this case, and the proton always emerges near the isobar direction.

In figure 38a the isobar and recoil cases are added, for several proton energies. Because θ_π' gives the only reference direction, the

Figures 37, 38, 39, 40

Proton Distribution in Center of Mass System

37a Isobar Model: Recoil Pion CM Angle 90^{o}

37b Isobar Model: Isobar Pion CM Angle 90^{o}

38 Distributions for Various CM Proton Energies, with Photon Energy 1000 Mev

- a Isobar Model
- b Density of States

39 Distributions for Various Photon Energies, with CM Proton Energy 40 Mev

- a Isobar Model
- b Density of States

40 Distributions from Isobar Model, with Anisotropic Isobar Production and Decay

Photon Energy 1000 Mev

CM Proton Energy 100 Mev

CM Pion Angle 90^{o}

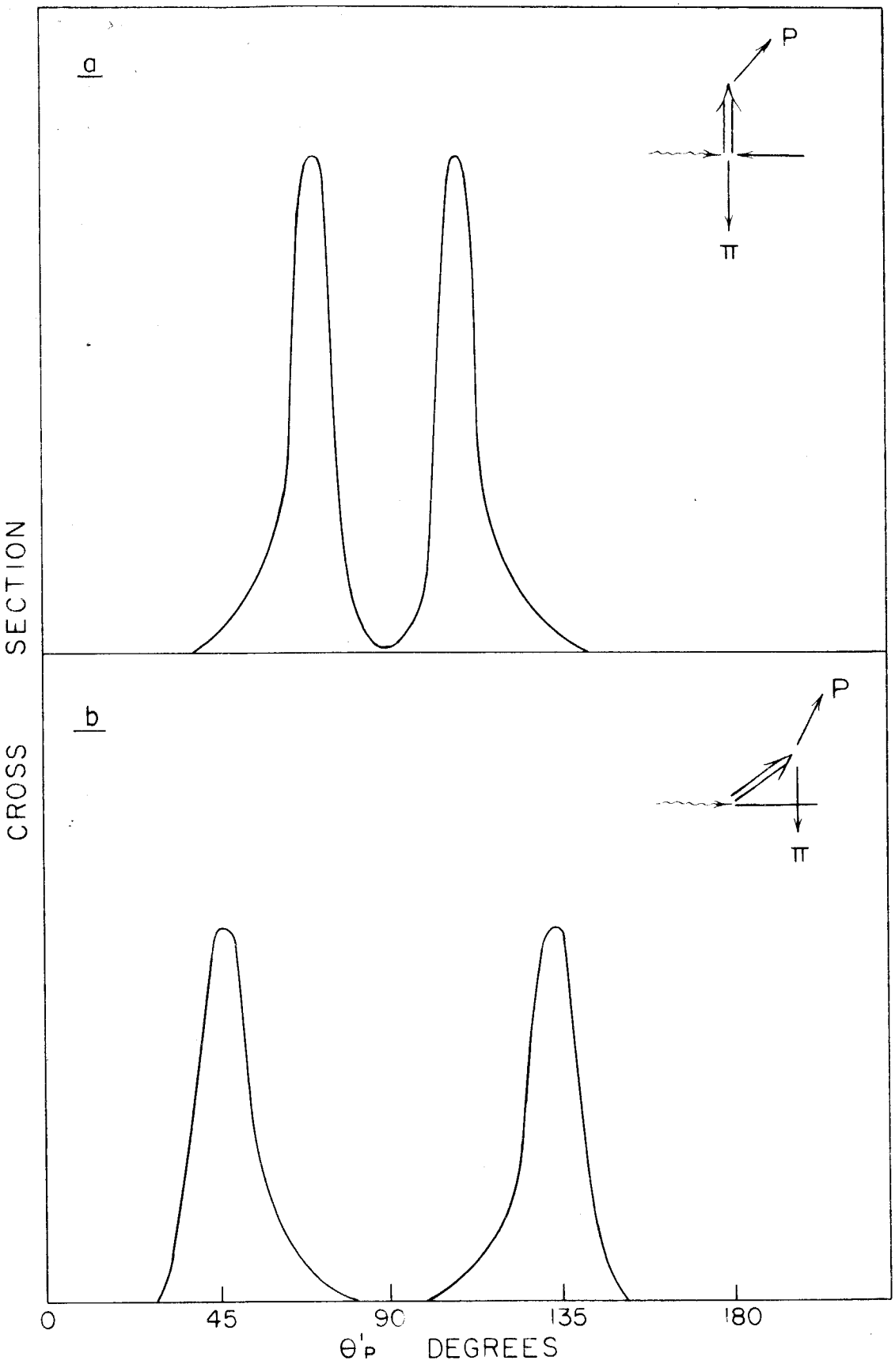
a
P
π
b
P
π
CROSS SECTION
0
45
90
135
180
θ'P DEGREES

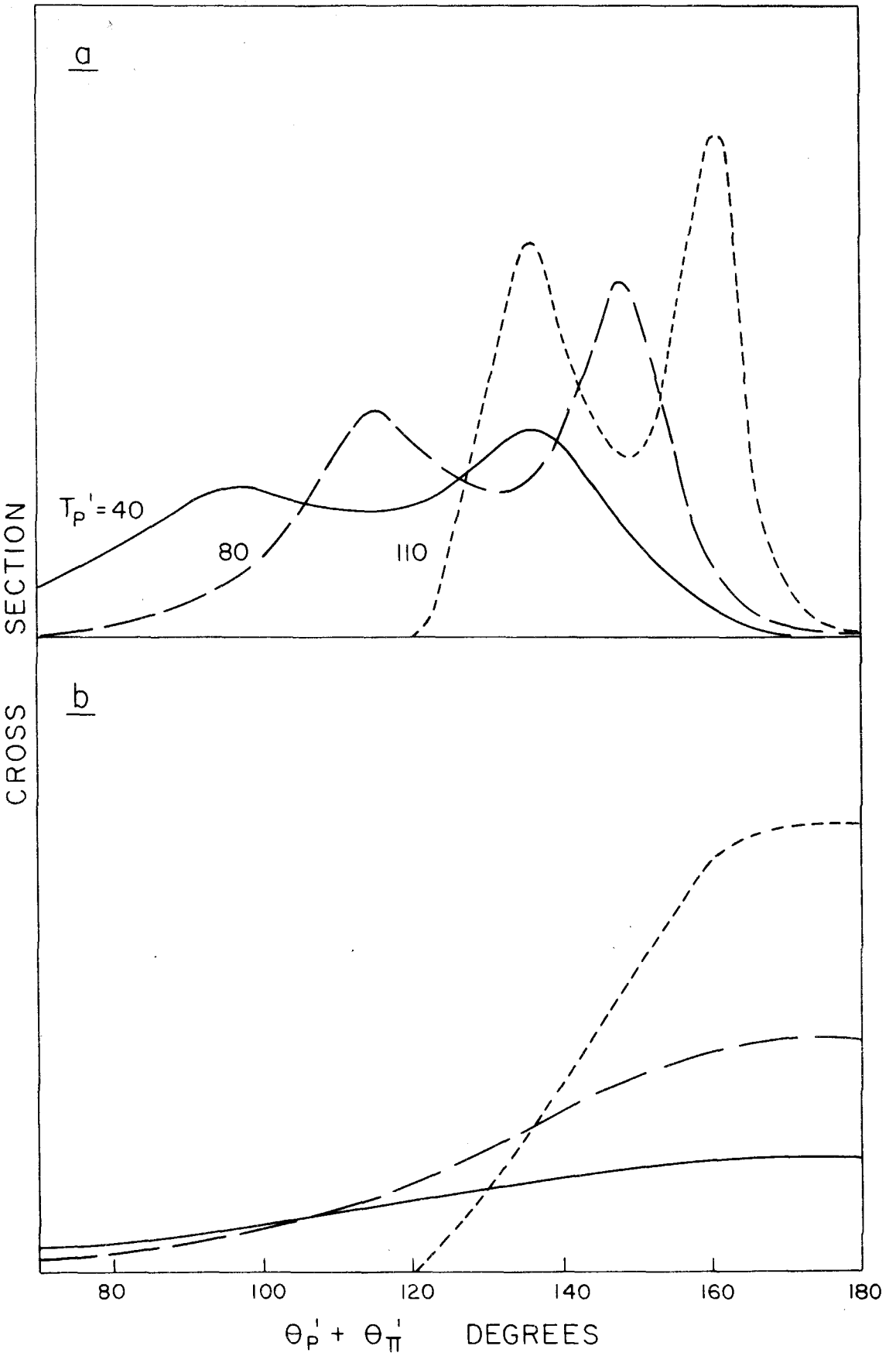
a
b
$T_p' = 40$
80
110
CROSS SECTION
80
100
120
140
160
180
$\theta_p' + \theta_\pi'$ DEGREES

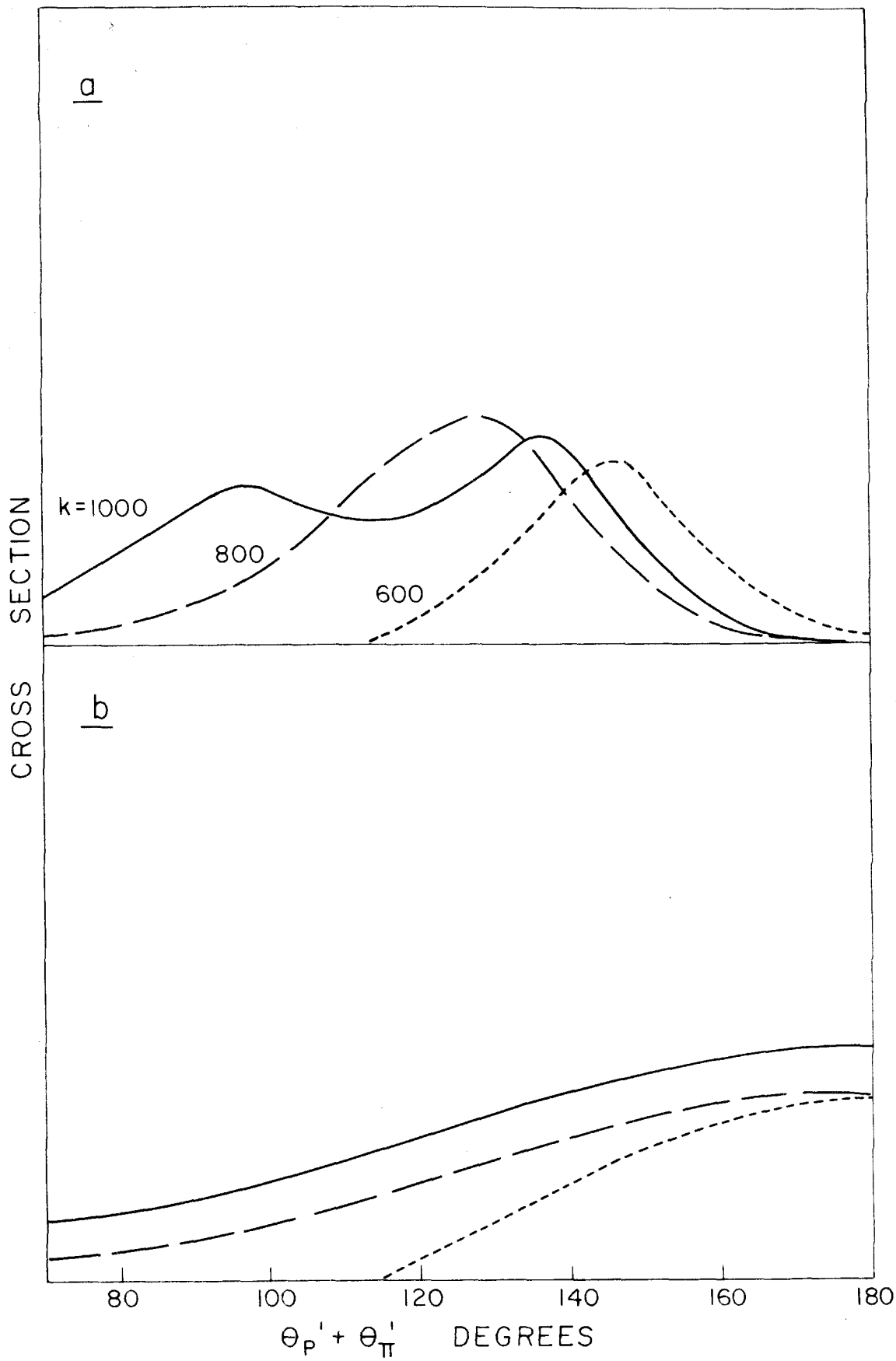
a
k=1000
800
600
CROSS SECTION
b
80
100
120
140
160
180
$\theta_p' + \theta_\pi'$ DEGREES

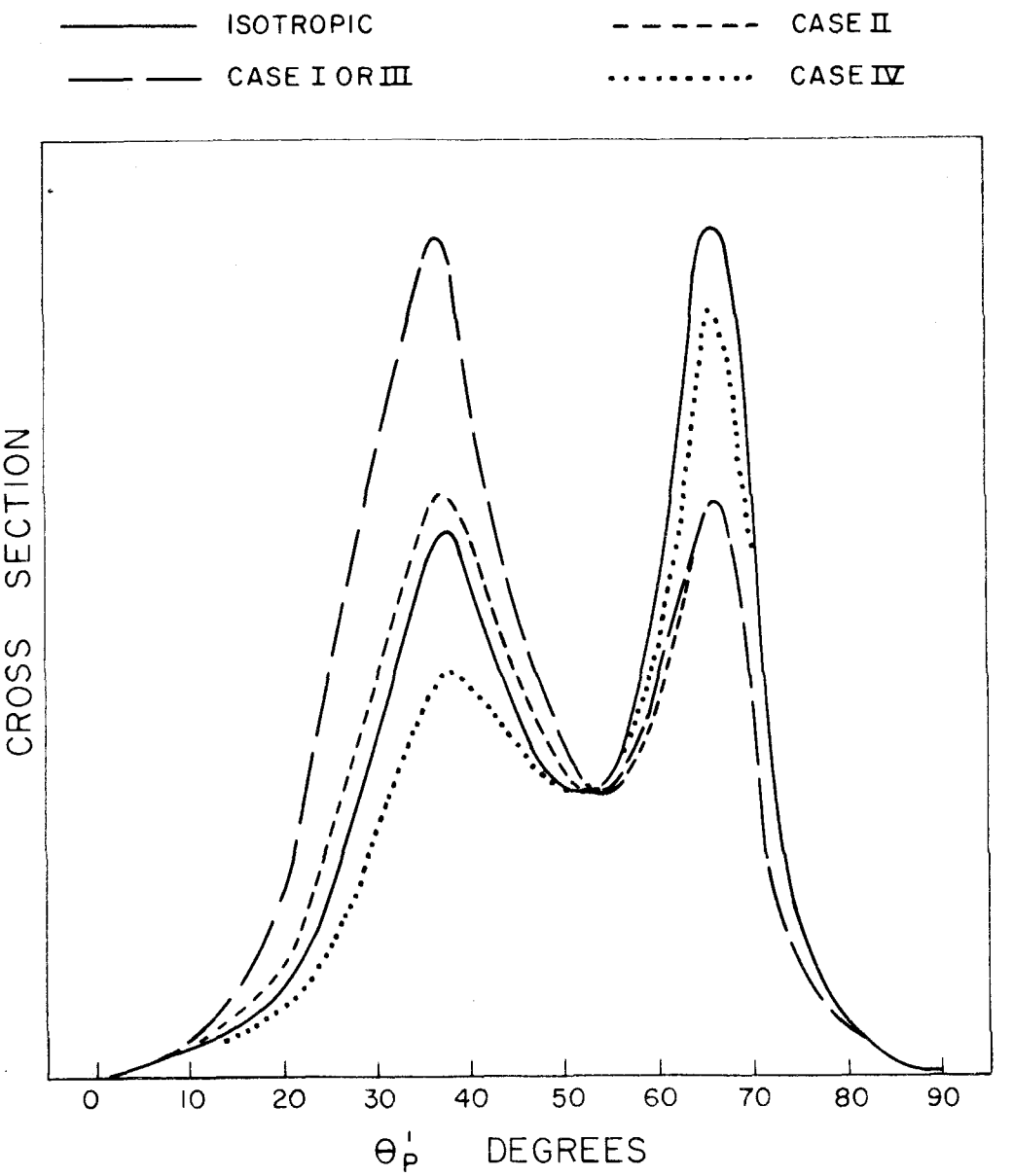
ISOTROPIC
CASE II
CASE I OR III
CASE IV
CROSS SECTION
0
10
20
30
40
50
60
70
80
90
θ_p' DEGREES

curves are plotted against $(\theta'_p + \theta'_\pi)$, the angle between pion and proton. The separate peaks from the two cases are quite distinct. The use here of a pion detector which could identify positive and negative mesons would give information about the doubly-charged or neutral isobar question. For example, if negative pions were counted at, say, 90° in the cm, the neutral isobar would give an 80 Mev proton peak near 58° while the doubly-charged isobar would give the protons near 25°.

Another interesting feature of the distribution is the very small cross section at $\theta'_p + \theta'_\pi = 180^\circ$. In contrast, the density of states formula indicates a large cross section at this angle (figure 38b). A clear distinction between the models could be made by counting protons 180° from the pions.

As the proton energy is lowered, the peaks from the isobar and recoil cases become less sharp, corresponding to the fact that lower energy protons make wider angles with the isobar direction. The smearing is even more pronounced for lower photon energies. Figure 39a shows that no separate 40 Mev proton peaks are distinguishable below 800 Mev.

Anisotropic production and decay of isobars has a more drastic effect on the cm distributions than was found in the lab. Calculations were made for the four anisotropic distributions of the previous section. Figure 40 shows typical results. The effect of the different distributions is to change the relative size of the peaks from the recoil and isobar cases. This is a definite change which might allow a decision as to the spin and parity of the pion-isobar compound state, if

the validity of the isobar were to be established.

In conclusion, it should be made clear that the preceding distributions were presented for the sake of completeness, rather than as definite suggestions for future work. Because of the lack of theoretical insight into the pair production process, detailed cloud chamber or bubble chamber experiments may be more appropriate at this time than such counter measurements as have been described here. Once a specific theory or model is suggested, counter experiments provide the easiest and most accurate method of checking predicted cross sections or distributions. Without a guiding theory, however, the complexity of pair kinematics--the large number of distributions which can be examined--makes it quite unlikely that further counter measurements will produce really significant or definitive results.

References

1. P. L. Donoho, Thesis, Cal Tech (1958)
2. Donoho and Walker, Phys. Rev. 107, 1198 (1957)
3. Peterson, Roos, and Terman, Private Communication
4. Silverman, Wilson, and Woodward, Phys. Rev. 108, 501 (1957)
5. McDaniel, Silverman, Wilson, and Coretllessa, Phys. Rev. Lett. 1, 109 (1958)
6. Brody, Wetherell, and Walker, Phys. Rev. 110, 1213 (1958)
7. Stokes, Northrop, and Boyer, Rev. Sci. Instr. 29, 61 (1958)
8. Wolfe, Silverman, and DeWire, Rev. Sci. Instr. 26, 504 (1955)
9. K. R. Symon, Thesis, Harvard University (1948)
10. B. Rossi, High Energy Particles, Prentice-Hall (1952)
11. R. M. Worlock, Thesis, Cal Tech (1958)
12. R. Gomez, "Preliminary Calibration of the Beam Monitor of the Cal Tech Synchrotron", unpublished (1957)
13. Donoho, Emery, and Walker, Private Communication
14. J. I. Vette, Phys. Rev. 111, 622 (1958)
15. Tollestrup, Keck, and Worlock, Phys. Rev. 99, 220 (1955)
16. Walker, Teasdale, Peterson, and Vette, Phys. Rev. 99, 210 (1955)
17. Clegg, Ernstene, and Tollestrup, Phys. Rev. 107, 1200 (1957)
18. R. Peierls, Proc. Roy. Soc. 149A, 467 (1935)
19. L. W. Alvarez, Proceedings of the Seventh Rochester Conference, Interscience (1957)
20. Motley and Fitch, Phys. Rev. 105, 265 (1957)
21. Birge, Perkins, Peterson, Stork, and Whitehead, Nuovo Cimento IV, 834 (1956)
22. Alexander, Johnston, and O'Ceallaigh, Nuovo Cimento VI, 478 (1957)

23. V. Z. Peterson, Private Communication

24. G. Puppi, Proceedings of the Seventh Rochester Conference, Interscience (1957)

25. Fitch and Motley, Phys. Rev. 101, 496 (1956)

26. R. L. Garwin, Rev. Sci. Instr. 21, 569 (1950)

27. W. A. Wenzel, University of California Report UCRL-8000 (1957)

28. Kessler and Lederman, Phys. Rev. 94, 689 (1954)

29. Plano, Samios, Schwartz, and Steinberger, Nevis Cyclotron Laboratories Report No. 46 (1957)

30. M. Bloch, Thesis, Cal Tech (1958)

31. Dixon and Walker, Phys. Rev. Lett. 1, 458 (1958)

32. Peterson and Henry, Phys. Rev. 96, 850 (1954)

33. Sands, Bloch, Teasdale, and Walker, Phys. Rev. 99, 625 (1955)

34. Friedman and Crowe, Phys. Rev. 105, 1369 (1957)

35. Cutkoski and Zachariasen, Phys. Rev. 103, 1108 (1956)

36. Sellen, Cocconi, Cocconi, and Hart, Preprint (1958)

37. D. Elliott, Thesis, Cal Tech (1959)

38. Yuan and Lindenbaum, Phys. Rev. 103, 404 (1956)

39. Walker, Hushfar, and Shephard, Phys. Rev. 104, 526 (1956)

40. Lindenbaum and Sternheimer, Phys. Rev. 105, 1874 (1957)

41. Crew, Hill, and Lavatelli, Phys. Rev. 106, 1051 (1957)

42. Sternheimer and Lindenbaum, Phys. Rev. 109, 1723 (1958)

43. R. Littauer, Rev. Sci. Instr. 29, 178 (1958)

44. M. Sands, Private Communication

45. M. Sands, "The Isobar Model in Pion Production", unpublished (1958)

46. A. B. Clegg, "Photoproduction of One and Two Pions from Hydrogen", unpublished (1958)